RIGA TECHNICAL UNIVERSITY
Faculty of Building and Civil Engineering
Institute of Heat, Gas and Water technology

Gints JAUDZEMS
Student of doctorate program of Heat, Gas and Water technology

MULTIPLE FLOOD IMPACT ON THE LOCAL SCOUR AT WATER ENGINEERING STRUCTURES ON A FLOODPLAIN

Doctoral Thesis

Scientific supervisor
Prof., Dr. Sc. Eng.
B.GJUNSBURGS

Riga 2015

Šis darbs izstrādāts ar Eiropas Sociālā fonda atbalstu projektā «Atbalsts RTU doktora studiju īstenošanai».

This work has been supported by the European Social Fund within the project «Support for the implementation of doctoral studies at Riga Technical University».

ANNOTATION

The flow parameters at the peak of the flood with unrestricted or restricted duration and the approach flow velocity are used in most accepted methods for local scour calculation, but in nature the flood has a form of hydrograph and unsteady flow conditions must be evaluated. At the present time, there is no formula or method for finding the scour depth near water engineering structures in the flow reflecting the changes of hydraulic and river bed parameters during multiple floods.

A new method to calculate the development of the depth, width and volume of the scour hole in time during multiple floods has been developed. Based on the agreement of experimental and calculated results, the computer program was carried out to model time-dependent scour development during a single flood with different slope of hydrograph and during multiple floods with different duration, probability, frequency and sequence.

The analysis of the influence of multiple floods with different probability, duration, sequence and frequency showed that, with less probability, increased duration and frequency of the floods, and certain sequences of different probability, the scour depth, width and volume increases. It was confirmed that the scour development for a single flood depends on the continuous changes of the hydraulic and river bed parameters because of the changes in flood discharge and the depth of the local scour hole near the water engineering structure. The scour which developed after the previous flood must be taken into account when the influence of the forthcoming flood on scour depth is evaluated.

The influence of the steepness of hydrograph limbs was also studied and analysed. Significant changes in maximum scour depth developed during single wave floods with a different hydrograph steepness were not found, however a direct impact to the time when maximum scour is developed was found.

It was confirmed that during the local scour evolution the local velocity increases and the critical one decreases because of increased discharge and the scour hole developed. The scour stops when the local and critical velocities become equal. The figures are presented which confirm the difference of local velocity from approach velocity near the water engineering structure. It was confirmed that the local velocity, but not the approach flow velocity as accepted by different authors, forms the scour hole.

The Thesis consists of: General Introduction, 5 chapters, General Conclusions, 2 appendixes, 121 references, 73 figures, 9 tables, 121 page together.

ANOTĀCIJA

Vietējo izskalojumu aprēķiniem vairumā no pieņemtajām metodēm tiek izmantoti plūmas parametri plūdu maksimuma laikā ar neierobežotu vai ierobežotu ilgumu, taču dabā plūdiem ir hidrogrāfa forma un aprēķinos jāņem vērā nestacionāras plūsmas apstākļi. Patreiz nav pieejamas formulas vai metodes, kas ļautu noteikt vietējā izskalojuma dziļumu pie ūdens tehnoloģiju būvēm plūsmā, ietverot hidraulisko un upes parametru izmaiņas laikā vairākkārtēju plūdu gadījumā.

Darba ietvaros izstrādāta metode, lai aprēķinātu izskalojumu bedres dziļuma, platuma un tilpuma izmaiņas laikā vairākkārtējos plūdos. Pamatojoties uz eksperimentālo un aprēķina rezultātu atbilstību, tika izstrādāta datorprogramma, lai modelētu izskalojumu attīstību laikā atsevišķiem plūdiem ar dažādu hidrogrāfa slīpumu un vairākkārtējiem plūdiem ar dažādu ilgumu, varbūtību, biežumu un secību.

Vairākkārtēju plūdu ar dažādu varbūtību, ilgumu, secību un biežumu ietekmes analīze parādīja, ka samazinoties plūdu varbūtības rādītājam, palielinoties ilgumam un biežumam, kā arī pie noteiktas plūdu ar atšķirīgu varbūtību secības, izskalojuma dziļums, platums un apjoms palielinās. Tika apstiprināts, ka izskalojuma veidošanās plūdu laikā atkarīga no nepārtrauktām hidraulisko un upes gultnes parametru izmaiņām, kas saistītas ar plūdu radītās plūsmas un vietējā izskalojuma bedres pie konstrukciju pamatiem izmaiņām. Vietējā izskalojuma dziļums, kas radies pirmo plūdu laikā ir svarīgs, lai izvērtētu sekojošu plūdu ietekmi uz tā izmaiņām.

Tika pētīta un analizēta hidrogrāfa līknes slīpuma ietekme uz vietējā izskalojuma dziļumu. Netika konstatēts, ka hidrogrāfa slīpums ietekmē maksimālo vietējā izskalojuma dziļumu, taču tika apstiprināts, kas hidrogrāfa slīpumam ir tieša ietekme uz laiku, kādā maksimālais izskalojuma dziļums tiek sasniegts.

Tika apstiprināts, ka plūdu laikā palielinoties vietējā izskalojuma dziļumam, vietējais un kritiskais plūsmas ātrums mainās, jo notiek plūsmas izmaiņas un izskalojuma bedres attīstība. Izskalojuma process apstājas, kad vietējais un kritiskais ātrums kļūst vienāds. Darbā parādīti grafiki, kas apliecina atšķirības starp vietējā plūsmas ātruma un pienākošās plūsmas ātruma vērtībām un to izmaiņām laikā. Izskalojuma bedres veidošanos ietekmē vietējais plūsmas ātrums, nevis pienākošās plūsmas ātrums, kā to apstiprinājuši dažādi autori.

Darbā ietverti: Ievads, 5 nodaļas, secinājumi, 121 literatūras avots, 2 pielikumi, 73 attēli, 9 tabulas, kopā 121 lapa.

CONTENTS

INTRODUCTION

The increase of unexpected and flash flood accidents in Europe in the past decade and information about environmental and economic losses caused by flooding confirm the impact of climate change on this phenomenon and the necessity for predicting of possible damages. The direct economic losses from the major events between 2003 and 2009 were about EUR 17 billion [91]. Exceptional flooding which produced significant impacts included the floods of summer 2007 in the United Kingdom, which accounted for overall economic losses of more than EUR 4 billion: the flooding of 2005 in Switzerland, Austria and Germany accounted for EUR 2.8 billion and the winter storms and flooding affecting France on December 2003 caused EUR 1.6 billion in losses. Several areas were affected several times in the relatively short period of time between 2003 and 2009. Fig.1.1. shows the occurrence of major floods in Europe during the period from 1998 to 2009 [28]. Up to nine flood accidents were registered for separate regions during a one decade period only and it is evidence of multiple flood events.

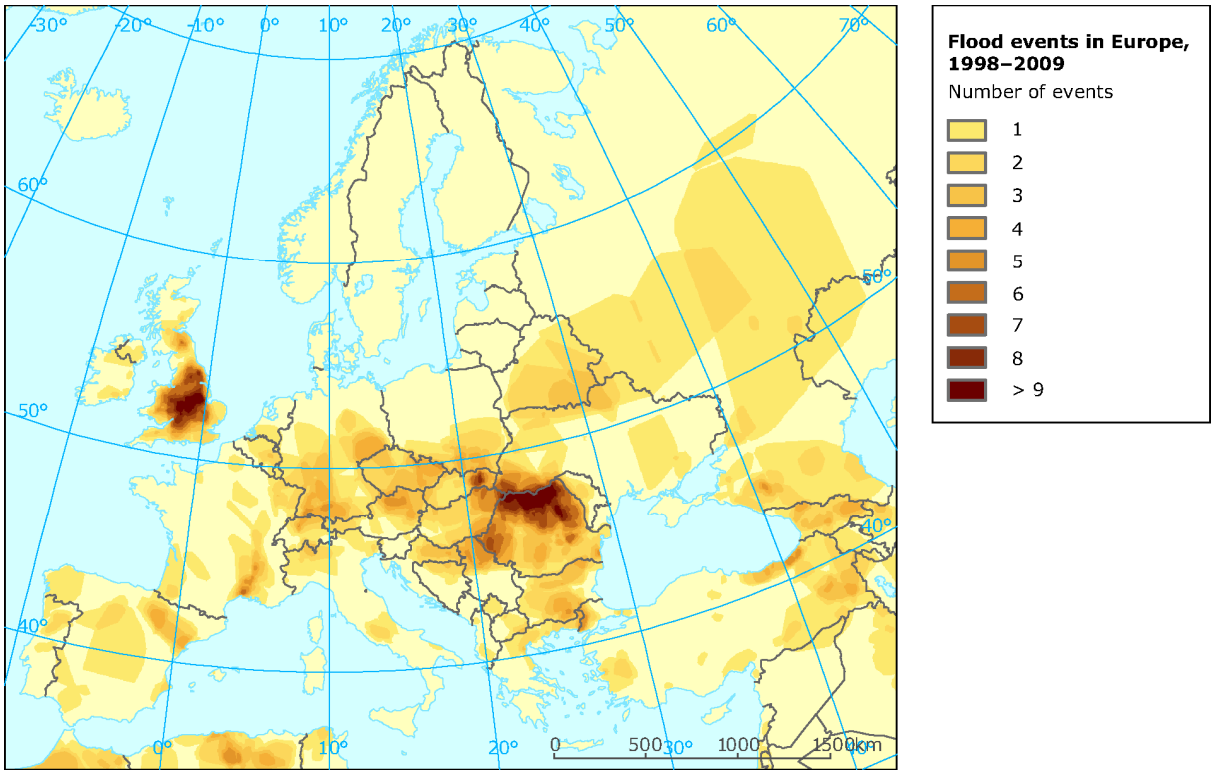

Figure 1.1 Flood events in Europe 1998-2009 [28]

Moreover, global climate change is projected to intensify the hydrological cycle and increase the occurrence and frequency of flood events in large parts of Europe, although estimates of changes in flood frequency and magnitude remain highly uncertain [29]. Climate change is generally expected to increase the magnitude and frequency of extreme precipitation events [20,31], which may lead to more intense and frequent river floods. The projected expected annual economic damages in Europe caused by floods in the 2080s range from 7.7 to 15 billion € depending on warming scenarios [22]. If Northern Europe would have lower damages, the Central Europe area and British Isles would undergo a significant increase in expected damages [22]. According to the European Commission, there have been more than 100 large flooding events in Europe over the last ten years [26]. These events have caused more than 700 casualties and damages of approximately 25 billion Euros. The EU Floods Directive 2007/60/EC [27] aims to estimate, reduce and manage damaging floods in order to protect the population, environment, cultural heritage and economic activity.

The local scour on hydraulic structures is one of the most significant problems which are always considered by hydraulic engineers. The local scour evaluation on foundations leads to the damage of water engineering structures and affects transport and engineering systems.

Water engineering structures (water intakes, effluent outflows or discharges, pipeline foundations etc.) as well as other hydraulic structures like bridge abutments, piers, dams and roads located on floodplain area are under the impact of multiple floods. If the local scour depth is estimated less than the real one it can lead the hydraulic structure to fail. On the other hand, if this depth is estimated more than the real local scour depth, that construction has no economic justification [23].

During the past few decades the equilibrium and temporal depth of scour has been studied and new approaches have been elaborated by Cardoso & Bettess [12], Kothyari & Ranga Raju [62], Balio & Orsi [3], Radice *et al.* [88], Hager *et al.* [53], Armitage & McGahey [2], Yanmaz & Celebi [111], Grimaldi *et al.* [51], Gjunsburgs *et al.* [35–38], Tregnaghi & Marion [106], and Yanmaz & Kose [74]. In most of them discharge on the peak of the flood is used for computing equilibrium or temporal depth of scour, they are not restricted in time for all the maintenance period of the structure or restricted in time for the temporal scour estimation; in field conditions, flow loads on water engineering structures are in the form of a hydrograph and the scour is formed by multiple floods with a different probability, duration, frequency, and sequence. Those parameters are not accepted in modern methods or formulas, they do not allow the computing of the depth of the scour formed in time near water engineering structures during multiple floods, therefore predicting the development of scour

depth before, during, or after the floods, proving the safety of the foundations, and taking the necessary protection measures.

The objective of this study is to develop a new method to determine the depth, width and volume evolution of the scour hole in time during multiple floods, and to estimate the influence of hydraulic and flow parameters to the depth of scour near engineering structures in the flow under unsteady conditions.

The test results were processed using previously published experimental data. The new method for the depth, width and volume evolution of the scour hole near water engineering structure during multiple floods of different probability, duration, frequency and sequence was elaborated. The method presented is confirmed by the test results. The computer modeling of time-dependent scour at water engineering structures under unsteady flow conditions was elaborated. Computer modeling was used to study an influence of the form of the flood hydrograph and the impact of multiple floods of different probability, duration, frequency and sequence to the scour evolution process at the foundations of engineering structures. The discharge, grain size of bed materials, flow contraction rate and duration were changed to study the interconnection of multiple floods and scour development.

It was found that the local flow modification, not the approach flow, is forming the scour hole near the water engineering structure. The changes of the local and critical velocities during scour development in time were studied to define the implications of their relation to the scour intensity. The local velocity depends on the contraction rate of the flow and on the backwater value, and is considerably greater than the approach flow. The interaction and changes of the local and critical velocity velocities during multiple floods was first described. The modeling of scour development in time during multiple floods of different probability, duration, frequency and sequence approved that, with less probability, increased duration and frequency of the floods, and certain sequences of different probability, the scour depth at the water engineering structures increases. The impact of the floods with different shapes of hydrograph on the maximum scour depth was found insignificant, however it was accepted that the intensity of scour development increases and the time when the maximum scour depth is reached reduces by increasing of the slope of hydrograph rising part.

The following conditions are taken into account in this study. Clear-water conditions and alluvial river bed with homogenous river bed material was supposed. Constant cross section of river bed and floodplain between floods was accepted.

Scientific novelty and the application. The new method for computing the depth of scour formed in time near water engineering structures during multiple floods was developed.

First established the impact of multiple flood probability, duration, frequency and sequence on the scour evolution at the structures foundations. It was confirmed that the value of the scour depth is different for various multiple flood scenarios. A new theory is proposed which confirms that the interaction of changes in the local and critical velocities is significant in scour formation. The influence of the hydrograph steepness at the time when the fixed scour depth is reached was accepted.

Since the proposed method reflects the situation in nature, it can be used for predicting the development of scour depth before, during, or after the floods, proving the safety of the water engineering structures, and taking necessary protection measures in due time. The method also allows modeling the scour development scenarios of forthcoming floods with different probability, duration, frequency, sequence, and flood hydrograph that can be used for evaluating whether the construction will be able to withstand flood impact.

The method suggested can be used as the part of an early warning system to evaluate the stability of structures in river flow by using the data from flood-forecasting models and multi-sensors networks for a real-time and distributed monitoring of hydrological measurements.

This work is a continuation of previous studies in the field of fluvial hydraulic developed by researchers of the Institute of Heat, Gas and Water technology of the Riga Technical University B.Gjunsburgs [36, 48], R.R. Neilands [81] and R.Neilands [82, 83]. Further studies on the riverbed layering impact on scour development and equilibrium time of the scour are in the process and studied by E.Govsha [40, 39] and O.Lauva [47] respectively.

Research objective and tasks

The objective of the study is to work out a new method for the scour hole depth, width and volume evolution in time during multiple floods, and to estimate the influence of hydraulic and flow parameters to the depth of scour near water engineering structures under unsteady flow conditions.

To achieve the research objective the following tasks are defined:

1. Make an overview of the methods for calculation of the local scour under steady and unsteady flow conditions to find out parameters used for evaluation of the scour depth at engineering structures in the river flow.
2. Develop a theoretical method for the local scour evolution during multiple floods.

3. Create a new program based on the developed method for the computer modeling of the local scour at engineering structures under unsteady flow conditions during multiple floods of different probability, duration, frequency and sequence.
4. Process experimental data to find the influence of different hydraulic flow parameters and time on the local scour parameters.
5. Analyse the changes in the local and critical velocity under unsteady flow conditions and the local and approach flow interaction and how it influences the scour hole evolution at structures.
6. Study the impact of the form of flood hydrograph on the scour evolution process.
7. Make a computer model of the real flow and study the impact of multiple floods of different probability, duration, frequency and sequence on the scour process at water engineering structures.

1 BACKGROUND AND LITERATURE REVIEW

The structures built in rivers are affected by scour around their foundations. Depending on the depth of scour at the foundations engineering structures keep their stability or become damaged. Many factors are involved in scour development; they are complex and differ due to the change of flow conditions and according to the type of structure. Natural changes of flow in the channel, long-term morphological changes of the river bed or man's activities are the reasons for the occurrence of scour. The scour generally means the removal of material from the bed and banks of a channel by the action of water and can be classified as natural scour, contraction scour and local scour [73]:

a) local scour- scour that results directly from the impact of individual structural elements (for example, piers and abutments) on the flow and occurs only in the immediate vicinity of those elements
b) constriction scour- scour affecting all or most of the channel bed in the vicinity of hydraulic structures, associated with higher velocities caused by the narrowing of the channel
c) natural scour- typically including bed degradation and lateral channel movement, bend scour etc.

The local scour rises because of the presence of a structure in flowing water which causes three-dimensional changes in the velocity field around the structure- increases local flow velocity in the horizontal plane, develops vertical velocities and separates flow from the downstream parts of the structure. Scour development varies according to the structures located in the flow therefore scour calculation methods for different structures vary as well.

1.1 Local scour at steady flow conditions

Scour calculation methods are used at the design stage of hydraulic structures to determine the depth of foundations and piles. The methods for the calculation of local scour at the foundations of hydraulic structures and the methods for the estimation of the equilibrium depth of scour can be found in literature. The regime approach was used to perform most of the early investigations where scour depth was related to the flow of discharge at the contracted cross section. The regime concept originated from the analysis of general scour in

live-bed conditions and was extended to local scour prediction at spur dikes, piers and abutments on the basis of observations.

Lacey [65] proposed a formula for the prediction of the maximum scour depth at piers and spur dikes based on field data from irrigation canals:

$$\frac{h_s}{h_{af}} = 0.47 k_1 \left(\frac{Q}{f \cdot h_{af}^3} \right)^{\frac{1}{3}} - 1 \ , \tag{1.1}$$

where h_s - scour depth measured from the initial bed level;
h_{af} - approach flow depth;
Q - flow discharge;
f – silt factor, $f = 1.76\sqrt{d_{50}}$;
k_1 - amplification factor depending on the type of obstruction;
d_{50} - medium grain size.

Based on the Lacey regime formula Claude Inglis [57] proposed a scour prediction equation (Inglis-Lacey):

$$d_s = 0.946 \cdot \left(\frac{q}{f} \right)^{\frac{1}{3}}, \tag{1.2}$$

where d_s - scour depth;
q - flow discharge;
f - silt factor (Lacey silt factor $f = 1.59\sqrt{d}$);
d - mean diameter of bed material.

The equation resulted from the collection of scour data at various bridge sites in India. He reasoned that the effect of bridge piers is to deflect the current like bend and therefore proposed that the maximum scour depth d_s is proportional to Lacey's [65] regime depth (mean depth, equal to cross-sectional area divided by surface width).

Inglis-Poona equation [57] after Melvil [75]

$$\frac{d_s}{h} = 2.32 \cdot \left(\frac{Q^{\frac{2}{3}}}{h} \right)^{0.78} \ , \tag{1.3}$$

where d_s - scour depth;
h - approach flow depth;

Q – regime discharge.

The result was based on model tests carried out by Inglis [57]. It was assumed that the maximum scour depth at an obstruction could be estimated by multiplying this flood regime depth by a factor dependent on the geometry of this obstruction.

In practice no distinction is made between clear-water scour and scour with continuous sediment motion, although Thomas [105] stated explicitly that the Poona experiments were run without sediment load.

Ahmad (1953) [1] used the regime approach based on laboratory experiments and proposed a maximum scour-depth relationship for spur dikes that used the "flow intensity" or flow rate per unit width in the contracted section, as the independent variable:

$$h_s + h_{af} = k_2 \cdot q^{\frac{2}{3}}, \tag{1.4}$$

where h_s - scour depth at spur dikes;
h_{af} - approach flow depth;
k_2 - constant depending on flow intensity and angle of inclination of spur dike;
q - flow rate per unit width.

Experiments in a flume were made by Laursen and Toch (1956) [70] to study the influence of foundation geometry, stream hydraulics,, the characteristics of sediments, the geometry of the channel shape and alignment to the local scour at piers and abutments. In the laboratory the maximum scour depth was observed at the upstream corner of abutment and authors accented that the contraction ratio was found to be an important factor in influencing abutment scour.

Another scour prediction approach is the empirical and semi-empirical approach, when scour control parameters are correlated through dimensional analysis.

Liu et al. (1961) [72] investigated the scour at spill-through and vertical-wall abutments in flume and used the regression analysis of experimental data to develop scour prediction equations under clear-water and live bed conditions. In a separate series of experiments, clear-water scour was studied by pre-forming the scour hole and determining the flow conditions necessary to just initiate sediment motion in the bottom of the scour hole. In this case, the dimensionless clear-water scour depth was found as follows:

$$\frac{h_s}{h} = 12.5\frac{Fr}{M}, \tag{1.5}$$

where h_s - scour depth;
h - normal flow depth;
Fr - Froude number;
M - geometric constriction ratio.

The geometric constriction ratio M is defined by the ratio of the constricted channel width to the approach channel width. Normal flow depth was determined with sediment in equilibrium transport before the abutment was placed in the flume.

Laursen (1963) [68] developed a relationship for vertical-wall abutment scour depth through a long flow constriction under live-bed and clear-water conditions. The contracted width was assumed to be equal to a scour-hole width of 2.75 times the scour-hole depth. This assumption resulted in a semi-empirical relationship for clear water ($\tau_0 < \tau_c$) scour depth:

$$\frac{L_a}{h_{af}} = 2.75 \frac{h_s}{h_{af}} \left[\frac{\left(\frac{1}{11.5} \frac{h_s}{h_{af}} + 1 \right)^{\frac{7}{6}}}{\sqrt{\frac{\tau_0}{\tau_c}}} - 1 \right], \tag{1.6}$$

where L_a - abutment length;
h_{af} - average upstream flow depth;
h_s - scour depth;
τ_0 - bed shear stress of approach flow;
τ_c - critical shear stress for initiation of sediment motion for sediment size d_{50}.

The maximum scour depth that should be accepted from Laursen's equation is $h_s = 4h_{af}$, because the filed observations of scour around spur dikes on the Mississippi River from which the equation was derived never exceeded $4h_{af}$.

Laursen's scour depth calculation Eq. (1.6) was proposed for abutments that do not extend over the floodplain into the river's main channel; for maximum clear-water scour at threshold conditions, and was approximated by Melville (1997) [76]:

$$h_{\max} \approx 1.93 \sqrt{L_a h_{af}} \ . \tag{1.7}$$

Gill (1972) [34] performed experiments on local scour at spur dikes in sand beds under clear-water and live bed conditions. He suggested that the maximum scour depth depends on the geometric contraction ratio (total width to the width of the contracted section),

on the ratio of the sediment size to the flow depth, and the ratio of the approach flow shear stress to the critical shear stress. The derived equation under clear-water conditions ($\tau_c / \tau_0 > 0$) is:

$$\frac{h_s + h}{h} = 8.375\left(\frac{d_{50}}{h}\right)^{\frac{1}{4}}\left(\frac{L}{L - L_a}\right)^{\frac{6}{7}}\left(\frac{\tau_0}{\tau_c}\right)^{\frac{3}{4}}, \tag{1.8}$$

where h_s - scour depth;
h - initial flow depth;
d_{50} - median grain size;
L - flume width;
L_a - length of the protruding structure;
τ_0 - bed shear stress of approach flow;
τ_c - critical shear stress of sediment particles.

Gill (1972) [34] noted that for bridge design prediction of maximum scour depth it is unimportant wherever clear-water or live-bed conditions exist. However maximum clear-water scour depth is about 10% larger than the equilibrium local live-bed scour, because clear-water conditions have greater sediment carrying capacity.

Tey (1984) [104] managed a wide range experimental study of the effect of flow depth on clear-water scour at abutment, with a constant ratio of approach flow shear stress to critical shear stress $\tau_0 / \tau_c = 0.90$, while varying the flow depth, abutment length and shape. The author concluded that length and shape of abutment protruding into flow influences obtained scour depth; scour depth increased with increasing flow depth, and at longer and blunter abutments shapes.

Froehlich (1989) [32] used dimensional and multiple regression analysis of a large number of clear-water laboratory experiment results on scour at abutments and spur dikes. Froehlich regression equation was proposed in HIRE:

$$\frac{h_s}{h_{af}} = 0.78K_1K_2\left(\frac{L_a}{h_{af}}\right)^{0.63} Fr_{af}^{1.16}\left(\frac{h_{af}}{d_{50}}\right)^{0.43} \sigma^{-1.87} + 1, \tag{1.9}$$

where h_s - scour depth;
h_{af} - approach flow depth;
K_1 - coefficient for abutment shape;
K_2 - $(\Theta / 90)^{0.13}$ - coefficient for angle of embankment to flow;
Θ - angle of embankment to flow;

L_a - abutment length;
Fr_{af} - $V_{ob}/\left(gh_{af}\right)^{0.5}$ - approach flow Froude number upstream of the abutment;
V_{ob} - approach flow velocity in obstructed area by embankment,
d_{50} - medium grain size;
σ - $\left(d_{84}/d_{16}\right)^{0.5}$ - geometric standard deviation of the sediment size distribution,
d_{84} and d_{16} - medium sediment grain size (particle size for which 84% and 16% are finer by weight, respectively);
g - gravitational acceleration.

Froehlich proposed that a factor of safety FS = 1 should be added to the value of h_s/h_{af} obtained from the regression analysis, and it has been included on the right-hand side of Eq. (1.9). The safety factor makes the equation predict a scour depth larger any of the measured scour depth in the data.

"Highways In The River Environment" (HIRE) by Richardson *et al.* (1990) [95] and the U.S. Department of Transportation recommended using the live-bed and clear-water abutment scour calculation equations obtained by Liu *et al.* (1961) [72], Laursen (1980) [69] and Froehlich (1989) [32] for bridge foundation design in the United States.

For predicting scour around long abutments (with $L_a/h_c > 25$) terminating in the main Channel, the original equation was presented in HIRE, while later HEC-18 [92] recommended using the modified HIRE equation by added coefficients of abutment shape and alignment

$$\frac{h_s}{h_c} = \frac{4}{0.55} Fr_{af}^{0.33} K_1 K_2, \tag{1.10}$$

where h_s - scour depth;
h_c - depth of flow at the abutment on the over-bank or in the main channel;
$Fr_{af} = V_{ob}/\left(gh_{af}\right)^{0.5}$ - approach flow Froude number upstream of the abutment;
K_1 - coefficient for abutment shape;
K_2 - coefficient for angle of embankment to flow calculated as for (1.9).

Equation (1.10) was developed from the U.S. Army Corps of Engineers field data for scour at the end of spur dikes on the Mississippi River, and it should be accented that scour depth was recommended to be calculated at bridge abutments if conditions are similar to the field conditions from which the equation was derived.

Melville (1992) [75] summarized a large number of experimental results on the abutment scour from the rectangular channels and proposed the generalized, empirical scour prediction equations. He termed temporal maximum scour depth as equilibrium scour depth

under a certain set of conditions and derived following the maximum scour depth calculation equations depending on empirical correction factors:

for short abutments $$\frac{h}{L_a} 2K_1 K_d K_\sigma K_S K_\theta K_G \,, \tag{1.11}$$

for long abutments $$\frac{h_s}{h_{af}} = 10 K_1 K_d K_\sigma K_s K_\theta K_G \,, \tag{1.12}$$

for intermediate abutments $$\frac{h_s}{\sqrt{L_a h_{af}}} = 2K_1 K_d K_\sigma K_s^* K_\theta^* K_G \,, \tag{1.13}$$

where h_s - local scour depth;
L_a - abutment length;
h_{af} - approach flow depth;
K_1 - flow intensity factor;
K_d - sediment size factor;
K_σ - sediment size factor;
K_S - abutment shape factor;
K_s^* - adjusted shape factor for intermediate abutments;
K_Θ - abutment alignment factor;
K^*_Θ - adjusted alignment factor for intermediate abutments;
K_G - channel geometry factor.

He classified abutments as short (L_a / h_{af} < 1), long (L_a / h_{af} < 25), and intermediate (1 ≤ L_a / h_{af} ≤ 25). Melville used experimental data to define other K factors.

Melville (1995) [77] used Dongol's (1994) [24] experimental data to investigate the compound channel geometry effect on abutment scour depth. The experiments were conducted in a rectangular laboratory flume with a modeled idealized compound channel with the wing-wall abutment placed perpendicular to the flow. It was proposed that the scour depth at abutment terminating into the main channel could be calculated as the scour in an equivalent rectangular channel of the same width and with a depth equal to the main channel depth by calculating the channel geometry factor in Eqs. (1.11), (1.12) and (1.13), as follows:

$$K_G = \sqrt{1 - \frac{L_a^*}{L_a}\left[1 - \left(\frac{h_{afl}}{h_c}\right)^{\frac{5}{3}} \frac{n_c}{n_f}\right]} \,, \tag{1.14}$$

where L_a - total length of the abutment projected into main channel;
L_a^* - projected length of abutment panning the floodplain (consequently, if abutment is terminating into main channel then L_a^* = width of floodplain);

h_c - flow depth in main channel;
h_{afl} - approach flow depth in floodplain;
n_c - Manning's roughness coefficient for main channel;
n_f - Manning's roughness coefficient for floodplain. For rectangular channels K_G = 1.

Sturm and Janjua (1994) [102] performed a series of experiments in a compound channel, i.e., a flume with a fixed-bed main channel and a movable-bed floodplain in which the abutment terminated. Flow depth, discharge, compound-channel geometry, and abutment length were varied, and measurements of approach velocity distribution and scour depth were obtained. On the basis of a dimensional analysis and the application of Laursen's analysis of relief bridge scour in a long contraction to compound channels, authors suggested a preliminary relationship for the dimensionless equilibrium scour depth to illustrate the compound-channel effects on scour:

$$\frac{h_s}{h_{afl}} = 7.70\left[\frac{\left(\frac{V_{afl}}{V_c}\right)}{M_1} - 0.35\right], \tag{1.15}$$

where h_s - scour depth;
h_{afl} - approach flow depth in floodplain;
V_{afl} - approach flow velocity in floodplain;
V_c - sediment critical velocity;
M_1 - discharge contraction ratio defined as the fraction of the total flow discharge in the bridge approach section.

The authors showed that the approach of flow distribution and its readjustment by the abutment in the contracted section are important factors that should be included in the equations for predicting scour depth in natural channels.

Lim (1997) [71] proposed a scour prediction equation based on the flow continuity equation before and after scour, scour geometry, and a generalized form of the power-law formula for flow resistance in an alluvial Channel, for the estimation of the dimensionless equilibrium clear-water scour depth at an abutment in a rectangular Channel for uniform sediments:

$$\frac{h_s}{h_{af}} = K_S\left(0.9X - 2\right), \tag{1.16}$$

where h_s - scour depth;
h_{af} - undisturbed approach flow depth;
K_S - abutment shape factor;
$X = \theta_c^{-0.375} Fr_d^{0.75} \left(d_{50} / h_{af}\right)^{0.25} \left[0.9\left(L_a / h_{af}\right)^{0.5} + 1\right]$,
$\theta_c = u_{*c}^2 / \left[(S-1) g d_{50}\right]$ - Shield's entrainment function;
$Fr_d = V_{af} / \left[(S-1) g d_{50}\right]^{0.5}$ - densimetric particle Froude number of approach flow;
d_{50} - median grain size;
L_a - abutment length;
V_{af} - average approach flow velocity;
u_{*c} - critical shear velocity of particle motion;
S - specific gravity of sediment;
g - gravitational acceleration.

The proposed equations were obtained for an abutment placed perpendicular to the flow direction in the rectangular laboratory flume, which evolves approach flow velocity, median size of cohesion-less sediment, and projecting length of an abutment. The author used a large amount of clear-water scour experiment data obtained by his own study, Dongol (1994) [24], Kandasamy (1989) [60], Kwan (1988) [64], Tey (1984) [104], Rajaratnam and Nwachkukwu (1983) [90], Wong (1982) [108], Zagloul (1974) [115], Gill (1972) [34], Garde *et al*. (1961) [33], and Liu *et al.* (1961) [72] to verify a developed method, however the method is limited to the range of experiment data conditions; $L_a / h_{af} \leq 1$; and $X > 2.22$. Under the maximum clear-water scour condition, i.e., $u_{*0} / u_{*c} \approx 1$, Lim (1997) [71] admitted that it achieved good agreement with the Melville (1992) [75] and Laursen (1963) [68] formulas for scour depth calculation in uniform sediments by reducing Eq. (1.16) to:

$$h_{\max} = 1.8\sqrt{L_a h_{af}} \ . \tag{1.17}$$

For scour calculation at abutment in sediment mixtures Lim (1997) [71] used the effective sediment size d_{50a}, which corresponds to the critical armour-layer criterion proposed by Chin et al. (1994) [17], and is introduced to account for the effect of non-uniform sediment: $d_{50a} = d_{max}/1.8$, where d_{50a} = median grain size of critical armor layer, and d_{max} = maximum particle size.

Chang (1996) [14] has applied Laursen's long contraction theory to both clear-water and live-bed scour. He suggested a velocity distribution in the contracted section, and a spiral-flow adjustment factor, k_f, at the abutment toe that depends on the approach Froude number. The value of k_v was based on potential flow theory, and k_f was determined from a collection

of abutment scour experiments in rectangular laboratory flumes. The resulting scour equation was:

$$\frac{y_2}{y_1} = k_f \left(\frac{k_v q_2}{q_1} \right)^{\Theta}, \tag{1.18}$$

where y_2 - flow depth in contracted section after scour;
y_1 - approach flow depth;
q_1 - flow rate per unit width in approach section;
q_2 - flow rate per unit width in contracted section;
Θ - 0.857 for clear-water scour.

The value of $k_v = 0.8(q_1/q_2)1.5+1$ and $k_f = 0.1+4.5F_1$ for clear-water scour, while $k_f = 0.35 + 3.2F_1$ for live-bed scour. The approach Froude number $F_1 = V_1/(gh_1)0.5$. The effect of sediment size on clear-water abutment scour is included in modified formula (Chang 2001) [15] and has the form:

$$h_2 = k_f (k_v)^{0.857} h_{sc}, \tag{1.19}$$

where h_2 - total depth of flow at the abutment including the contraction scour depth only;
k_f and k_v - are unchanged from the previous formulation;
h_{sc} - is calculated from q_2/V_c;
q_2 - unit discharge at the contraction;
V_c - critical velocity obtained from expressions given by Neill (1973) [84].

The evaluation of q_2 is unclear for the case of the contracted section having a compound section with a variable q_2 across the cross section.

For scour calculation at abutment in sediment mixtures Lim used the effective sediment size d_{50a}, which corresponds to the critical armor-layer criterion proposed by Chin *et al.*, and is introduced to account for the effect of non-uniform sediment: $d_{50a} = d_{max}/1.8$, where d_{50a} is median grain size of critical armor layer, and d_{max} is maximum particle size.

Kouchhakzadeh, S. & Townsend, R.D. (1997) [63], shows that the ratio of flow obstructed by abutment, Q_a, to flow at a specific width near the tip of abutment, Q_w, was a significant parameter in estimating the equilibrium scour depth. The formulation of the functional relationship is based on:

$$\frac{d_{SE}}{h_f} = f\left(F_c, F_f, \frac{Q_a}{Q_w}, S \right), \tag{1.20}$$

where Q_w - specific discharge for a certain width "w" near the abutment tip;
h_f - approach flow depth;
S – construction shape factor;
Q_a - discharge for width "w" at the approach section;
F_f - Froude number of at approach section;
F_c - Froude number when the sediment is at incipient motion condition.

Young *et al.* (1998) [112] developed a regression equation for abutment scour prediction under clear-water and live-bed conditions using the calculated contraction scour as a non-dimensional parameter for the local scour depth at abutment:

$$h_{af} + h_s = 1.37\left[\frac{n^2}{\tau_{*c}(S-1)d_{50}}\right]^{\frac{3}{7}}\left(h_{af}\cdot V_R\right)^{\frac{6}{7}}, \tag{1.21}$$

where h_{af} - approach flow depth;
h_s - scour depth;
n - Manning's roughness coefficient;
τ_{*c} - critical value of Shields' parameter;
S - specific gravity of sediment;
d_{50} - median grain size;
V_R - resultant flow velocity adjacent to the end of the abutment due to contraction.

The resultant local velocity was calculated from $V_R = V_x / \cos\theta^*$, where V_x is an average contraction velocity from continuity, and $\theta^* = 69.85(a/A)^{0.2425}$, where a is blocked flow area by the embankment and abutment, and A is total unobstructed flow area including floodplain and to the centre of main channel.

The U.S. Maryland State Highway Administration developed methods for abutment scour prediction by using coefficients applied to contraction scour. These methods were based on research by Chang and Davis (1999) [13], who applied Laursen's long contraction theory. The authors defined a velocity adjustment factor k_v to account for the non-uniform flow velocity distribution in the contracted section, and a spiral-flow adjustment factor k_f, was based on potential flow theory, and k_f was determined from the analysis of abutment scour experiments in laboratory flumes. The abutment scour depth including contraction scour under clear-water conditions, when the shear stress of approach section is less than critical shear stress, $\tau_0 < \tau_c$, can be found:

$$h_s = \left(k_f \cdot k_v^{0.857}\frac{q_2}{V_c} - h\right)\cdot K_1 \cdot K_2, \tag{1.22}$$

where h_s - total scour depth;
h - average flow depth in contraction prior to scour;
k_f - spiral-flow adjustment factor equal to $0.1+4.5Fr_{af}$;
Fr_{af} - approach flow Froude number upstream abutment, $V_{ob}/(gh_{af})0.5$;
V_{ob} - approach flow velocity in obstructed area by embankment;
g - gravitational acceleration;
k_v - dimensionless velocity adjustment factor, equal to $0.8(q_1/q_2)^{1.5}+1$;
q_1 - flow rate per unit width in the approach section;
q_2 - flow rate per unit width in contracted section;
V_c - sediment critical velocity;
K_1 - abutment shape factor;
K_2 - coefficient for angle of embankment to flow as for Froehlich's equation (1.9).

The values of k_v were limited to the range from 1.0 to 1.8, and k_f within range from 1.0 to 3.3. A factor of safety of 20-40% of computed scour value was proposed to be used for engineers.

Hamill (1999) [56] recommended using a modified version of Froehlich's equation presented in HEC-18 for clear-water abutment scour prediction.

Hydraulic Engineering Circular No. 18 (HEC-18) issued by U.S. Federeal Highway Administration for bridge engineers in the U.S. by Richardson and Davis (2001) [93] recommended a modified version of Froehlich's live-bed abutment scour equation for both, live-bed and clear-water scour depth calculations in conditions that Eq. (1.23) is not consistent with the fact that as L' tends to 0, y_s also tends to 0:

$$\frac{h_s}{h_f} = 2.27K_1K_2\left(\frac{L'}{h_f}\right)^{0.43} Fr^{0.61} + 1, \qquad (1.23)$$

where h_s - scour depth;
h_f - average depth of flow in floodplain, equal to A_e/L;
A_e - flow area of the approach cross section obstructed by the embankment;
L - length of embankment projected normal to the flow;
K_1 - coefficient for abutment shape;
K_2 - coefficient for angle of embankment to flow;
L' - length of active flow obstructed by embankment;
Fr - Froude Number of approach flow upstream of the abutment, equal to $V_e/(gh_f)^{0.5}$
V_e - Q_e/A_e, approach flow velocity in the obstructed area by embankment;
Q_e - flow obstructed by the abutment and approach embankment;
g - gravitational acceleration.

Gjunsburgs and Neilands (2001, 2004) [36,37] and Gjunsburgs *et al*. (2006) [49] used the differential equation of equilibrium of the bed sediment movement under clear-water

conditions, and worked out a fundamental method for calculating the scour development under unsteady flow conditions:

$$h_s = 2h_f\left(x-1\right)\cdot k_m \cdot k_s \cdot k_a\,, \tag{1.24}$$

where h_s - scour depth;
h_f - flow depth in floodplain;
x - parameter determined from graphical relation $N = f(x)$, $N_i = (t_i/(4D_ih_f^2)) + N_i\text{-}1 = 1/6x_i^6 - 1/5x_i^5$;
t_i - time interval;
D_i - constant parameter in steady flow time step;
k_m - coefficient depending on the side wall slope of the abutment (by Yaroslavcev [121]);
k_s - coefficient depending on the angle of flow crossing (by Richardson *et al.* [92]).

Oliveto and Hager (2002) [85] presented a scour equation that involves the scour depth z as a function of time t:

$$Z = z / z_R = 0.068 \cdot N \cdot \sigma^{-1/2} \cdot F_d^{1.5} \cdot \log T\,, \tag{1.25}$$

where $z_R = (h_0D^2)^{1/3}$ for the cylindrical pier;
$z_R = (h_0b^2)^{1/3}$ for the rectangular abutment;
$N = 1$ or $N = 1.25$ - a shape factor for circular-shaped cylindrical pier and vertical abutment, respectively;
$\sigma = (d_{84}/d_{16})^{1/2}$ - the sediment uniformity parameter;
$T = t / t_R$ - the relative time.

The authors found that the dominant parameter governing scour processes is the densimetric particle Froude number $F_d = V / (g'd_{50})^{1/2}$ with approach velocity V, the relative gravitational acceleration $g' = [(\rho_s - \rho)/\rho]g$, where ρ_s is sediment density, ρ is fluid density and d_{50} is a median grain size. The limitations of this method were also described by authors: (1) sediment size $d_{50} \geq 0.80$ mm in order to exclude viscous effects; (2) channel geometry; (3) relative flow depth to exclude macroroughness effects; and (4) approach flows producing essentially clear-water bridge scour.

Rahman and Haque (2003) [89] used Lacey's equation and compared the results against the observed maximum scour depth around abutment-like pier-like structures along the major rivers in Bangladesh. They found out that the calculated scour values usually over-predicted the observed ones. The authors accepted Lacey's equation applicability, but accented that equations do not take into account the structure's dimensions, therefore using the flow-continuity approach and concept of flow concentration into a restricted region of the

scour hole, Rahman and Haque (2003) [89] derived modified Lacey's equation for the prediction of maximum scour depth at abutments:

$$\frac{h_s}{h_{af}} = 0.47 M_2^{1/3} \left(1 + 1.5 \frac{L_a}{h_{af}} \right)^{\frac{1}{3}} - 1, \tag{1.26}$$

where h_s - scour depth;
h_{af} - approach flow depth;
L_a - abutment length;
M_2 - constant for a specific river equal to $\Psi L u_{*c}/(1.76 d_{50}^{0.5} h_{af}^2)$;
$\Psi = 8.5+5.75\log(h_{af}/k_{gr})$ - for turbulent flow;
L - channel width;
u_{*c} - approach flow critical bed shear velocity;
d_{50} - median grain size;
k_{gr} - grain roughness, equal to $2.5 d_{50}$.

Rahman and Haque (2003) concluded that modified, Lacey's equation is applicable for abutment-like structures adopted in the major rivers of Bangladesh within $L_a/h_{af} < 10$, but the applicability is questionable when the equation is used for sloped-wall abutments.

Sturm (2004) [100] performed a large number experiments on the abutment scour in a compound channel flume. The scour depth was measured as a function of discharge, sediment size, abutment shape and length, as well as water-surface profiles, velocities and scour hole contours were also measured. Sturm observed that the discharge distribution factor is the appropriate variable to use rather than abutment length to measure the effects of flow contraction and flow redistribution in the contracted section on local scour depths. He suggested the scour prediction equation for either setback (shorter abutments terminating in floodplain) and bank-line abutments (located at the edge of the main channel) under clear-water conditions:

$$\frac{h_s}{h_f} = K_{ST} \cdot C_r \cdot \left(\frac{q_{afl}}{M_1 \cdot V_c \cdot h_f} - C_0 \right) + FS, \tag{1.27}$$

where h_s - scour depth;
h_f - normal flow depth in floodplain for un-constricted conditions;
K_{ST} – spill-through abutment shape factor;
C_r - best-fit coefficient in proposed equation, equal to 8.14;
C_0 - best-fit constant in proposed equation, equal to 0.40;
$M_1 = [Q_c+(Qfl-Qa)]/Q$ - discharge distribution factor in approach section;
Q - total flow discharge;
Q_c - flow discharge in main channel for uniform flow in compound channel;
Q_{fl} - flow discharge in approach floodplain;

Q_a - flow discharge in obstructed area over a length equal to abutment length;
$q_{afl} = V_{af}/h_{afl}$ - flow rate per unit width in the approach obstructed portion of floodplain;
V_{afl} - average approach flow velocity in the obstructed portion of floodplain;
h_{afl} - average approach flow depth in the obstructed portion of floodplain;
V_c - V_{flc} sediment critical velocity for abutments located on the floodplain;
V_c - V_{cc} sediment critical velocity for abutments located near the bank of the main channel;
V_{flc} - critical velocity for the un-constructed approach flow in the floodplain evaluated for h_f;
V_{cc} - critical velocity for the un-constructed approach flow in the main channel evaluated for normal flow depth h_c in the main channel.

Sturm recommended adding a value of $FS = 1$, because FS is greater than the standard error of 0.75 for h_s/h_f for the best-fit of the experimental data. The spill-through abutment shape factor is: $K_{ST} = 1.52(\xi\text{-}0.67)/(\xi\text{-}0.40)$ for $0.67 \leq \xi \leq 1.2$; $K_{ST} = 1$ for $\xi \geq 1.2$; and $K_{ST} = 0$ for $\xi \leq 0.67$, where $\xi = q_{afl}/(M_1 V_c H_f)$. Sturm (2004) [100] concluded that the abutment shape was important for shorter abutments, while no experimental differences in the abutment shape effects was detected with increased length abutment when more contraction is caused with encroachment on the main channel. Sturm (2004) [100] admitted that opinion where contraction and local scour are independent is overly conservative, therefore his proposed abutment scour prediction method does not distinguish between contraction and local scour.

Sturm (2005) [101] presented a conversation relation between approach hydraulic variables and local hydraulic variables: $V_R/V_c\text{-}1 = 1.56[q_{afl}/(M_1 q_{flc})\text{-}0.4]^{1.78}$, where V_R is resultant depth-average velocity at the upstream corner of the abutment face, V_c is a critical velocity at the upstream corner of the abutment face, $q_{flc} = V_c h_f$ is a critical flow rate per unit width in un-constructed floodplain at normal flow depth h_f. However, the author did not use resultant depth-average velocity in his scour calculation equation.

Benedict *et al.* (2006) [5] using Young's *et al.* (1998) [112] abutment and contraction scour equation and unpublished data presented the contraction adjustment factor K, which was derived from a multiple regression laboratory test analysis of contraction and abutment scour, and modified original Young's equation:

$$\frac{h_f + h_s}{h_f} = 3K\left[\frac{(n \cdot V_R)^2}{d_{50} \cdot \sqrt[3]{h_f}}\right]^{3/7} K_1 K_2, \tag{1.28}$$

where h_s - scour depth;
h_f - normal flow depth in floodplain;

K = $1+1.5393(a/h_f^2)^{0.3798}$ - adjustment factor as a ratio of total scour at the abutment to contraction scour;
a - blocked flow area by the embankment and abutment;
n - Manning's roughness coefficient;
d_{50} - median grain size;
V_R - resultant local velocity adjacent to the end of the abutment due to contraction;
K_1 – coefficient for abutment shape;
K_2 - coefficient for angle of embankment to flow.

Resultant local velocity at the abutment end due to contraction depends on the geometric constriction of the flow area and average un-constricted flow velocity: $V_R = V\{[A/(A-a)]^2+\{a/(0.43A)]^2\}^{0.5}$, where A is the total unobstructed flow area including the floodplain and to the centre of the main channel, V is the average flow velocity over area A. Previously defined constants for specific gravity S = 2.65 for sand, and the critical value of Shield's parameter τ_{*c} = 0.047 for sand motion were used in Eq. (1.28).

Various scour prediction models have been developed and reported in the literature. Most of these models are of empirical character, which are based on clear water scour conditions. A comparison of the methods of different authors as well as a comparison of the results achieved by methods and measured in laboratory tests is objective of many studies. Grimaldi & Gaudio (2006) [52] analysed laboratory data by different authors to verify the onset of the equilibrium state and this compared with the empirical formulae on time evolution of the scour depth at piers and abutments. The results of studies showed that the scour depth at the abutments was generally overestimated by Shen *et al.* (1966) [96] and Melville & Coleman (2000) [78], Franzetti *et al*. (1994) [30] and Hager & Oliveto (2002) [53] formulas, while Lauchlan *et .al*. (2001) [67] formula gave the best prediction. The authors did not accept the extrapolation of the test results with Bertoldi & Jones' (1998) [6] formula because the results showed that the percentage of relative error on the assessment of scour depth presented strong oscillation over time.

Yanmaz (2008) [110] discussed the results obtained from various scour-prediction models dealing with the temporal variation of clear water scour depth. It was found that time-dependent scour depths obtained from Melville and Chiew's (1999) [79] equations are slightly smaller than those of Hager and Oliveto's (2002) [53] equation. The discrepancy between the Hager and Oliveto (2002) [53] equations and Melville and Chiew (1999) [79] equation decreases with increasing duration [110].

1.2 Scour development during unsteady flow conditions

The severity of a flood is a function not only of its flood peak, volume, and duration, but also of the shape of its hydrograph. Various methods have been proposed to construct the shape of a design-flood hydrograph (DHF) and these methods may be placed into the following four classes [113]: (1) the traditional unit-hydrograph (TUH) methods (Sherman 1932 [97]; Dooge 1959 [25]; Chow 1964 [18]; Chow *et al.* 1988 [19]; Pilgrim and Cordery 1993 [87]; Yue and Hashino 2000 [114], Yang and Han 2006 [109]); (2) the synthetic unit hydrograph (SUH) method, such as the Snyder method (Snyder 1938 [98], Bhunya *et al.*2004 [8], Bhunya *et al.* 2011 [7]) and the Soil Conservation Service (SCS)-method (US-SCS 1985 [107]); (3) the typical hydrograph (TH) method (Nezhikhovsky 1971 [117]; Sokolov *et al.* 1976 [99]); and (4) the statistical method (SM) (Gray 1961 [50]; Sokolov *et al.* 1976 [99]; Ciepielowski 1987 [21]; Haktanir and Sezen 1990 [55]).

The shape of a flood hydrograph is a random event. Yue *et al.* (2002) [113] developed a method for describing the statistical properties of the shape of a flood hydrograph. Two shape variables, namely, shape mean (S_m) and shape variance (S_v), were defined to express the randomness of a flood hydrograph. The shape of the flood hydrograph was represented by employing the Beta Probability Density Function (pdf) with two parameters *a* and *b*.

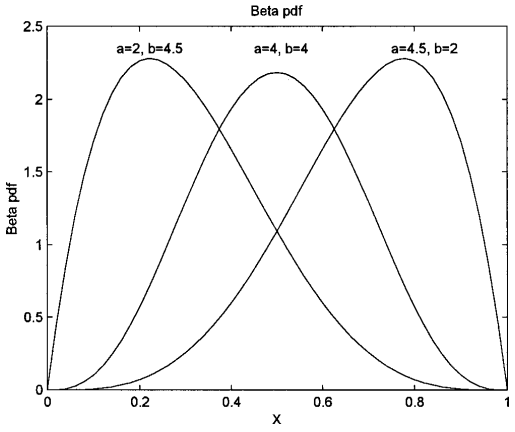

Figure 1.1 Different shapes of Beta pdf [113]

The shape of the pdf is shown in Figure 1.1:

positively skewed or prior-peak shape, when $b > a > 1$

symmetrical or mid-peak shape, when $a = b$

negatively skewed or posterior-peak shape when $a > b > 1$

According to the relationship between the flood peak-occurrence time from the origin (t_p) and the horizontal distance of the centroid of a flood hydrograph from the origin (t_c), flood

hydrographs can be roughly classified into the following three shape types: (1) Positively skewed or prior-peak shape ($t_p < t_c$); (2) symmetrical or mid-peak shape ($t_p = t_c$); and (3) negatively skewed or posterior-peak shape ($t_p > t_c$) and schematic illustrated as shown in Fig. (1.2) [113].

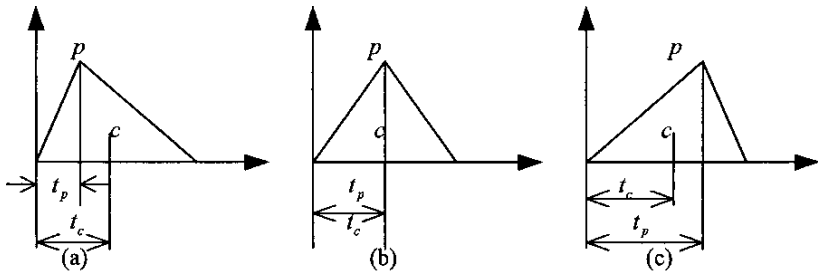

Figure 1.2 A schematic illustration of different shapes of flood hydrographs: (a) prior-peak shape; (b) midpeak shape; (c) posterior-peak shape [113]

Although bridge foundations fail mainly during floods, the effect of an unsteady hydraulic load on bridge piers and abutments has received no systematic attention so far [86]. Many researchers have reported that the failures of cross-river bridges mainly occur during floods. The scouring process during a flood is totally different from that under steady-flow conditions. This is because during floods, the bridge piers become exposed to flood hydrographs with varying flow conditions. Hence, it is very important to investigate the scouring process during unsteady flows. Briaud *et al.* (2001) [11] proposed the SRICOS method to predict the depth of the local scour hole versus time curve around a bridge pier in a river for a given velocity hydrograph and for a layered soil system. The method was limited to cylindrical piers and water depths larger than two times the pier width. Chang *et al.* (2004) [16] and Oliveto and Hager (2005) [86] used a similar concept to calculate the temporal variation of pier scour depth under unsteady flows at uniform piers and abutments.

Lai *et al.* (2009) [66] investigated the temporal effect of different rising hydrographs on local scour depth under clear water scour conditions at bridge piers. A relation for estimating the maximum scour depth in uniform depth was proposed where the flow unsteadiness effect is taken into account by an unsteady flow parameter combining the peak-flow intensity and time-to-peak factors. Two types of hydrograph in the form of approaching flow velocity V versus time t were considered (Fig. 1.3.).

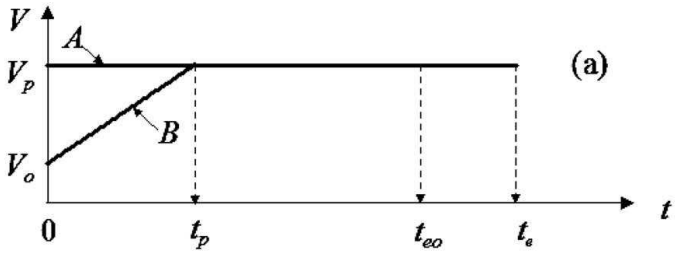

Figure 1.3 Two types of hydrograph in the form of approaching flow velocity *V* versus time *t*. Hydrograph A with steady flow, hydrograph B with linear rising limb[66]

The method for maximum scour depth d_{sm} calculation was proposed:

$$\frac{d_{sm}}{D} - \alpha K_d K_h P, \tag{1.29}$$

where α - coefficient equal to 3.9;
K_d - adjustment factors for sediment size effect and flow depth effect respectively;
K_h - adjustment factors for sediment size effect and flow depth effect respectively;
P - unsteady flow parameter incormporating the peak-flow intensity factor (V_p/V_c) and the time-to-peak factor t'_p/t_{eo};
V_p - approach velocity at peak discharge;
V_c - critical approaching velocity;
t'_p - equivalent scour duration under hydrograph A;
t_{eo} - equilibrium scour time (days).

Chang *et al.*2004 [16] investigated and analyzed experimental data on the scour-depth evolution at circular piers in nonuniform sediment. A scheme for computing the scour-depth evolution under unsteady flow was proposed using a hydrograph with stepwise discharge (Fig. 1.4).

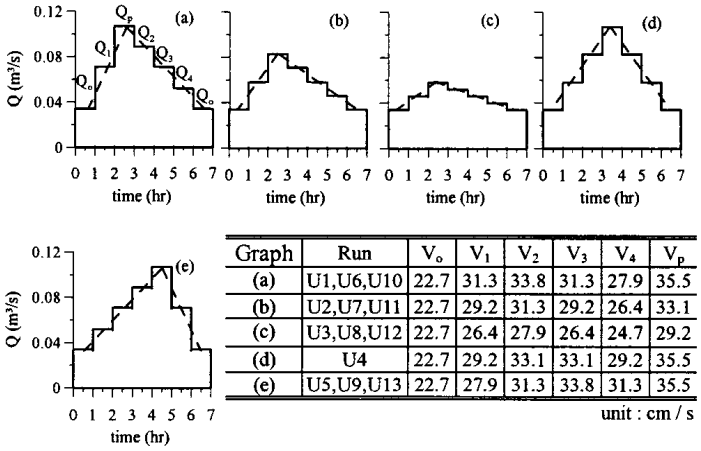

Graph	Run	V_o	V_1	V_2	V_3	V_4	V_p
(a)	U1,U6,U10	22.7	31.3	33.8	31.3	27.9	35.5
(b)	U2,U7,U11	22.7	29.2	31.3	29.2	26.4	33.1
(c)	U3,U8,U12	22.7	26.4	27.9	26.4	24.7	29.2
(d)	U4	22.7	29.2	33.1	33.1	29.2	35.5
(e)	U5,U9,U13	22.7	27.9	31.3	33.8	31.3	35.5

unit : cm / s

Figure 1.4 Stepwise hydrographs for Runs U1–U13[16]

In the unsteady flow experiments of Chang *et al*. 2004, general observations showed that the scour depth increases steadily during the rising period of the hydrograph, and changes only slightly during the recession period. Simulations of scour-depth evolution under a stepwise hydrograph for the experimental runs were made and good agreement between the simulated and experimental results indicated that the proposed scheme may be employed to simulate scour depth evaluation under the stepwise hydrograph flow. The method proposed by Melville and Chiew (1999) [79] was used for scour depth calculation during this investigation.

Oliveto and Hager (2005) [86] carried out research on the effect of unsteady flow on scour development at bridge elements. Two types of flood waves were defined: (1) single-peaked floods with time to peak t_p = 1,800 s and peak discharges Q_p = 0.070, 0.090, and 0.110 m^3/s, plus two runs with t_p = 900 and 3,600 s with a peak discharge Q_p = 0.090 m^3/s; and (2) a double-peaked flood wave with times to peak t_p = 1,800 and 3,600 s for Q_p = 0.090 m^3/s.

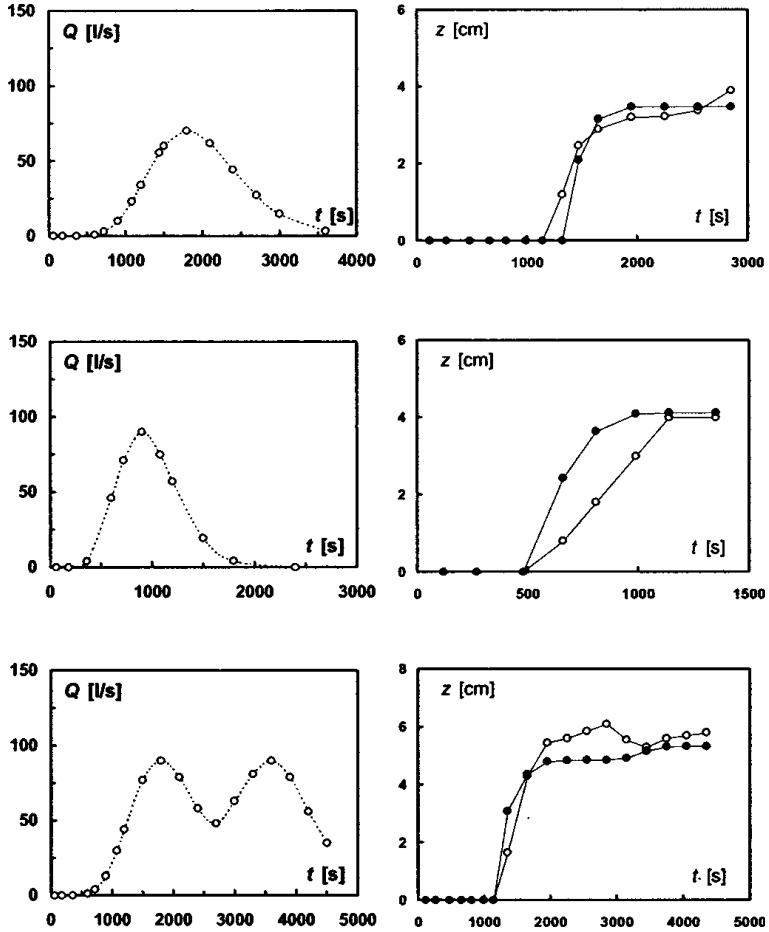

Figure 1.5 Scour advance due to unsteady discharge Q(t) (left) with resulting scour depth z(t) (right) with (white circle) observations and (black circle) predictions for runs: single-peaked floods (**a**) 11.11.00 (1); (**d**) 03.03.01 and double-peaked flood wave (**f**) 04.03.01[86]

It was demonstrated that the basic scour Eq. (1.25) represented by Oliveto and Hager 2002 [85] applies also to such phenomena, provided the parameters are adapted to the experimental configurations. . The authors' confirm that all present experiments followed the nonuniform data well when using a constant but reduced coefficient in Eq. (1.25) and the computational procedure is straightforward, allowing a prediction of the scour depth with a simple subroutine.

Hager and Unger 2010 [54] investigated the effect of a single-peaked flood wave on pear scour. It was made theoretically using Oliveto and Hager's 2002 [85] equation and confirmed by the experimental results. By the application of form coefficient $N = 1$ for the circular bridge pier and $N = 1.25$ for the abutment in the formula, the results also related to the scour at the bridge abutments. Based on scour Eq. (1.25) for a steady approach flow and a model flood hydrograph, the evolution of maximum scour depth was predicted. It was found that the end scour depth depends essentially on the peak approach flow velocity, neutrally on the element shape parameter, the pier diameter, the sediment nonuniformity, the fluid and sediment densities, and the sediment size, but only slightly on the additional variables.

The influence of the unsteady flow hydrograph shape on local scouring around the bridge pier was studied by Borghei *et al.* 2012 [10]. Triangular shaped hydrographs with repeatable peaks where used to simulate the unsteady flow (Fig.2.6). It was found that both sharp and flat increases to the peak of the hydrographs have a negligible effect on the scour depth of the same base time.

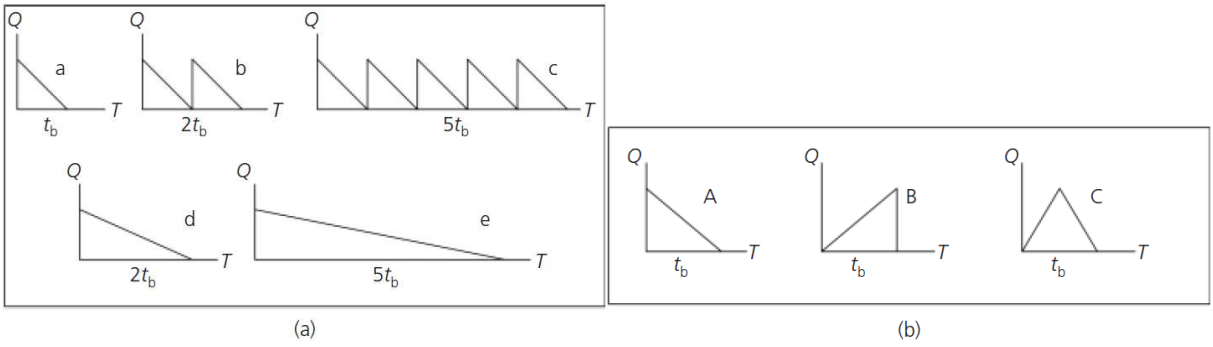

Figure 1.6 (a) Different tested hydrographs and (b) different hydrograph shapes to reach to the peak [10]

Experimental and numerical investigations on the dynamic behaviour of bed-load sediment transport under unsteady flow conditions can be found in literature from a hydrology point of view (De Sutter *et al.* 2001 [103], Bombar *et al.* 2011 [9]). It confirms the

topicality of research necessity for natural flow conditions, when the flow has a form of hydrograph.

Kothyari *et al.* [61] studied the temporal variation of scour depth at bridge piers under clearwater scour conditions with unsteady flow, as approximated by a stepwise discharge hydrograph. Mia and Nago [80] considered the development of bed-shear stress around the pier incorporated with the bed-load sediment transport theory, and they proposed a method for computing the local scour depth varying with time.

Chang *et al.* [16] accepts that the general practice of employing peak-flow discharge to evaluate the maximum scour depth for design may be questioned because the maximum scour depth occurring under a flood hydrograph can be much smaller than the calculated value using peak-flow discharge and using the peak-flow discharge for design can greatly overestimate the maximum scour depth in comparison to the actual conditions under the flood hydrograph.

1.3 Conclusions

Although many studies on local scour around bridge piers have been found in the literature, investigations dealing with time dependent scour studies at abutments under an unsteady flow are still limited. The study of local scour described in chapter 2.1 shows that in line with base variables, like construction length and shape, flow depth, critical velocity and grain size of sediments, there are several which are included or avoided. Most of the methods described include the average approach flow velocity although local scour at constructions is formed by a flow with a velocity near it. Most of the research describes scouring for unsteady flow conditions at the foundations of bridge piers [11], [16], [66], [10]. Hager and Unger [54] suggest using coefficient $N = 1$ for the circular bridge pier and $N = 1.25$ for the abutment in their formula, though tests were carried out for bridge piers. Oliveto and Hager's [86] investigation was based on scour experiments for bridge piers and abutments. All the methods proposed are focused on the comparison of the maximum scour value developed during temporal scour, calculated using temporal scour methods or taking into account varying flow conditions according to the flood hydrograph.

In the unsteady flow experiments and calculations described in literature, general observations show that the scour depth increases steadily during the rising period of the hydrograph, and changes only slightly during the recession period. Despite of comparatively

similar experimental tasks, decisions according to calculation results differ. The common decision of authors is that scour depth calculated by simple methods and those including changes of flow conditions give results with an insignificant difference, however only approach flow characteristics were used in all research.

Literature overview highlights the following conclusions:

1) Approach flow parameters are used for scour calculation at steady or unsteady flow conditions, although local flow modification as local velocity, vortex structures and increased turbulence form the scour hole.
2) The influence of the hydrograph steepness on the value of the depth, width and volume of the scour hole is not studied well in literature.
3) At present there are no formulae or methods found in literature for scour depth calculation during multiple floods.
4) A theoretical analysis of scour development during multiple floods with different probability, duration, sequence and frequency was not found in literature.

2 THEORY AND METHOD OF SCOUR EVALUATION DURING MULTIPLE FLOODS

The flow obstruction at the engineering structure causes flow acceleration, vortex structure development, local increase in velocity and scour hole. The hydraulic characteristics, the contraction rate of flow, the local and critical velocities, the grain size in different layers of the bed, the sediment discharge, the depth, the width and the volume of the scour hole varied during the flood and influence scour development in time.

The method for computing the development of scour depth in time at the water engineering structures during multiple floods is described in this section. The method is confirmed by experimental results in Chapter 4.

The differential equation of equilibrium for the bed sediment movement in clear water conditions has the form:

$$\frac{dw}{dt} = Q_S, \tag{1.1}$$

where t - time, d;
w - volume, m^3;
Q_s - sediment discharge out of the scour hole, m^3/d.

According to laboratory tests, $w = 1/6\pi m^2 h_s^3$ (volume of cone is $w = 1/3\pi r^2 h_s$, steepness of right angle triangle $m = \mathrm{ctg}\alpha$ and $r = mh_s$, (Fig.2.1). Steepness m is defined according to the river bed material size.

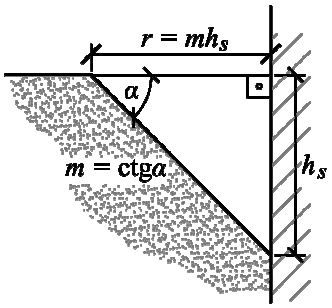

Figure 2.1. Steepness, depth and radius of scour hole

The left-hand part of Eq. (1.1) can be written as

$$\frac{dw}{dt} = \frac{1}{2}\pi m^2 h_s^{\,2} \frac{dh_s}{dt} = a h_s^{\,2} \frac{dh_s}{dt}, \tag{1.2}$$

where h_s - scour depth, m;
m - steepness of the scour hole (Fig. 2.1);
a - equal to $1/2\pi m^2$.

The sediment discharge was determined by the Levi (1969) [116] formula:

$$Q_s = AB \cdot V_l^4, \tag{1.3}$$

where Q - sediment discharge, m^3/d;
B - the width of a scour hole, equal to mh_s, m;
V_l - the local velocity at the water engineering construction, m/s;
A - a parameter in the Levi (1969) [116] formula (Eq. 1.4).
The sediment discharge concept by Levi is presented in Appendix II (Eqs. A2.1 – A2.13).

$$A = \frac{5.62}{\gamma}\left(1 - \frac{\beta V_0}{V_l}\right)\frac{1}{d^{0.25} h_f^{0.25}}, \tag{1.4}$$

where γ - the specific weight of sediments, t/m^3;
β - the coefficient of reduction in critical velocity V_0 due to the vortex system;
V_0 - the velocity required to start the movement of sediments, m/s;
d - the grain size of the bed material, m;
h_f - the depth of water on the floodplain, m.

The sediment discharge concept by Levi is described in Apendix II.

The local and critical velocities vary during a flood. An investigation of the critical and local velocities changes during flood was carried out by and a calculation method for critical and local velocities was derived [37] [41].

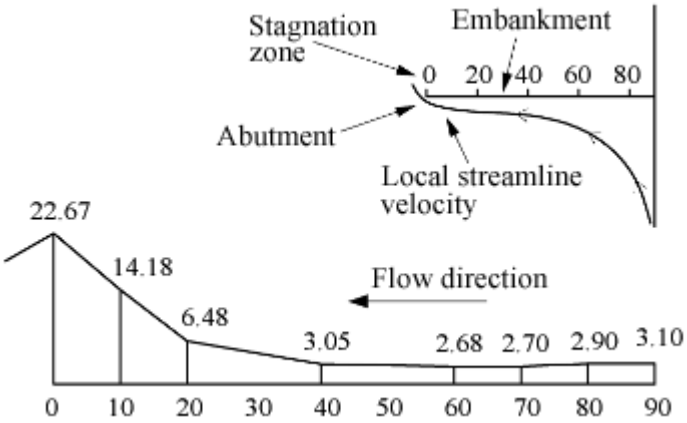

Figure 2.2. Velocity distribution in the vicinity of an abutment [37]

When approaching the contraction of the bridge, the streamlines were bent by the embankment, and then the flow went parallel to it. The velocities along the extreme streamline dropped down almost to the minimum and then gradually increased (Fig. 2.2), and

a spiral vortex system developed. At the corner of the abutment, the concentration of streamlines, a sharp drop in water level, and a rapid increase in velocity were found (Fig. 2.3). Tests accepted that the local velocity near the abutments existed at any contraction of the flow.

To calculate the local velocity, the Bernulli equation for two cross sections of a unit streamline is used. Then the formula for the local velocity near the abutment is:

$$V_l = \varphi\sqrt{2g\Delta Z}\,, \tag{1.5}$$

where V_l - local velocity, m/s;
φ - the local velocity coefficient [48] (Fig.3.4);
ΔZ - the difference in water levels at the corner of the abutment, m;
g - gravitational constant, m/s^2.

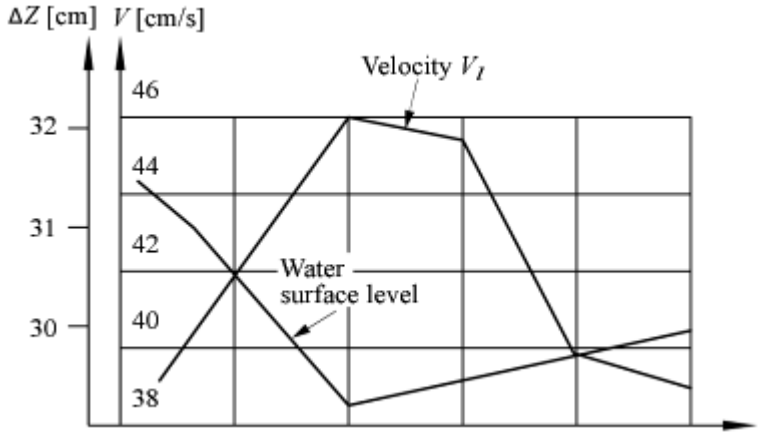

Figure 2.3. Changes in the velocity and water level near the abutment [37]

It was found in tests that the water level difference ΔZ is equal to the maximum backwater Δh. The maximum backwater value can be determined by using the Rotenburg (1969) [118] formula

$$\Delta h = Dh_b + \frac{L \cdot i}{2}\sqrt{\frac{Fr}{i}}\left[\left(\frac{Q}{Q_b}\right)^2 + 1\right] + \frac{V^2}{g}\,, \tag{1.6}$$

where Δh - the maximum backwater, m;
D - the coefficient depending on flow contraction rate Q/Q_b and kinetic parameter P_{KB} of the flow in bridge opening (Eqs. 1.7, 1.8 and 1.22)
h_b - the average depth in the opening
Q_b - the discharge through the bridge opening under open-flow conditions, m^3/s;
Q - approach flow discharge, m^3/s;
L - the flow width, m;

i - the slope of the river bed;
Fr - the Froude number;
V - approach flow velocity, m/s;

$$P_{KB} = \frac{V_b^{\,2}}{g h_b}, \tag{1.7}$$

where h_b - the average depth in the bridge opening.
V_b - the flow velocity in the bridge opening under uncontracted conditions, m/s;

$$D = \frac{P_{KB}}{2}\left[\left(\frac{Q}{Q_b}\right)^2 - 1\right]. \tag{1.8}$$

The velocity coefficient in Eq. (1.5) depends on the rate of contraction of the flow (Fig. 2.4).

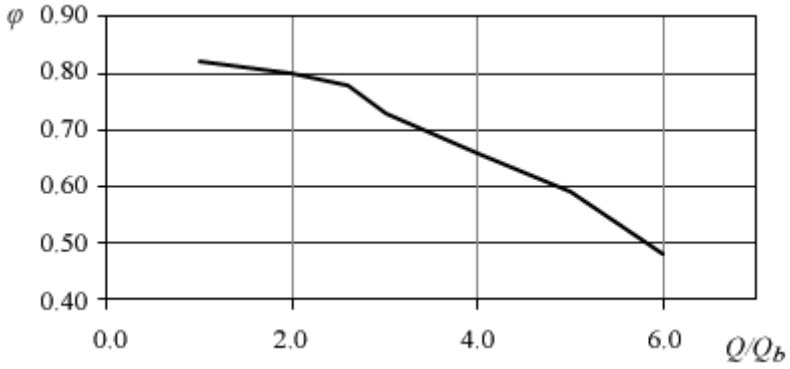

Figure 2.4. Coefficient φ versus the contraction of the flow [37]

The critical velocity V_0 can be found by Studenitcnikov formula [120]:

$$V_0 = 3.6 d^{0.25} h_f^{\,0.25}, \tag{1.9}$$

where V_0 - the critical velocity, m/s;
d - the grain size of the bed material, m;
h_f - the depth of water on the floodplain, m.

The critical velocity concept by Studenitchnikov is presented in Appendix II (Eqs. A2.14 – A2.24).

The hydraulic characteristics, the contraction rate of flow, the velocities V_0 and V_l, the grain size in different layers of the bed, the sediment discharge, the depth, the width and the volume of scour hole varied during the flood. Intermediate values V_{lt}, V_{0t} and h_m must be used in formulas to study time dependant scour development.

The local velocity at any depth of the scour hole can be found based on flow-continuity relation. According to it, the discharge across the width of a scour hole before and after the scour can be defined as:

$$Q_f = k \cdot Q_{sc}, \tag{1.10}$$

where Q_f - discharge across the width of the scour hole with a plain bed, m^3/s;
Q_{sc} - discharge of the scour hole with a scour depth h_s, m3/s;
k - coefficient depending on flow contraction rate (Fig. 2.5) [48].

The Eq. (1.10) can be written as follows:

$$mh_s \cdot h_f V_l = k\left(mh_s h_f + \frac{mh_s}{2} \cdot h_s \right) \cdot V_{lt}, \tag{1.11}$$

where V_{lt} – the local flow velocity after time t at a scour depth h_s, m/s;
m - steepness of the scour hole (Fig.2.1).

From Eq. (1.11) the local velocity at any depth of the scour hole can be determined by formula [37]:

$$V_{lt} = \frac{V_l}{k\left(1 + \frac{h_s}{2h_f}\right)}, \tag{1.12}$$

where k - the coefficient of changes in the discharge due to the scour, depends on the flow contraction rate (Fig. 2.5).

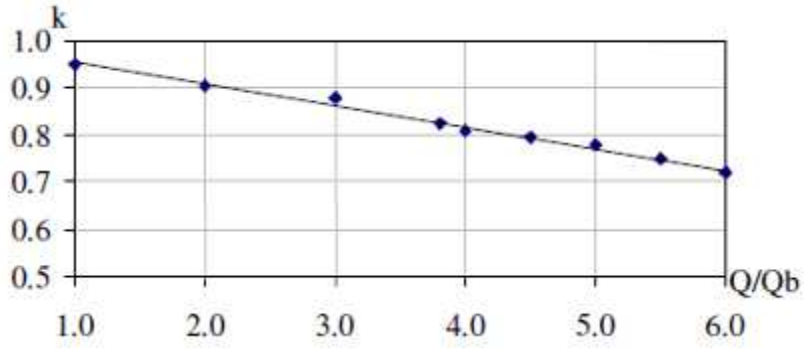

Figure 2.5. Coefficient k versus flow contraction rate [48]

The medium scour depth during the flood is (Gjunsburgs, 2004) [42]:

$$h_m = \frac{w}{B} = \frac{mh_s \cdot h_f + \frac{1}{2} mh_s \cdot h_s}{mh_s} = h_f \left(1 + \frac{h_s}{2h_f}\right), \quad (1.13)$$

where h_m - medium scour depth, m.

Then from Eq. (1.9) and (1.13) the critical velocity at any depth of scour:

$$V_{0t} = 3.6d^{0.25} \cdot h_m{}^{0.25} = 3.6d^{0.25} \cdot h_f{}^{0.25} \left(1 + \frac{h_s}{2h_f}\right)^{0.25}, \quad (1.14)$$

where V_{0t} - the critical flow velocity after time t at a scour depth h_s, m/s.

From Eq. (1.3) and (1.12) the sediment discharge upon development of the scour can be found:

$$Q_{st} = A \cdot m \cdot h_s \cdot V_{lt}{}^4 = Amh_s \frac{V_l{}^4}{\left(1 + \frac{h_s}{2h_f}\right)^4} = b \frac{h_s}{\left(1 + \frac{h_s}{2h_f}\right)^4}, \quad (1.15)$$

where b – equal to $Am \cdot V_l^4 k$;
k - the coefficient of changes in the discharge due to the scour, depends on the flow contraction rate (Fig. 2.5).

The hydraulic characteristics, the contraction rate of flow, the velocities V_0 and V_l, the grain size in different layers of the bed, the sediment discharge, the depth, the width and the volume of scour hole varied during the flood.

Upon the development of the scour, we have

$$A_i = \frac{5.62}{\gamma}\left(1 - \frac{\beta V_{0t}}{V_{lt}}\right) \cdot \frac{1}{d^{0.25} h_m{}^{0.25}} = \frac{5.62}{\gamma}\left[1 - \frac{k\beta V_0}{V_l}\left(1 + \frac{h_s}{2h_f}\right)^{1.25}\right] \cdot$$
$$\cdot \frac{1}{d^{0.25} h_f{}^{0.25}\left(1 + \frac{h_s}{2h_f}\right)^{0.25}}. \quad (1.16)$$

Taking into account Eq. (1.2) and (1.15), differential Eq. (1.1) can be presented as

$$ah_s^2 \frac{dh_s}{dt} = b \frac{h_s}{\left(1+\frac{h_s}{h_f}\right)^4}, \tag{1.17}$$

or

$$D_i \cdot h_s \left(1+\frac{h_s}{2h_f}\right)^4 dh_s = dt, \tag{1.18}$$

where $D_i = a/b$ - constant inside time interval.

After integration we have

$$t = D_i \int_{x_1}^{x_2} h_s \left(1+\frac{h_s}{2h_f}\right)^4 dh_s . \tag{1.19}$$

According to the method [37], the flood hydrograph was divided in time steps, and each step in turn was divided into small time intervals (Fig. 2.6).

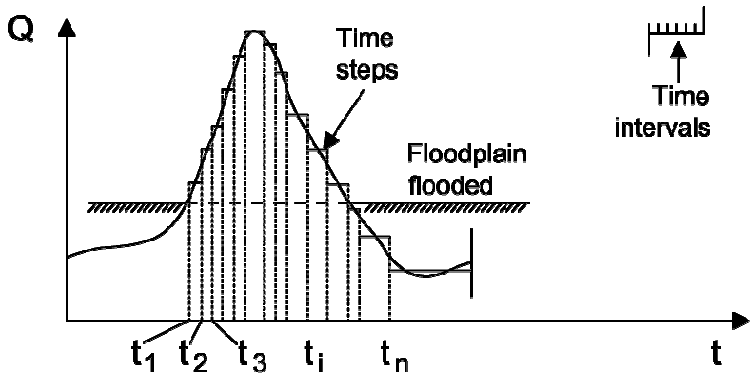

Figure 2.6. Flood hydrograph dividend in time steps and time intervals

After integration with new variables $x = 1 + h_s / 2h_f$, $h_s = 2h_f(x - 1)$ and $dh_s = 2h_f dx$ we obtain

$$N_i = \frac{t_i}{4D_i h_f^2} + N_{i-1}, \tag{1.20}$$

where $N_i = 1/6x_i^6 - 1/5x_i^5$;
t_i - time interval, d;
N_{i-1} - the value of N_i in previous step.

Using the graph $N = f(x)$ or the data from Table 2.1 for the calculated N_i, we find x_i and the depth of scour at the end of time interval:

$$h_s = 2h_f(x-1). \tag{1.21}$$

Table 2.1

The value of N_i as a function of x_i

x_i	1.0	1.2	1.4	1.6	1.8	2.0	2.2	2.4	2.6	2.8
N_i	-0.033	0.0002	0.18	0.70	1.90	4.29	8.62	15.98	27.2	46.07

The flow discharge is determined as the ratio between the discharge through the bridge opening Q_b and floodplain discharge Q_f under open-flow conditions. Discharge through the bridge opening under open-flow conditions can be found by Rotenburg (1965) [119] formula:

$$Q_b = \frac{Q}{1+\frac{K_f}{K_b}}, \tag{1.22}$$

where Q_b - discharge through the bridge opening, m^3/s;
Q - approach flow discharge, m^3/s;
K_f - discharge modules of floodplain;
K_b - discharge modules of bridge opening;

$$K_f = \frac{\omega_f}{n_f} h_f^{0.75}, \tag{1.23}$$

$$K_b = \frac{\omega_b}{n_b} h_b^{0.75}, \tag{1.24}$$

where ω_f - cross section of the flow in floodplain, m^2;
ω_b - cross section of the flow in bridge opening, m^2;
n_f - roughness coefficient for floodplain (0.025 – 0.08) [4],
n_b - roughness coefficient for channel bed (0.05 – 0.2) [4],
h_f - average depth of the flow on the floodplain, m;
h_b - average depth of the flow in bridge opening, m.

To determine the scour depth development during the flood, the hydrograph is divided into time steps, and each time step is divided into time intervals. For each time step, the following parameters must be determined: h_f – depth of water on the floodplain, Q/Q_b – contraction rate of the flow, Δh – maximum backwater, d – grain size, H – thickness of the

bed layer with d – size, and γ – specific weight of the bed material. As a result, V_l, V_0, A, D, N_i, N_{i-1}, and h_s must be found at the end of the time intervals and finally at the end of the time step. For the next time step, the flow parameters changed because of the flood and the scour developed during the previous time step.

From this, the method for the calculation of **scour development during multiple floods was derived**. At first flood scour starts from the moment when the floodplain is flooded. According to the method presented the hydrograph of each following flood wave is divided in time steps (Fig. 2.7).

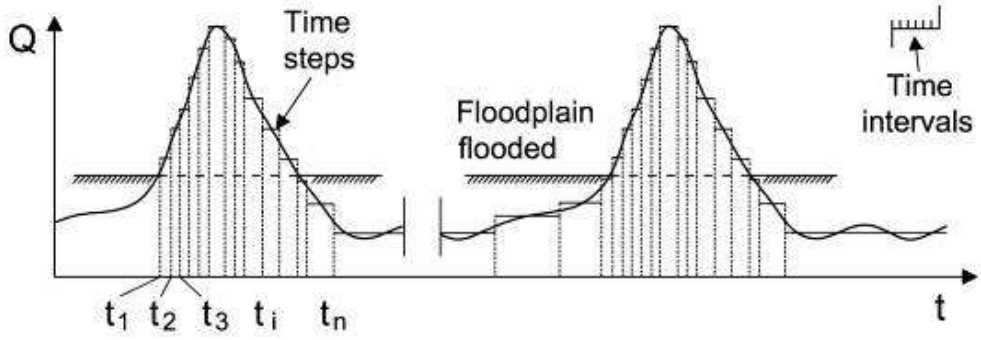

Figure 2.7. Multiple floods hydrographs dividend in time steps and time intervals

The steady flow condition is considered within the time step. The local velocity $V_{l\ I}$ and the critical velocity $V_{0\ I}$ are found at the start of the scour process. Because of the steady flow conditions considered, the value of local velocity V_{lt} is reducing and the value of critical velocity V_{0t} is increasing because of the scour within the time step. At the end of time step, values of local velocity $V_{lt\ I-1}$, critical velocity $V_{0t\ I-1}$ and the scour depth developed during first step $h_{s\ I-1}$ can be found (where the Roman numeral in a subscript of variables indicates number of flood and the Arabic numeral indicates number of time step).

For the second time step new values of local and critical velocities should be found because of the increased discharge and taking into account the scour depth $h_{s\ I-1}$ evolved in first step. The scour depth $h_{s\ I-2}$ is found at the end of the second time step and calculation continued for further steps.

For time steps in the rising limb of hydrograph the local velocity leads to a reduction because of the scour and at the same time it increases because the depth of the flow, discharge and backwater value are increasing. The critical velocity is increasing in time from step to step of hydrograph, because of the constant increase of the average depth of the flow, including the depth of scour.

At the recession limb the local velocity is considerably reducing from step to step because of the flood as well as this, the critical velocity is reducing. The scour stops at some point of recession limb of hydrograph X_{I-2}, when the local velocity $V_{lt\ I-n}$ becomes equal to the critical one $V_{0t\ I-n}$, and the scour depth $h_{s\ I}$ reached during the first flood wave can be found (Fig 2.8).

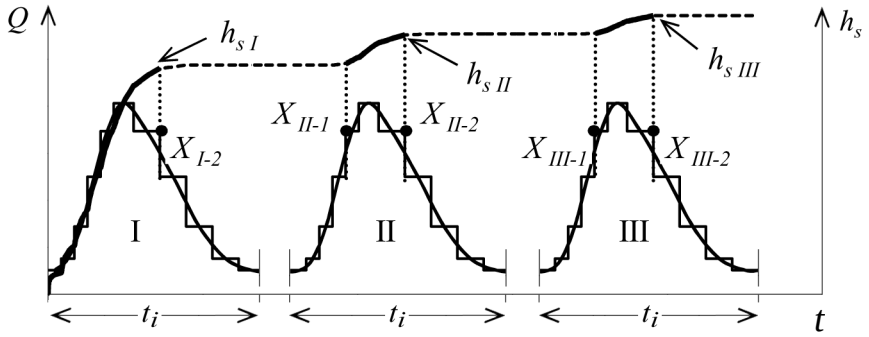

Figure 2.8. Scour evolution during multiple floods; I, II and III are a number of floods

Taking into account the scour depth $h_{s\ I}$ reached in the first flood, the new values of $V_{lt\ II}$ and $V_{0t\ II}$ are found for the first time step of the second flood hydrograph.

$$V_{lt\ II} = \frac{V_{l\ II}}{k\left(1+\frac{h_{s\ I}}{2h_{f\ II}}\right)}, \tag{1.25}$$

where $V_{lt\ II}$ - local velocity at the depth of the scour hole $h_{s\ I}$, m/s;
$V_{l\ II}$ - local velocity of the second flood, with the flat river bed supposed, m/s;
$h_{s\ I}$ - scour depth developed during the first flood, m;
$h_{f\ II}$ - depth of the floodplain of the second flood, m,

and

$$V_{0t\ II} = 3.6d^{0.25} \cdot h_{f\ II}{}^{0.25}\left(1+\frac{h_{s\ I}}{2h_{f\ II}}\right)^{0.25}, \tag{1.26}$$

where $V_{0t\ II}$ - critical velocity at the depth of the scour hole $h_{s\ I}$, m/s.

The calculation is continued for each time step while the condition when the local velocity $V_{lt\ II}$ is higher than the critical one $V_{0t\ II}$ is found and the scour starts (point X_{II-1}, Fig. 2.8).

Because of the scour evolved during a previous flood, the scour process starts only at the sufficient flood discharge when the local velocity is higher than the critical one. According to the method presented and Eqs. (1.21, 1.12 and 1.14), the scour depth achieved during the second flood $h_{s\ II}$ is found. The scour stops at the point of the recession limb of hydrograph $X_{II\text{-}2}$, when the local velocity $V_{lt\ II\text{-}n}$ becomes equal to the critical one $V_{0t\ II\text{-}n}$.

For the third flood the scour depth developed during the second flood $h_{s\ II}$ is taken into account and the new values of the local and critical velocities found, while $V_{lt\ II\text{-}n} > V_{0t\ II\text{-}n}$. The scour starts at some point of hydrograph rising limb $X_{III\text{-}1}$ and stops on recession limb at some point $X_{III\text{-}2}$ when condition $V_{lt\ II\text{-}n} = V_{0t\ II\text{-}n}$ is reached.

The method presented is taking into account local and critical velocities evolution in time from step to step and from flood to flood.

The scour in nature nowadays is a result of multiple floods, and to predict it possible with the method presented if we know the history of the multiple flood of the river.

3 EXPERIMENTAL DATA PROCESSING AND COMPARISON RESULTS

The test results were processed using previously published experimental data [46]. The tests were carried out in a flume 3.5 m wide (L in Table 3.1) and 21 m long. Experimental data obtained in the flumes in open flow conditions are presented in Table 2.1. The flow distribution between the channel and the floodplain was studied under open channel flow conditions. The rigid-bed tests were performed for different flow contractions and Froude numbers to investigate the changes of velocity and water level near the modelled abutment. The Froude number Fr_f varied from 0.01 to 0.124, Re_c varied from 7500 to 16010 and Re_f varied from 4390 to 14300, where Re_c and Re_f are the Reynolds numbers for the channel and floodplain, respectively; the slope of the flume was 0.0012. The floodplain depth h_f was 7 and 13 cm. The condition that $Fr_R = Fr_f$ was fulfilled, where Fr_R and Fr_f are the Froude numbers for the plain river and for the flume, respectively. The approach flow velocity V_{ap} varied from 6.47 cm/s to 10.30 cm/s for the discharge Q from 16.66 l/s to 47.10 l/s.

Table 3.1

Experimental data for open flow conditions

Test N^o	L [cm]	h_f [cm]	V_{ap} [cm/s]	Q [l/s]	Fr_f	Re_c	Re_f
(1)	(2)	(3)	(4)	(5)	(6)	(7)	(8)
L1	350	7	6.47	16.66	0.078	7500	4390
L2	350	7	8.58	22.70	0.103	10010	6060
L3	350	7	10.30	23.60	0.124	12280	7190
L7	350	13	7.51	35.48	0.067	13700	9740
L8	350	13	8.74	41.38	0.076	16010	11395
L9	350	13	9.90	47.10	0.088	14300	14300

To study the local scour process, tests in the conditions of different contraction rates of the flow, grain sizes of bed material, Froude numbers of the open flow, different depths of the floodplain, and steady and unsteady flow conditions were carried out. The time intervals were one 7-h step and two steps, 7 hours each, for the steady and unsteady flow conditions respectively. The tests were carried out with one floodplain model and one side contraction of the flow.

Table 3.2 presents flow parameters during tests for steady flow conditions. The flume width was 350cm and the bridge model opening was 80cm. The grain sizes d_i were 0.24 and 0.67 mm. For steady flow tests, the flow contraction rate Q/Q_b (where Q is the discharge and

Q_b is discharge through the bridge opening under open-flow conditions) varied, respectively, from 3.66 to 3.87 for the floodplain depth h_f 7 cm, the Froude number Fr varied from 0.078 to 0.124. The local velocity V_l varied from 35.0 cm/s to 45.2 cm/s and the backwater value Δh from 1.19 cm to 2.35 cm respectively. The sand-bed tests were carried out under clear water conditions. The tests in the flume lasted for 7 hours (t).

Table 3.2

Experimental data for steady flow conditions

Test N^o	hf [cm]	Q [l/s]	Q/Q_b	V_l [cm/s]	Fr	t [hours]	d_i [mm]	Δh [cm]
(1)	(2)	(3)	(4)	(5)	(6)	(7)	(8)	(9)
AL 4	7	16.66	3.66	35.0	0.078	7	0.24	1.19
AL 5	7	22.7	3.87	39.0	0.103	7	0.24	1.8
AL 6	7	23.6	3.77	45.2	0.124	7	0.24	2.35
AL 16	7	16.66	3.66	35.0	0.078	7	0.67	1.19
AL 17	7	22.7	3.87	39.0	0.103	7	0.67	1.8
AL 18	7	23.6	3.77	45.2	0.124	7	0.67	2.35

Unsteady flow tests were performed with the flow parameters presented in Table 3.3. Two stages of the hydrograph were modelled with the depth of flow h_f 7 cm and 13 cm, and different discharges Q [l/s] at both stages. For example, at the test TL1 the discharges were 16.66 l/s and 35.48 l/s for the first and second stage respectively.

Table 3.3

Experimental data for unsteady flow tests

Test N^o	hf [cm]	Q [l/s]	Q/Q_b	V_l [cm/s]	t [hours]	d_i [mm]	Δh [cm]
(1)	(2)	(3)	(4)	(5)	(6)	(7)	(8)
TL1	7	16.66	3.66	35.0	14	0.24	1.19
	13	35.48	4.05	33.6			1.42
TL2	7	22.7	3.87	39.0	14	0.24	1.8
	13	41.38	3.99	38.3			1.8
TL3	7	23.6	3.77	45.2	14	0.24	2.35
	13	47.1	4.05	49.15			2.7
TL4	7	16.6	3.66	35.0	14	0.64	1.19
	13	35.48	4.05	33.6			1.42
TL5	7	22.7	3.87	39.0	14	0.64	1.8
	13	41.38	3.99	38.3			1.8
TL6	7	23.6	3.78	45.2	14	0.64	2.35
	13	47.1	4.05	49.15			2.7

Duration t was 7 hours at each stage or 14 hours for whole test. From test to test the discharge at the first and second stage of the hydrograph increased, as well as the Froude number of the

flow at open flow conditions, the local Froude number and the densimetric Froude number increased. The grain sizes d_i were 0.24 or 0.67 mm for both stages of the tests. The contraction rate Q/Q_b, the local velocity V_l and the backwater value Δh were calculated for each step of the test.

The test results were compared with those calculated by the method proposed.

3.1 Comparison of test and calculated results of scour at steady flow conditions

At steady flow conditions scour, local and critical velocities change in time are presented in Fig.3.1. According to the test results and the method presented in Chapter 3, the scour is developing rapidly at the initial stage of scour and the rate of the development in time is gradually reducing. For long test periods the depth of scour is going to reach the equilibrium stage. The local velocity is reducing in time because of the scour hole developed, while the critical velocity is increasing in time because of dependence on the floodplain depth and the grain size diameter. The scour stops, when the local velocity becomes equal to the critical one. According to the method, for this and further calculation of the critical velocity, the coefficient β is applied because of the reduction in critical velocity due to the vortex system.

The calculated and measured values of scour depth and the development of local and critical velocities (Test AL 4, Table 4.2) are presented in Fig.3.1.

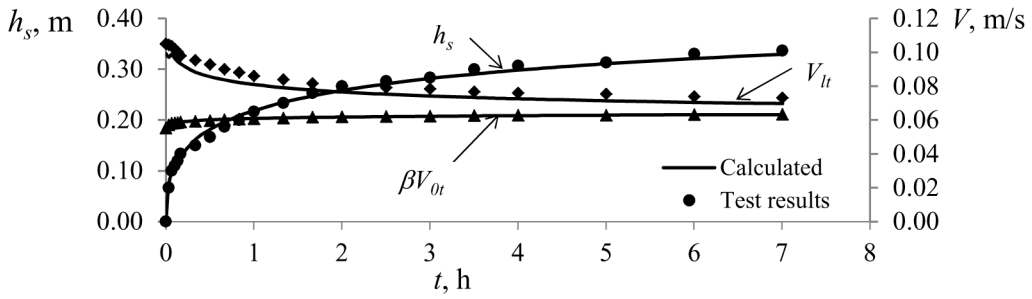

Figure 3.1. Scour depth h_s, local velocity V_{lt} and critical velocity βV_{0t} changes in time at steady flow conditions (test AL4)

The development of the scour-hole width (Eq.1.1) and volume (Eq.1.3) increases together with the increase in its depth. The left and right parts of Fig. (3.2) present the development of

the scour width B and volume w respectively, calculated for Test AL4 at steady flow conditions.

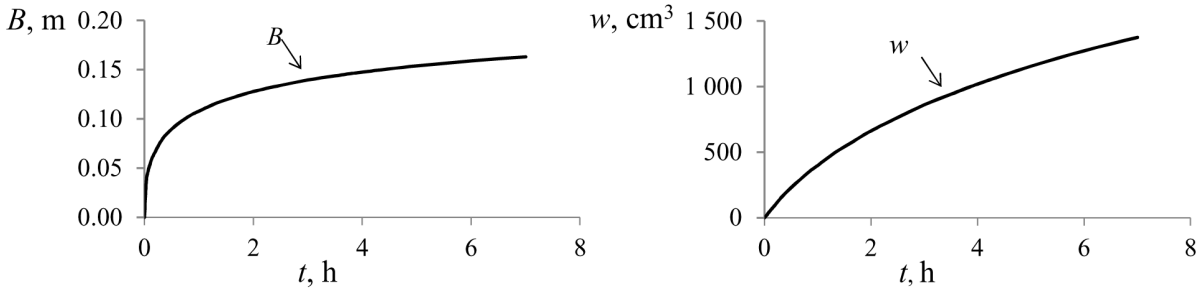

Figure 3.2. Development of the scour hole width B and volume w in time at steady flow conditions (test AL4)

The changes of the relative local velocity V_{lt} / V_l in time are presented in Fig. 3.3. At the same contraction rate of the flow, the local velocity at the initial stage of scour is V_l. During scour process, both the local velocity V_{lt} and relative local velocity reduce.

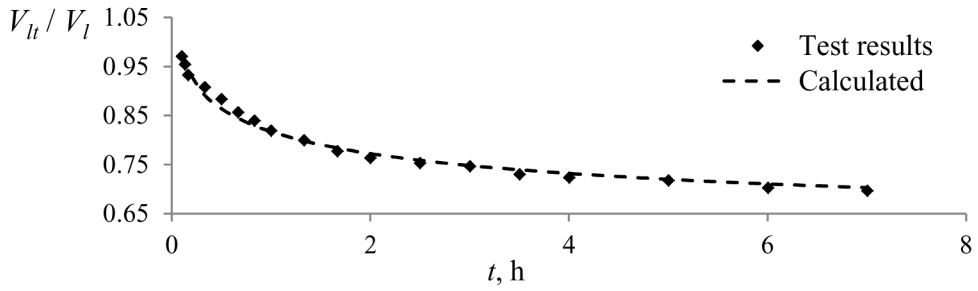

Figure 3.3. Relative local velocity V_{lt} / V_l changes in time at steady flow conditions

The changes in time under steady flow conditions for the relative critical velocity V_{0t} / V_0 are presented in Fig. 3.4. At the initial stage of scour at the floodplain depth h_f and grain size d_{50} the critical velocity is equal to V_0 (Eq.1.9). The critical velocity at any depth of scour V_{0t} (Eq.1.14) increase due to the increase in the depth of scour h_s, therefore the relative critical velocity V_{0t} / V_0 also increase.

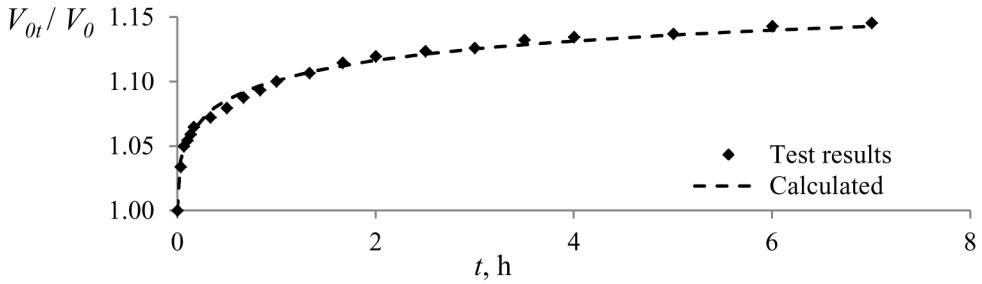

Figure 3.4. Changes of relative critical velocity in time at steady flow conditions

Using the test results, the scour development cases with different flow rates were compared. Fig. 3.5 shows a comparison of scour development during tests AL16, AL17 and AL18. In all of those tests, the geometrical characteristic of the channel was equal, h_f was 7cm and ground particle size d_i was 0.67mm. The flow rate was different in the tests, therefore the calculated maximum backwater value Δh and flow contraction rate Q/Q_b also differed (Table 3.2)

As can be seen from Fig. 3.5, the scour develops more intensively and the scour depth has a higher value during test AL18 with the highest discharge.

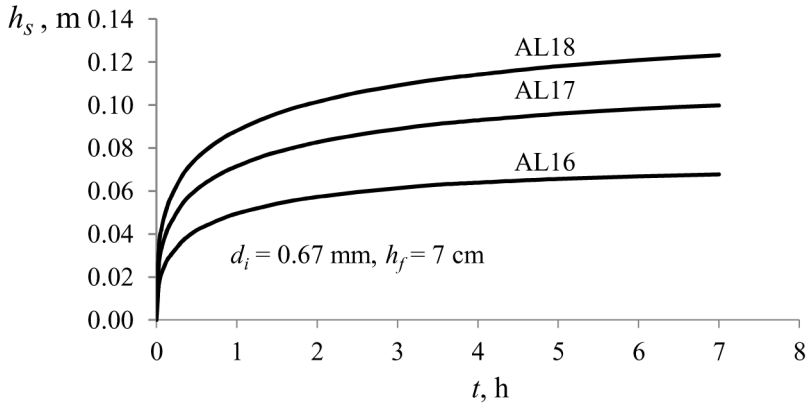

Figure 3.5. Scour development during tests with different discharge under steady flow conditions

Based on the conformity of the test results compared to the calculated ones, the modeling of further scour development for tests AL4 and AL16 was made to find results for a discharge time equal to 14, 21 or 28 hours. The difference in tests AL4 and AL16 is the grain size used for bed material. Grains with a size of 0.24mm and 0.67mm were used for tests AL4 and AL16 respectively. Fig.3.6 shows the results achieved for test AL4 when the discharge time from 7 hours was prolonged to 14 hours, 21 hour and 28 hours. The modeling results show

the increase of scour depth due to the increase of the discharge duration. The reduction of scour development intensity by each following time step also is shown.

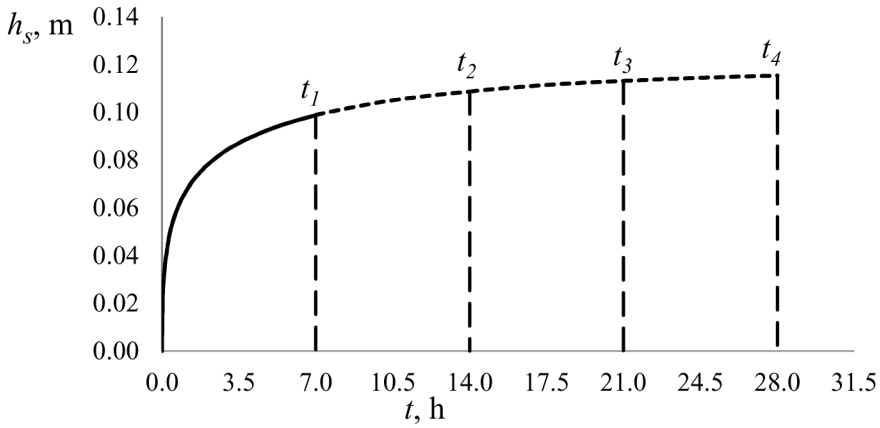

Figure 3.6. Test AL4 with modelled increased duration at steady flow conditions

In addition, for test AL 16 scour depth increases if the duration of flow impact is prolonged (Fig. 3.7), however the intensity of scour development is not as high as for test AL 4 and the scour stops at time t_2, because a greater grain size was used in test AL 16 and because of the lack of flow power to remove sediments from the scour hole.

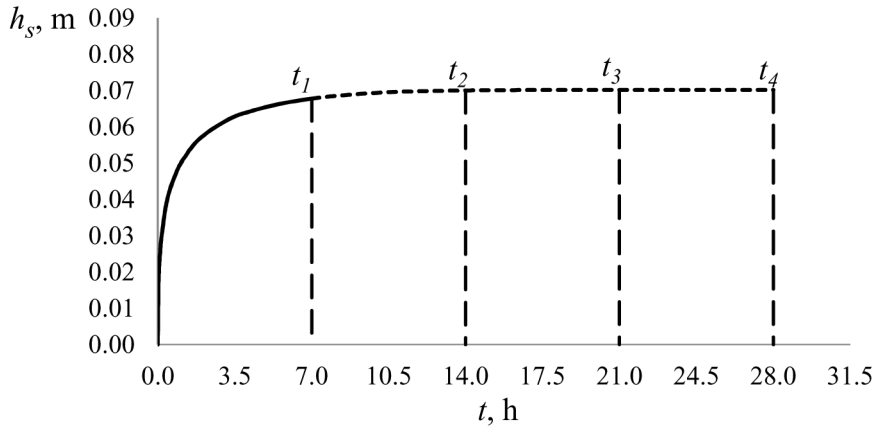

Figure 3.7. Test AL16 with modelled increased duration under steady flow conditions

The test results and those achieved by calculation were in good agreement. As can be seen from the figures presented, the main facts are observed, i.e. a higher scour depth is reached due to a higher discharge, with less sediment size and by longer flow impact. At the same time the results showed changes in critical and local velocities and relative depth of scour in time therefore it can be confirmed that the local scour process at the foundations of engineering structures is connected to continuous changes of the flow and river bed parameters.

Figures (3.1 –3.7) describe the changes of important parameters: h_s, V_{lt}, V_{0t}, V_{lt} / V_l and V_{0t} / V_0 used for scour depth calculation at steady flow conditions. However, in nature, a flood is in the form of a hydrograph, therefore, it is more important to study the scour process under unsteady flow conditions.

3.2 Comparison of test and calculated results of scour at unsteady flow conditions.

The results for a two stage hydrograph at unsteady flow conditions are presented. A comparison of experimental results and data calculated by applying the presented in Chapter 3 method was made. In Figs. (3.8 – 3.12) scour depth, width and volume, as well as local and critical velocities changes in time are presented. The dependence of the changes of the relative depth of scour h_s/h_f in time on the ratios $\beta V_{0t}/V_{lt}$, V_{lt}/V_l and V_{0t}/V_0 are presented.

For unsteady flow conditions the depth, width and volume of the scour hole at the initial stage- during the first step develops similarly as under steady flow conditions. However, when the discharge increases for the next step of unsteady flow, the intensity of the scour development also increases (Fig. 3.8).

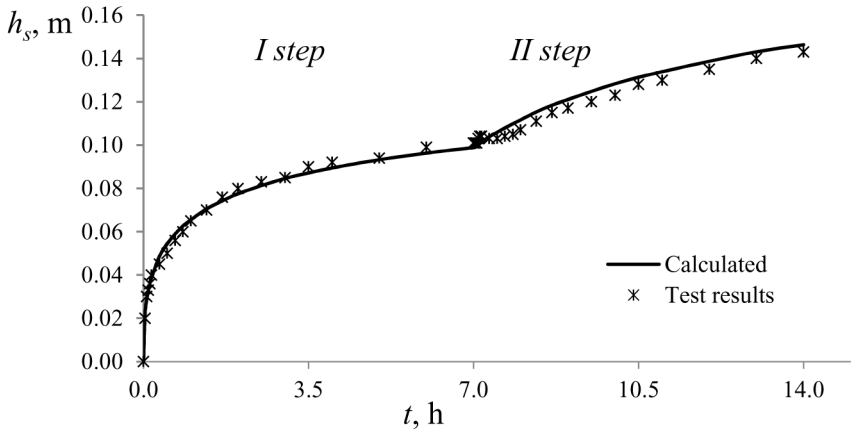

Figure 3.8. Scour development in time during unsteady flow conditions (test TL1)

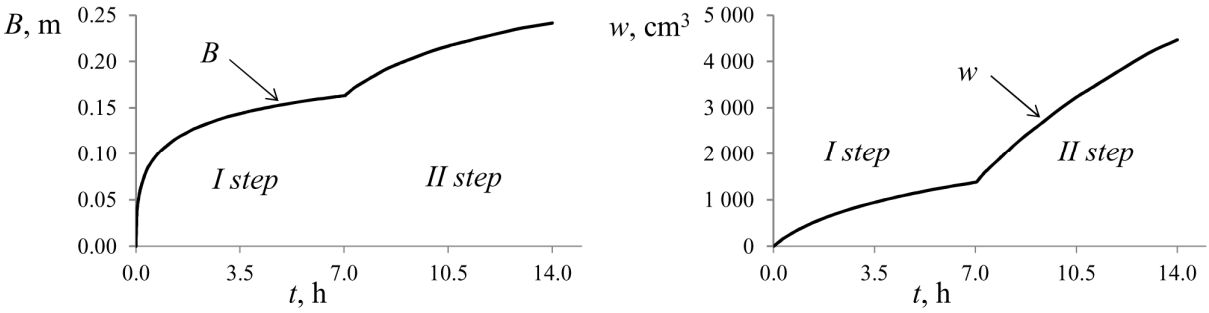

Figure 3.9. Development of the scour-hole width *B* and volume *w* in time at unsteady flow conditions (test TL1)

The development of the scour-hole width (Eq. 1.1) and volume (Eq. 1.3) was calculated and is presented in Fig. 3.9. The left and right parts show the development of scour width *B* and volume *w* respectively, calculated for test TL1 at unsteady flow conditions.

The local velocity V_{lt} gradually reduce in time at the first step because of the scour hole developed (Fig. 3.10). At the beginning of the second step the local velocity increases, because of the higher discharge value used for the second step, but also it takes into account the influence of the scour hole formed in the first step. During the second step the local velocity reduces again because of the scour hole formed in this period.

At the same time the critical velocity V_{0t} tends to increase during scour development at unsteady flow conditions. The critical velocity gradually increases in the first or second step because of the increased depth of scour. At the beginning of the second step the critical velocity rises rapidly because of the rapid increase of the depth on the floodplain and the scour depth developed in the previous step (Fig. 3.10).

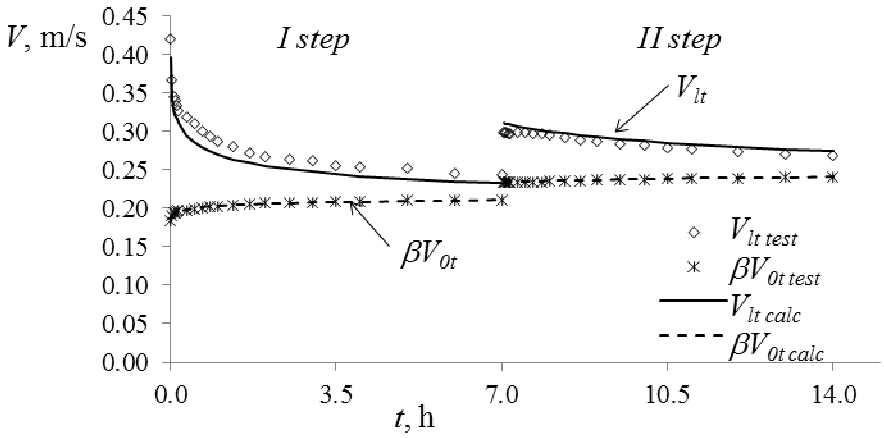

Figure 3.10. Local and critical velocities changes in time at unsteady flow conditions

As can be seen in Fig. (3.10), the values of the local and critical velocities tend to approach one other. The intensity of scour development is higher for the higher ratio between local and critical velocities. By using formulas for local velocity (Eq.1.12) and critical velocity (Eq.1.14), the calculation can be made and the new understanding of the scour process for unsteady flow conditions can be explained. For local velocity development in time at unsteady flow conditions, there are two simultaneous processes during the scour. On one hand, the local velocity V_{lt} is reducing because of the scour hole developed, but on the other hand it is increasing because of the increasing discharge during floods. The critical velocity is increasing because of increase of the depth of scour and the increasing discharge during floods.

The relative local velocity V_{lt}/V_l is reducing with the development of scour hole (Fig 3.11). The rapid increase at the beginning of the second step is based on the rising of the discharge for the second step. The relative velocity at the beginning of the second step is less than at the beginning of the first one, but it is higher at the end of the second step than at the end of the first one.

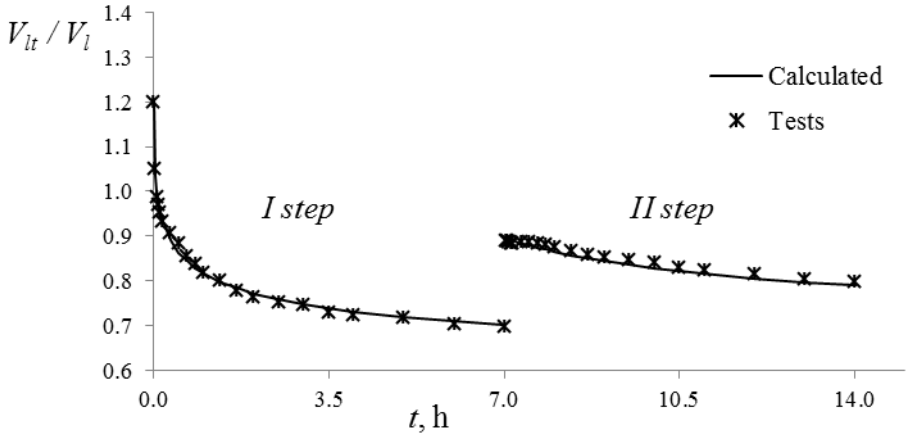

Figure 3.11. Relative local velocity V_{lt}/V_l changes in time at unsteady flow conditions

The relative critical velocity V_{0t}/V_0 is increasing in time (Fig. 3.12). At the beginning of the second step it is rapidly reducing because of the sharp rise of the value of critical velocity V_0 calculated for the second step, and is further increasing. The critical velocity at the beginning of the second step is higher than at the beginning of the first one, and it is less at the end of the second step than at the end of the first one.

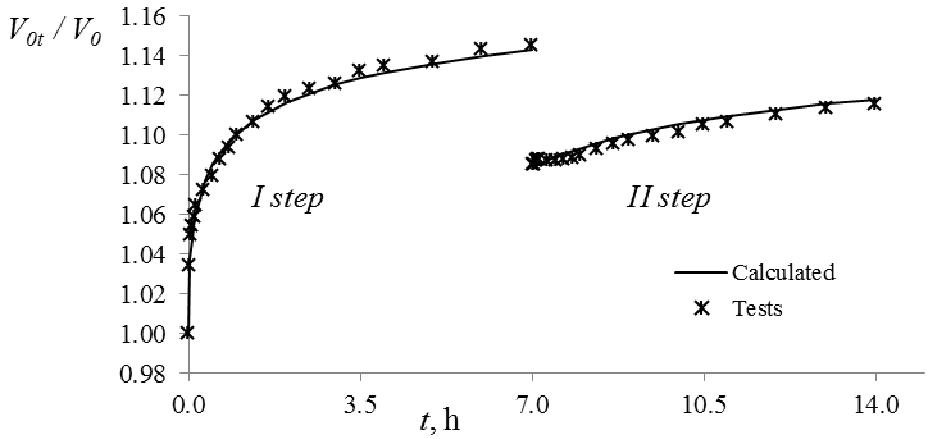

Figure 3.12. Relative critical velocity V_{0t}/V_0 changes in time at unsteady flow conditions

The ratio between critical velocity βV_{0t} and local velocity V_{lt} is determined by the rate of scour development in time and its value (Fig. 3.13). During the scour process the ratio $\beta V_{0t}/V_{lt}$ increases. At the beginning of the second step, with the increase of the depth of water on the floodplain and discharge of the flow, the ratio $\beta V_{0t}/V_{lt}$ reduces and then increases again. During the scour process the ratio $\beta V_{0t}/V_{lt}$ approaches 1. The scour stops when the critical velocity βV_{0t} becomes equal to the local velocity V_{lt}.

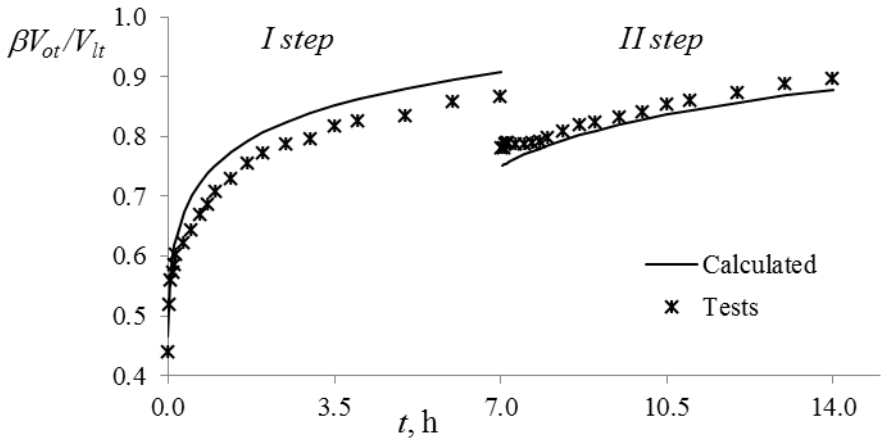

Figure 3.13. Changes of the ratio $\beta V_{0t}/V_{lt}$ in time at unsteady flow conditions

The relative depth (width, volume) of scour gradually increases during the first step, than because of the sharp increase of the floodplain depth it reduces at the beginning of the second step, after that it gradually increases again (Fig. 3.14).

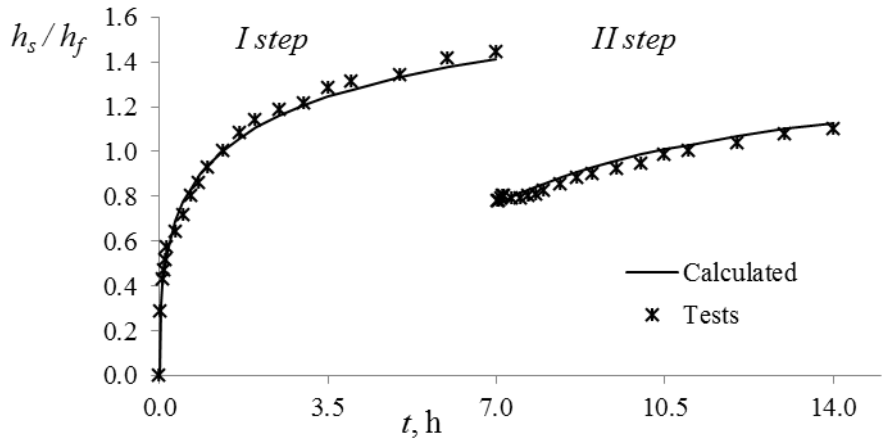

Figure 3.14. Development of the relative depth of scour in time at unsteady flow conditions

The relation between the relative depth of scour and the ratio of the critical and local velocities is presented in Fig. 3.15. Due to the increase of the relative depth of scour, the ratio of critical and local velocities within the step limits is increasing. There is a reduction in both – the relative depth of scour and the ratio of critical and local velocities between steps with different discharge and the depth of water on the floodplain.

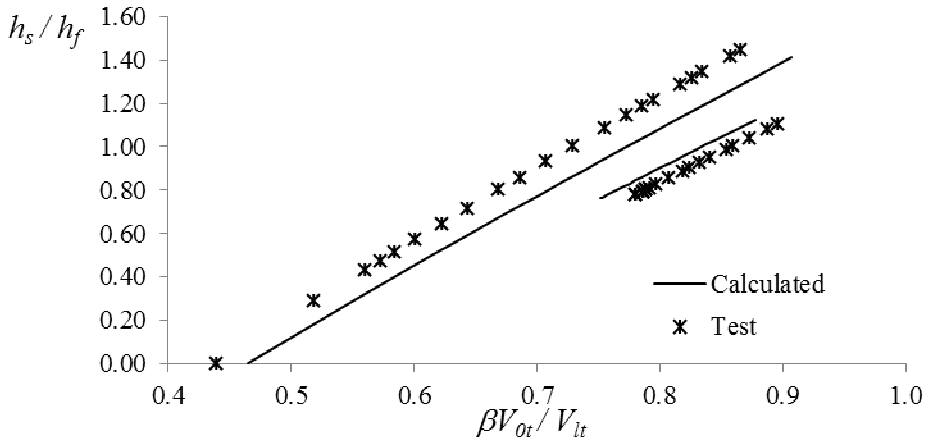

Figure 3.15. Relation of the relative depth of scour h_s/h_f to the ratio of critical and local velocities $\beta V_{0t} / V_{lt}$ at unsteady flow conditions

The value of the relative critical velocity V_{0t}/V_0 increases when there is a reduction in the relative local velocity V_{lt}/V_l (Fig. 3.16). The relation between the values of the relative critical velocity V_{0t}/V_0 and the relative local velocity V_{lt}/V_l is almost the same in both steps.

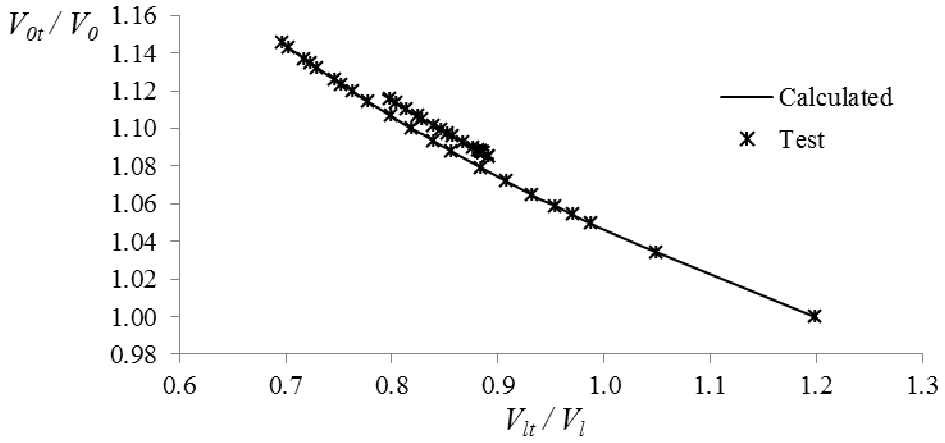

Figure 3.16. Relation of the relative local velocity V_{lt} / V_l and the relative critical velocity V_{0t}/V_0 at unsteady flow conditions

An evaluation of the relative depth of scour under changes of the relative local velocity is presented in Fig. 3.17. The relation between the values of the relative depth of scour h_s/h_f and the relative local velocity V_{lt}/V_l leads to be similar in both steps.

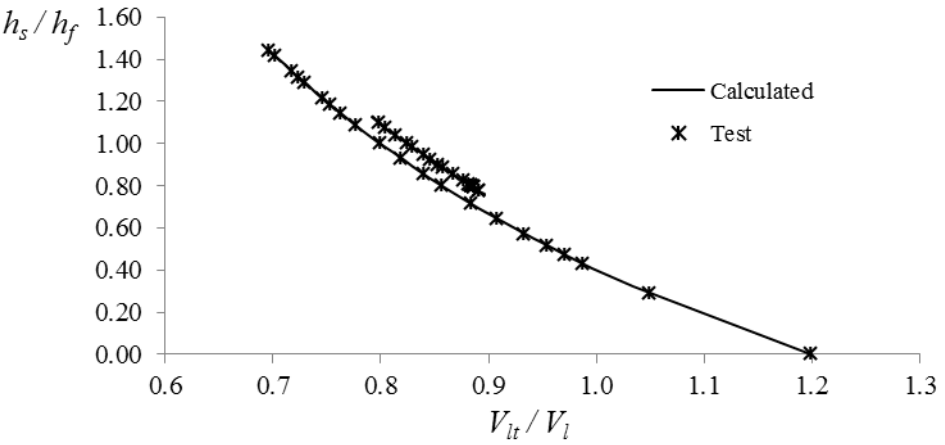

Figure 3.17. Relation between relative depth of scour h_s/h_f and the relative local velocity V_{lt}/V_l at unsteady flow conditions

An evaluation of the relative depth of scour under changes of the relative critical velocity is presented in Fig. 3.18. The relation between the values of the relative depth of scour h_s/h_f and the relative critical velocity V_{0t}/V_0 is practically the same in both steps.

From the Figs. (3.15 - 3.18) it can be concluded that with the increase of the depth of floodplain h_f the relative local velocity V_{lt}/V_l increases, the relative critical velocity V_{0t}/V_0 reduces and also relation between the critical and local velocities $\beta V_{0t}/V_{lt}$ reduces.

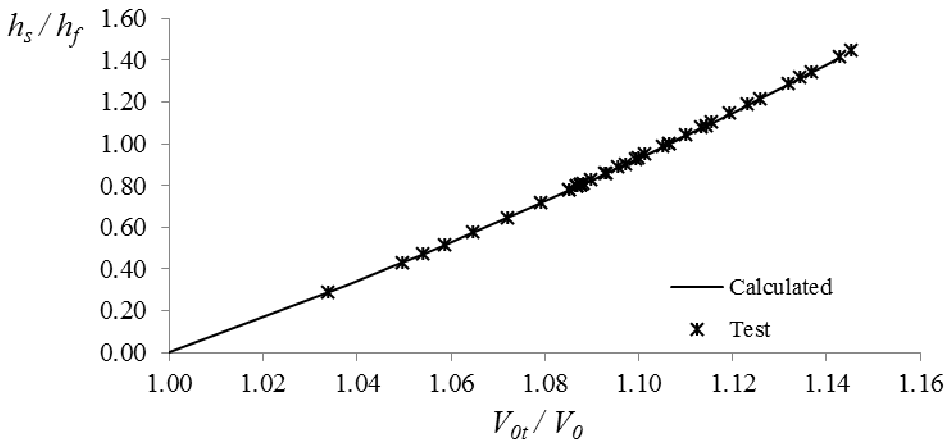

Figure 3.18. Relation between relative depth of scour h_s/h_f and the relative critical velocity V_{0t}/V_0 at unsteady flow conditions

With the increase of the scour depth h_s the relative local velocity V_{lt}/V_l reduces, the relative critical velocity V_{0t}/V_0 increases and also relation between the critical and local velocities $\beta V_{0t}/V_{lt}$ increases. With the increase in the local velocity V_l the relative critical velocity V_{0t}/V_0 increases, as well as the relative local velocity V_{lt}/V_l increases by rising of the critical velocity V_0. It indicates that both the local and critical velocity changes have simultaneous impacts- the floodplain depth and scour depth changes. The local velocity increases with a higher floodplain depth but decreases because of the developed scour depth. The critical velocity increases with the increase in both the floodplain depth and the scour depth.

3.3 Influence of the local, critical and approach velocities on the scour depth

With the development of scour in time, under steady flow conditions, the local velocity reduces and the critical one increases. Velocities become more equal with the increase in depths of scour (Figs. 3.1, 3.3, 3.4). With the increase of relative depth of scour h_s / h_f at uniform sand bed, the ratio of critical to local velocity $\beta V_{0t} / V_{lt}$ increases and approaches one, when the scour stops (Fig. 3.19).

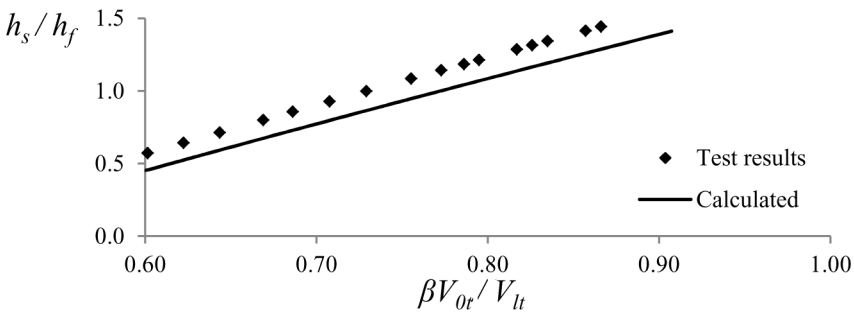

Figure 3.19. Relative depth of scour h_s/h_f development in time versus relative critical velocity $\beta V_{0t}/V_{lt}$ in one uniform sand bed layer at steady flow (Test AL 4)

The ratio V_l / V_{ap} (local to approach velocity) is dependent on the Froude number of the flow (Fig. 3.20). With an increased Froude number, the difference between local and approach velocity of the flow is decreasing.

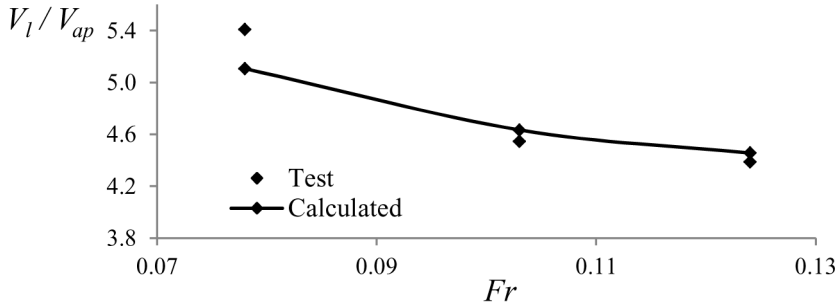

Figure 3.20. Ratio of the local to approach flow velocity V_l/V_{ap} versus Froude number (Tests AL 4,5,6)

The ratio V_l / V_{ap} (local to approach velocity) is dependent on the contraction rate of the flow (Fig. 3.21). With an increased contraction rate, the difference between local and approach velocity of the flow increases.

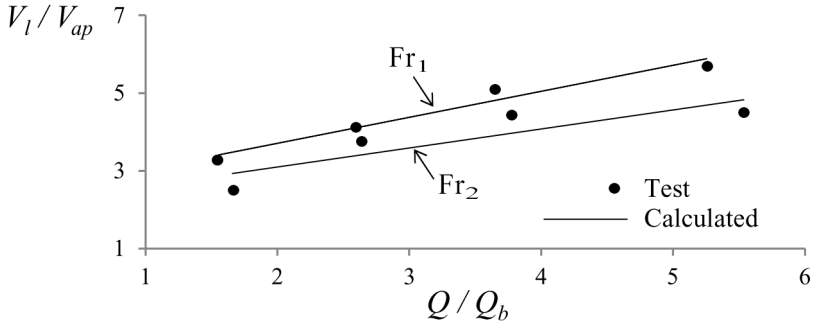

Figure 3.21. Ratio of the local to approach flow velocity versus contraction rate of the flow

The difference in local velocity at any depth of scour V_{lt} and approach flow velocity V_{ap} changes during scour (Fig. 3.22). The ratio of velocities is higher at the start of the scour

process and gradually reduces because of reduced local velocity due to the scour hole developed in time.

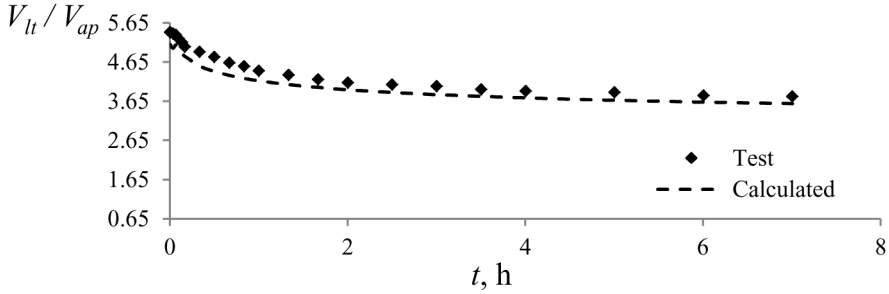

Figure 3.22. Changes of the ratio of the local velocity at any depth of scour V_{lt} to the approach flow velocity V_{ap} at steady flow conditions (test AL4)

The research on the test results described in this chapter confirmed the influence of the local velocity on the local scour evolution at the structures, but not approach flow velocity as it is accepted now by different authors.

At steady flow conditions, when scour is developing in time, the local velocity reduces and the critical velocity increases due to the scour hole developed. The scour stops when the local velocity becomes equal to a critical one.

For local velocity development in time at unsteady flow conditions, there are two simultaneous processes during the scour. On one hand, the local velocity V_{lt} is reducing because of the scour hole developed, but on the other hand it is increasing because of the increasing discharge during floods. The critical velocity is increasing because of the increase of the depth of scour and the increasing discharge during floods.

It was confirmed by test result processing and by the method presented that the scour evolution depends and can be evaluated by the local and critical velocities. As both of them are changing in time because of the scour evolution, also the local to critical velocities ratio to the approach flow velocity is changing.

4 COMPUTER MODELING PROGRAM

Based on the method described in Chapter 3, the computer program was elaborated using Microsoft Excel to calculate and evaluate time dependant scour development at the foundation of engineering structure in river flow during multiple floods with different duration, probability, frequency and sequence. For one flood wave the influence of flood hydrograph steepness on the scour depth was investigated. The program can be divided in to the following parts- initial data field, modeling field, calculation field and output field.

4.1 Description of the computer modelling program

The initial data data should be prepared first to be used for flood hydrograph modeling. The cross section of river flow, floodplain relief, contraction rate of the flow and flow discharge during a flood was assumed and calculated by the formulas described in Chapter 3. Input data for multiple flood modeling are shown in Table 4.1. A flood hydrograph is built step by step using the data in this table. Column No.1 includes flood probability P_n from number 0,33 to number 90,6%.

Table 4.1

Initial data for multiple flood modeling

P_n	N	h_f [m]	Δh [m]	Q/Q_b	Q [m^3/s]
1	2	3	4	5	6
90,60%	1	0,185	0,2172	1,047	510
77,10%	2	0,975	0,1926	1,542	760
63,60%	3	1,720	0,3156	1,865	1440
50,00%	4	2,300	0,4242	2,021	2200
36,50%	5	2,500	0,4646	2,052	2500
23,00%	6	2,700	0,5698	2,112	3000
10,00%	7	2,900	0,6400	2,124	3470
9,50%	8	3,000	0,6636	2,206	3500
5,00%	9	3,250	0,7147	2,177	4065
2,00%	10	3,600	0,8292	2,221	4858
1,00%	11	3,800	0,9002	2,243	5354
0,33%	12	4,000	0,9879	2,392	6208

The second column indicates the number of flood steps. h_f and Q are given for assumed flood discharge, Q_b is the discharge through the bridge opening under open-flow conditions calculated by Eq. (1.22) and maximum backwater Δh is calculated by Eq. (1.6).

The characteristics of river bed material are described in another data-input table belonging to the program. The river bed grain size d_{50} (mm), the specific gravity of the river bed material γ and the thickness of the layer with specified river bed material H_d must be entered in this table (Table 4.2). As mentioned before, a current investigation is being made for a case with a homogenous river bed. However, in further investigation this input field can be enlarged by the possibility to present a river bed with different layers of the river bed material. As only one layer of river bed is used, the value of layer thickness is used as a large number.

Table 4.2

Initial data describing river bed material

River bed material		Layer thickness
d_i [mm]	γ	H_d [m]
0.24	1.60	20
0.50	1.70	20
0.67	1.70	20
1.00	1.80	20

Coefficients k_m, k_s, k_α and β and are written in the data-input field. Coefficient β of the reduction in critical velocity according to the method is 0.8, k_m, k_s, k_α are the coefficients depending on the side-wall slope [121], shape and the angle of flow crossing [94] of the foundation of water engineering structure and are equal to 1 in this research.

Flood modeling field

Using the data from the flow data input table (Table 4.1) the flood hydrograph or multiple flood hydrographs are built in the flood modeling field. As it follows from the method, the flood hydrograph was divided into time steps- this is a field where time steps are inputted and the duration of each separate time step indicated. The calculation program allows adding information up to 4-5 flood hydrographs (65 input lines), depending on the step number chosen for each hydrograph. A sample of input data for one triangle-shaped flood hydrograph is shown in Table 4.3. According to the entered number in column N^{o}2, columns N^{o}3-N^{o}6 are filled from the data shown in Table 4.1. Column N^{o}7 allows us to input the time

of each flood step, it can be changed to model flood hydrographs with a different duration. Hydrograph steepness can be changed using column N°7 by changing the ratio between the time of the hydrograph steps in the rising part and recession part of the hydrograph.

Table 4.3

Flood hydrograph (-s) modeling field, sample for one flood of 7 day duration

Step N^0	N	h_f [m]	Q/Q_b	Δh [m]	Q [m^3/s]	t_{step} [h]
1	2	3	4	5	6	7
1	1	0.185	1.047	0.2172	510	10.5
2	2	0.975	1.542	0.1926	760	10.5
3	3	1.720	1.865	0.3156	1440	10.5
4	5	2.500	2.052	0.4646	2500	10.5
5	7	2.900	2.124	0.6400	3470	10.5
6	9	3.250	2.177	0.7147	4065	10.5
7	7	2.900	2.124	0.6400	3470	21
8	5	2.500	2.052	0.4646	2500	21
9	3	1.720	1.865	0.3156	1440	21
10	2	0.975	1.542	0.1926	760	21
11	1	0.185	1.047	0.2172	510	21
						168 h total, or 7 days

Table 4.3 presents data for one flood of 7 days duration and includes 11 steps of hydrograph. Steps N^{0}1 – 5 are chosen for the rising limb of hydrograph, steps N^{0}7 – 11 for the recession limb of hydrograph. Step N^{0}6 indicates a peak discharge of flood. The time of the step of peak discharge was chosen equal to the time of step in the hydrograph rising limb. The time of the peak discharge step is divided in two parts according to the ratio of hydrograph steepness when time of the rising and recession parts must be defined. If the ratio of the rising and recession parts of hydrograph is 1:2, then 1/3 of the peak discharge time is concerned to the rising and 2/3 to the recession time of hydrograph. For the sample in Table 4.3 the rising time is 5x10.5h plus 1/3 of the time of the step N^{0}6 or 3.5h so the time of rising part is 56h. The recession time is 5x21h plus 2/3 of the time the step N^{0}6 or 7h so the time of recession time is 112h, and the ratio of the rising and recession parts is equal to 1:2.

The multiple flood models were created by repeating the input of the initial data of hydrograph steps for forthcoming floods.

Calculation field

By using data inputted and prepared for use in the calculation method described, the program works out the calculation of scour depth for each time step and in the frame of time step for each time interval.

	A	B	C	D	E	F	G	M	N	O	P	Q	R	S	T
1		Nr.	ti	di	Yi	V_o (m/s)	V_l (m/s)	h_s	h_s	B	W	V_{lt}	V_{0t}	$ßV_0/V_l$	$ßV_{0t}/V_{lt}$
2		0	0	0.0067	1.70	0.6755	1.69	0.00	0.0000	0.0000	0.0000	1.783	0.675	0.3197	0.3030
3		1	0.0018	0.0067	1.70	0.6755	1.69	0.22	0.2207	0.3099	0.0111	1.117	0.759	0.3197	0.54379
4		2	0.0018	0.0067	1.70	0.6755	1.69	0.25	0.2537	0.3561	0.0168	1.058	0.770	0.3197	0.5819
5		3	0.0035	0.0067	1.70	0.6755	1.69	0.29	0.2945	0.4135	0.0264	0.993	0.782	0.3197	0.6300
6		4	0.0035	0.0067	1.70	0.6755	1.69	0.32	0.3202	0.4495	0.0339	0.956	0.789	0.3197	0.6606
7		5	0.0035	0.0067	1.70	0.6755	1.69	0.34	0.3395	0.4765	0.0404	0.930	0.795	0.3197	0.6837
8		6	0.0069	0.0067	1.70	0.6755	1.69	0.37	0.3685	0.5173	0.0516	0.893	0.803	0.3197	0.7189
9		7	0.0069	0.0067	1.70	0.6755	1.69	0.39	0.3880	0.5447	0.0603	0.871	0.808	0.3197	0.7427
10		8	0.0069	0.0067	1.70	0.6755	1.69	0.41	0.4055	0.5692	0.0688	0.851	0.813	0.3197	0.7641
11		9	0.0069	0.0067	1.70	0.6755	1.69	0.42	0.4179	0.5866	0.0753	0.838	0.816	0.3197	0.7794
12	1	10	0.0104	0.0067	1.70	0.6755	1.69	0.43	0.4348	0.6103	0.0848	0.820	0.820	0.3197	0.8003
13		11	0.0104	0.0067	1.70	0.6755	1.69	0.45	0.4486	0.6297	0.0931	0.806	0.824	0.3197	0.8175
14		12	0.0104	0.0067	1.70	0.6755	1.69	0.46	0.4592	0.6446	0.0999	0.796	0.826	0.3197	0.8308
15		13	0.0104	0.0067	1.70	0.6755	1.69	0.47	0.4690	0.6583	0.1064	0.787	0.829	0.3197	0.8431
16		14	0.0208	0.0067	1.70	0.6755	1.69	0.49	0.4857	0.6819	0.1182	0.771	0.833	0.3197	0.8642
17		15	0.0208	0.0067	1.70	0.6755	1.69	0.50	0.4979	0.6989	0.1273	0.760	0.836	0.3197	0.8796
18		16	0.0208	0.0067	1.70	0.6755	1.69	0.51	0.5086	0.7140	0.1358	0.751	0.839	0.3197	0.8932
19		17	0.0208	0.0067	1.70	0.6755	1.69	0.52	0.5181	0.7273	0.1435	0.743	0.841	0.3197	0.9052
20		18	0.0208	0.0067	1.70	0.6755	1.69	0.52	0.5247	0.7366	0.1490	0.738	0.842	0.3197	0.9137
21		19	0.0208	0.0067	1.70	0.6755	1.69	0.53	0.5307	0.7450	0.1542	0.733	0.844	0.3197	0.9214
22		20	0.0418	0.0067	1.70	0.6755	1.69	0.54	0.5417	0.7604	0.1640	0.724	0.846	0.3197	0.9354

Figure 4.1 Fragment of calculation table

Fig.(4.1) presents part of a calculation table for one hydrograph time step divided into twenty time intervals. The following variables are calculated by the equations described in Chapter 3:

V_0 - critical velocity (Eq. 1.9),
V_l - local velocity (Eq. 1.5),
A_i - parameter in the Levi (1965) [116] formula (Eq. 1.16),
m - steepness of scour hole (Fig. 2.1),
B - width of scour hole, equal to mh_s (Eq. 1.3),
D_i, N_i and x_i - intermediate variables (Eqs. 1.18, 1.20).

Graphs of modelling results

Basically the program provides hydrograph, scour evolution and velocity graphs, however, graphs which describe velocity changes versus flow contraction rate can also be acquired as well as graphical descriptions of other factors which affect or interact during scour development in time.

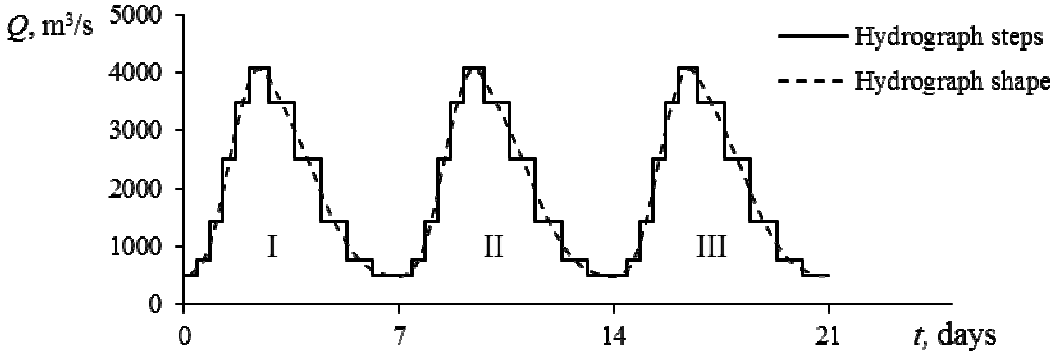

Figure 4.2 Multiple flood hydrograph, I, II and III are numbers of flood

Three flood hydrographs with equal probability are shown in Fig. 4.2. They are not separated in this graph. That is because there is no water on the floodplain during the low-water period and any significant changes of scour hole geometry happen. As it was found from further research, scour development stops short after achieving flood peak discharge, at the beginning of the flood hydrograph recession part. The removal of sediments from the scour hole returns only, when the local velocity of the next flood exceeds the critical velocity.

Each flood in this sample has duration of 7 days, a similar peak discharge and distribution to time steps. Using an input field of flood hydrograph those parameters can be changed to simulate floods with a different duration, probability, frequency and sequence. The graph presented in Fig. 4.2 shows the main parameters of the hydrograph input table – discharge and duration of each time step (continuous line). The dashed line indicates the average form of the hydrograph.

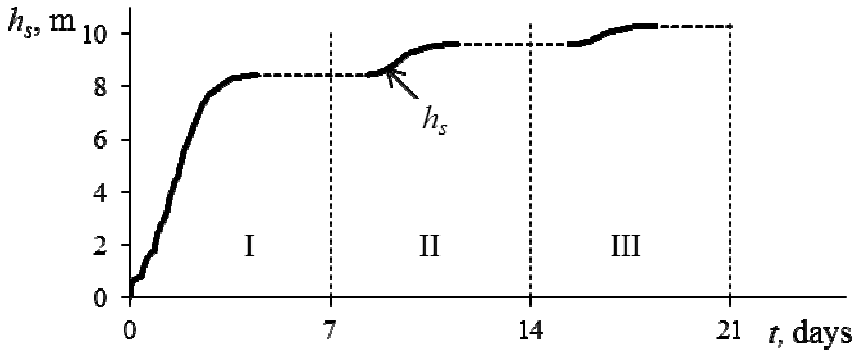

Figure 4.3 Results of the scour evolution during three floods

A graph of time dependant scour development according to the sample of multiple flood model is presented in Fig. 4.3. The bold continuous line represents the time and the development of scouring; the dashed line appears when scour does not proceed because local velocity becomes less than critical velocity. The changes of local and critical velocities during

multiple floods are printed in the velocity graph (Fig. 4.4). Scour develops when local velocity exceeds the value of the critical one multiplied by reduction coefficient β.

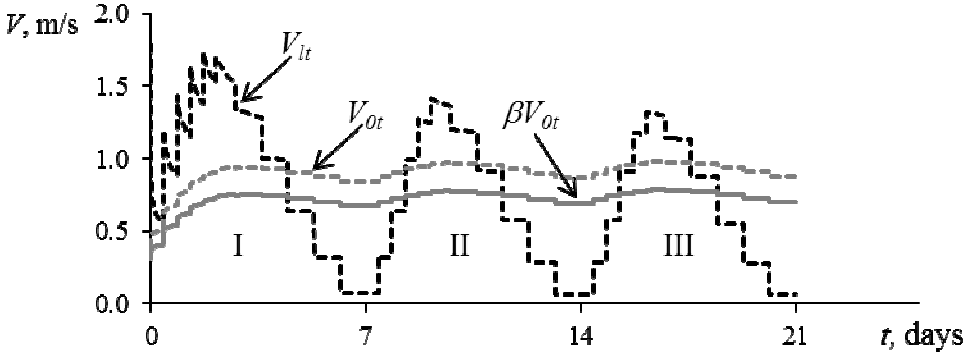

Figure 4.4 Output of local (V_{lt}) and critical (V_{0t} and βV_{0t}) velocities

For a better description of flood and scour development interaction, joined graphs can be used. Figure 4.5 presents a joined graph of velocities and scour development while Fig. 4.6 presents a joined graph of flood hydrograph and scour development.

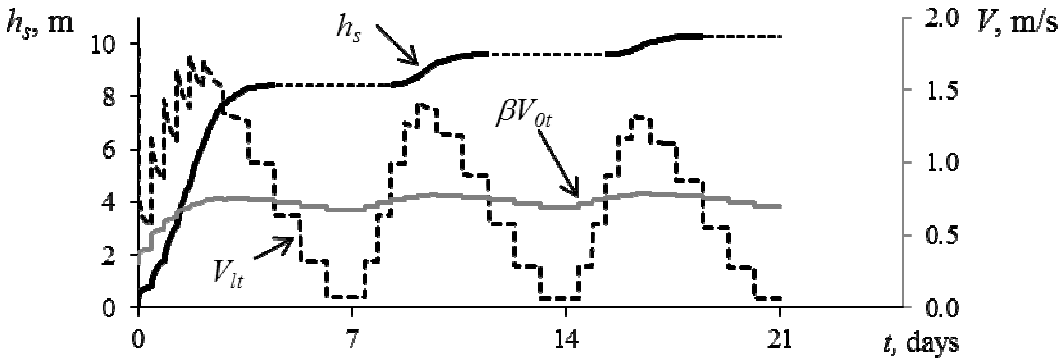

Figure 4.5 Joined graph of local (V_{lt}) and critical (V_{0t}) velocities and scour depth h_s

The joined graph of velocities and scour depth (Fig. 4.5) shows the relationship between the changes in local and critical velocities and scour development. The curve of scour depth moves up only when the curve of local velocity V_{lt} exceeds one of critical velocity V_{0t} multiplied by coefficient β.

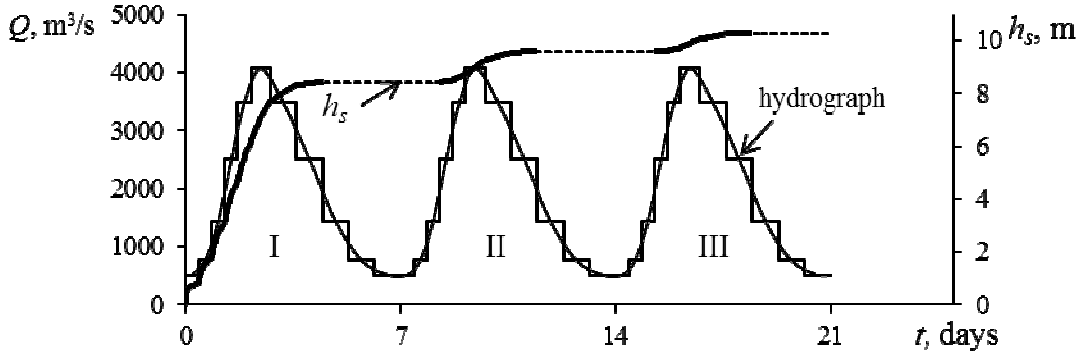

Figure 4.6 Joined graph of flood hydrographs and scour depth

As can be seen from Fig. 4.6, scouring between flood events does not proceed because of the lack of flow power to remove sediments from the scour hole. It confirms the assumption that during the modeling of scour development, the separation of flood hydrographs is not required. This confirms the scour holes developed at the foundations of water engineering structures located in floodplain areas. It must be taken into account that in nature, flow channel geometry can change over time and scour development during forthcoming flood events must be calculated using new input parameters.

4.2 Modeling task

Based on the method described in Chapter 3, a computer modeling of the time-dependent scour during multiple floods with different probability, duration, frequency, and sequence was performed. The impact of flood hydrograph shape was studied and the influence of multiple floods with different probability, duration, frequency and sequence on the scour process was investigated. The triangle-shaped hydrograph was used during the investigations of multiple floods and the hydrograph shape impact on scour development at the foundations of engineering structures located on the floodplain of river flow.

The influence of the hydrograph steepness on scour development in time was investigated. The duration of floods t includes the time t_{rise}, when the flood discharge reaches its peak value, and the time t_{reces}, when the flood discharge decreases down to the low-water level; $t = t_{rise} + t_{reces}$ (Fig. 4.7).

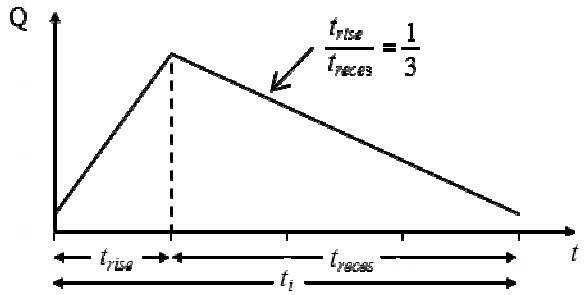

Figure 4.7 Ratio between the time periods of the rising and recession parts of hydrograph is equal to 1/3

The steepness of the rising part of the hydrograph depends on many factors, namely rainfall intensity, relief, soil type, etc. Aforementioned reasons also have an influence on the steepness of the hydrograph recession part. The form of the hydrograph is also characterized by the ratio between the time periods of the rising and recession parts t_{rise} / t_{reces} (Fig. 4.7).

The impact of the floods with different shapes of hydrograph on the scour at engineering structures was studied. The shape of the hydrograph was changed at the time of the rising and recession parts of the flood. Two types of the hydrograph shape were studied. For the first one the discharge and the rising time was the same for all models, however the flood duration was changed by increasing the recession time of the flood. For the second type the flood discharge and duration remain the same, but the steepness of the hydrograph was changed by the ratio between the time of rising and recession parts.

The impact of multiple floods with different duration, probability, frequency and sequence was studied using triangular-shaped hydrographs with a ratio 1:2 between rising and recession parts for all models. A certain time period was assumed, in the example 5 years, and a series of floods were modelled by changing the before mentioned parameters within this period. For each flood the duration t_i and the peak discharge Q_i can be changed, as well as the number of floods during a certain time period. The sample of multiple flood models with three forthcoming floods of similar discharge and duration is presented in Fig. 4.8.

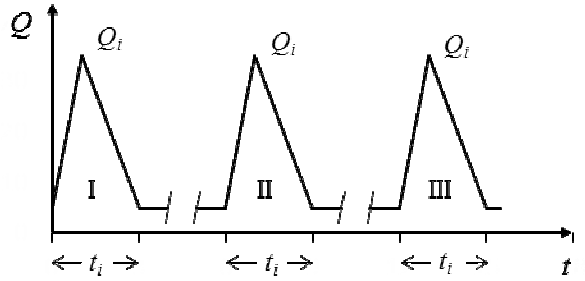

Figure 4.8 Series of three floods of similar probability Q_i and duration t_i

The results of computer modeling as well as conclusions about the impact of the form of flood hydrograph and the impact of multiple floods of different probability, duration, frequency and sequence to the scour development at engineering structures in flow are presented in Chapter 7.

The initial data of each flood model according to which the calculation was made and results are presented in Chapter 7, are shown in Appendix I.

The following conditions are taken into account in this study. Clear-water conditions and alluvial river bed with homogenous river bed material was supposed. Constant cross section of river bed and floodplain between floods was accepted.

5 RESULTS OF COMPUTER MODELING

A computer modeling of the time-dependent scour during single flood with different shape of hydrograph or during multiple floods with different probability, duration, frequency, and sequence was performed. The patterns of the scour development in time in all modeling results are similar, namely the rapid development at the start of the scour process and gradual reduction with time was observed.

According to the method described in Chapter 3, scour stops when the local velocity V_{lt} becomes less than the critical velocity βV_{0t}. The scour process usually stops just after the peak of the flood, therefore the scour development time t_s, when the maximum depth is reached, is less than the duration of the flood t_i (Fig. 5.1).

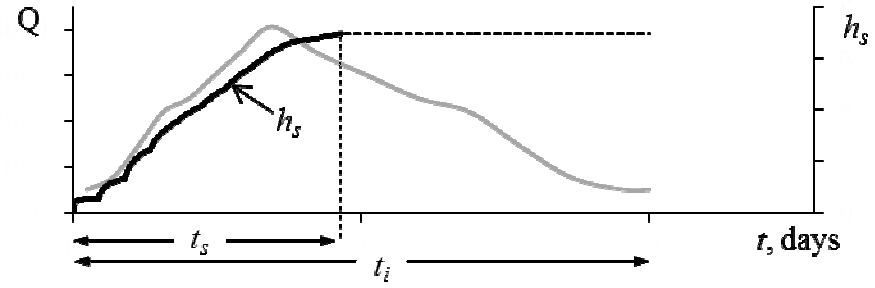

Figure 5.1 Scour development in time. Comparison between the flood duration t_i and scour development time t_s when the maximum scour depth is reached during a current flood event [43]

5.1 The influence of the steepness of flood hydrograph

A computer modeling of the time-dependent scour during floods with different shapes of hydrograph was performed. The shape of the hydrograph was changed by time of the rising and recession parts of the flood. Two types of the hydrograph shape were studied.

For the first type of hydrograph, the rising time of the flood has the same value, but the flood duration t_i was different because of the increase of recession time. The ratios between the time of rising and recession parts of the hydrograph were: 1:2, 1:3, 1:4, 1:6 and 1:8 (Fig. 5.2).

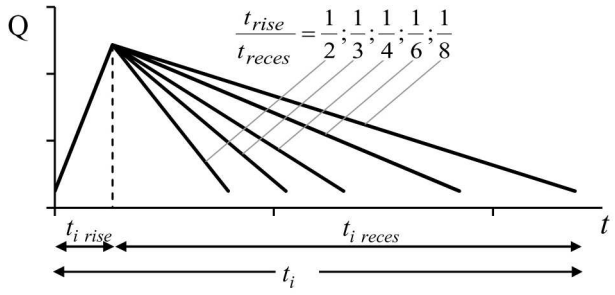

Figure 5.2 Hydrographs with constant time of rising part of the flood

The sediment size of 0.67mm was used for this model. Rising time t_{rise} was equal to 24h for each model and recession time t_{reces} increased according to the ratio t_{rise} / t_{reces}. The scour depth achieved during each flood model is presented in Table 7.1 and Fig. 5.3. The flow parameters used for flood time steps are presented in the Appendix I, Chapter 7.9 (Table A1.12 and A1.13).

Table 5.1

Flood duration and scour depth according to the ratio of rising and recession time if t_{rise} is constant

t_{rise} / t_{reces}	t_{rise} [h]	t_{reces} [h]	t_i [h]	h_s [m]
1 / 2	*24*	48	72	6.88
1 / 3	*24*	72	96	7.22
1 / 4	*24*	96	120	7.50
1 / 6	*24*	144	168	7.95
1 / 8	*24*	192	216	8.30

The higher the recession time of floods, the greater their duration, and the greater the scour depth (Fig. 5.3).

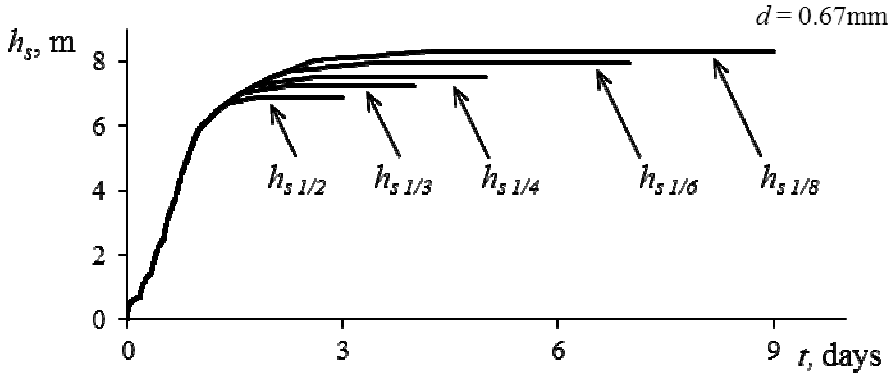

Figure 5.3 Scour development with time for triangle-shaped hydrographs at constant time of the rising part

However it must be taken into account that the regular triangle-shaped hydrograph was used in the model. In nature the reduction of flow discharge during floods varies and is not regular.

It was found that even during the reduction of flood discharge the removal of sediments from scour-hole continued, but only while the local velocity is higher than critical velocity multiplied by reduction coefficient.

For the second type (Fig. 5.4), the duration of the flood was the same.

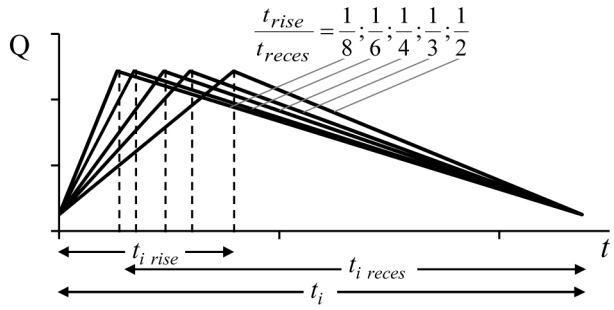

Figure 5.4 Hydrographs with equal duration, but different time ratio between the rising and recession parts of the flood

The time of the rising and recession parts of the flood had different ratios, for example, 1:2, 1:3, 1:4, 1:6, and 1:8, where the first and second numbers are the rising and recession time periods of the flood. It was found that the influence of its shape on the scour depth h_s was small, but the scour process was different at the initial stage (Fig. 5.5). After an equal period of time t_i at the beginning of the flood, the depth of scour was not the same for different hydrograph shapes (Table 5.2). The shorter the time of the rising part of the floods, the greater the depth of scour. According to the calculation results, the maximum scour depth develops more intensively during the floods with a higher slope of the rising limb of hydrograph.

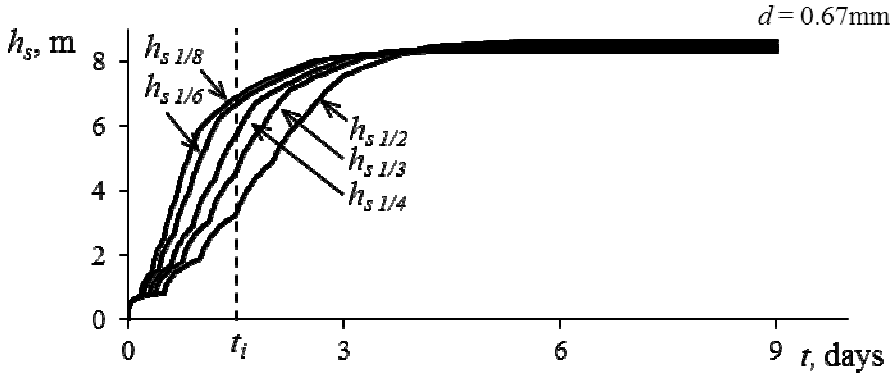

Figure 5.5. Scour development for floods with an equal duration and a different ratio between the rising and recession parts of hydrograph

Table 5.2

Scour hole depth after t_i = 1.5 days of floods with an equal duration but a different ratio between the rising and recession parts of hydrograph (Fig. 5.5)

t_{rise} / t_{reces}	t_{rise} [h]	t_{reces} [h]	t_i [h]	$h_{s\ 1.5days}$ [m]	$h_{s\ max}$ [m]
1 / 2	72	144	*216*	3.24	8.61
1 / 3	54	162	*216*	4.55	8.51
1 / 4	43.2	172.8	*216*	5.70	8.43
1 / 6	30.84	185.16	*216*	6.66	8.35
1 / 8	24	192	*216*	6.90	8.30

The time T_s, when the maximum depth $h_{s\ max}$ is reached, varies for different shapes of the hydrograph. The shorter the time of the rising part of the floods, the faster the maximum scour depth is reached (Table 5.3) [44], [45].

Table 5.3

Dependence of the time T_s, when the maximum scour depth is reached, on the ratio between the rising and recession parts of hydrograph (Fig. 5.5)

$\frac{t_{rise}}{t_{reces}}$	$\frac{1}{2}$	$\frac{1}{3}$	$\frac{1}{4}$	$\frac{1}{6}$	$\frac{1}{8}$
T_s, days	5.4	4.95	4.68	4.37	4.2

5.2 The influence of multiple flood probability, duration, frequency and sequence on scour at engineering structures in river flow

5.2.1 The influence of multiple flood probability

First the single flood model was studied. Single wave flood with a different return period was modelled to evaluate the influence of flood probability on scour depth.

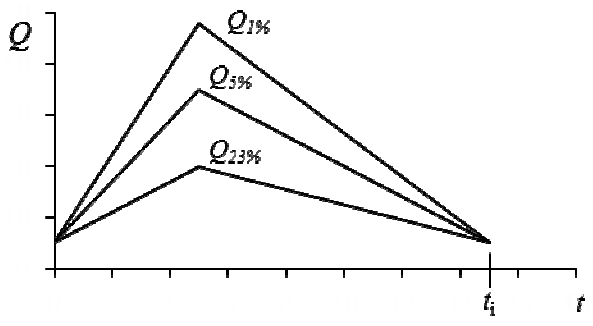

Figure 5.6. Floods with discharges of different probabilities

Figure 5.6 shows triangle-shaped hydrograph models for single floods with a probability of 1%, 5% and 23%.

Figure 5.7 shows the scour development in time for the discharge of a single flood with a probability of 1%, 5% or 23%. The initial data used for flood models are presented in the Appendix I, Chapter 7.1. (Tables A1.1 –A1.3). A duration of 7 days and the median grain size of 0.67mm was chosen for floods. Even though the flood duration is 7 days, the sediment discharge from the scour hole stops earlier, in this sample- around 5th day. The continuous line in Fig. 5.7 corresponds to the time when scour develops, but the dashed line shows a period when the depth of the scour hole remains the same. The sediment discharge proceeds more intensely and the scour hole at the foundation of the engineering structure is deeper for the flood of a lower probability during the same duration of flood.

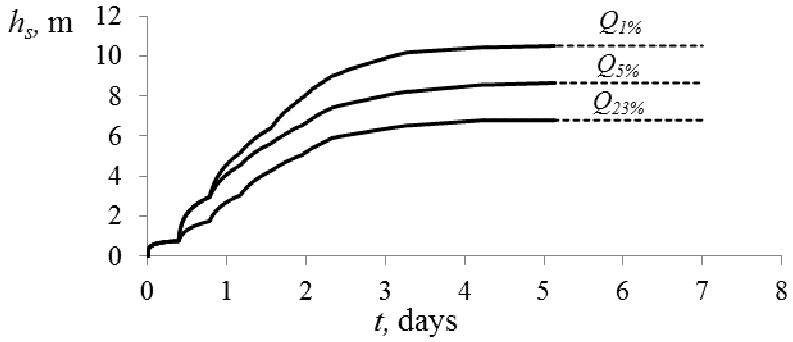

Figure 5.7 Time-dependent scour development with discharges of different probabilities, t = 7 days, d_i = 0.67mm

The time dependant development of the local velocity V_{lt} (dashed line) and the critical velocity βV_{0t} (continuous line) during single floods of 23% probability is presented in Fig. 5.8. According to the method the flood hydrograph was divided in to steps and each time step-in to smaller time intervals. The local velocity V_{lt} gradually reduces and the critical velocity βV_{0t} tends to increase within the time step because of the increase of the scour hole depth. The rapid increase or reduction of velocities at the start of each time step is related to the increase or reduction of the flood discharge according to the flood hydrograph. The scour develops only while the local velocity at the engineering structure is higher than the critical velocity.

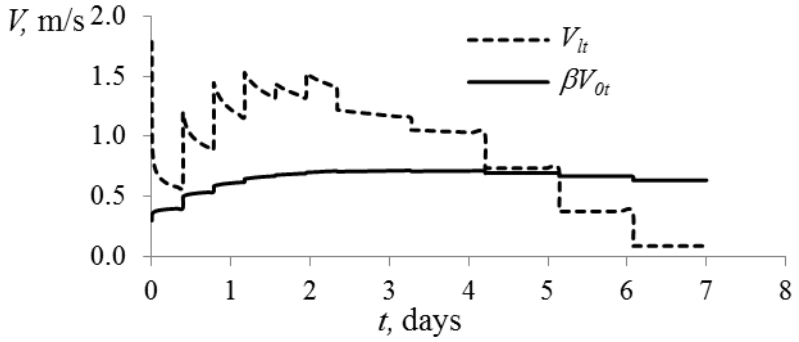

Figure 5.8 Development in time of the local velocity V_{lt} and the critical velocity βV_{0t} during single flood of 23% probability, t = 7 days, d_i = 0.67mm

The influence of probability on scour development during multiple floods was evaluated. Two series of floods with similar duration and hydrograph shape were used; however the discharge of multiple floods was changed for each model (Fig. 5.9).

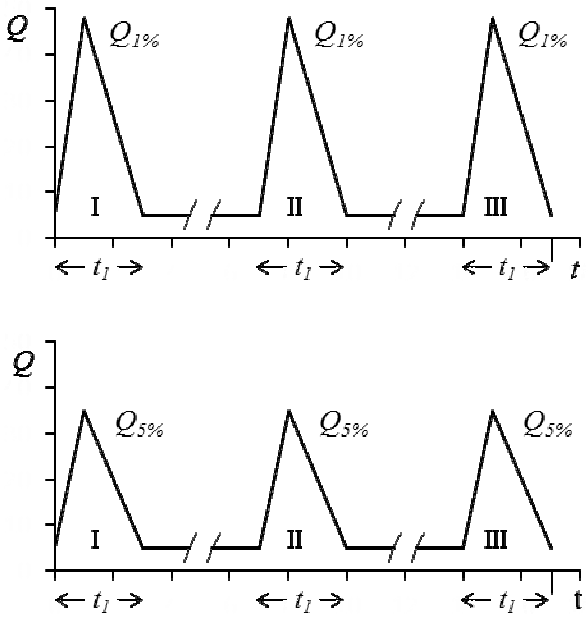

Figure 5.9 Multiple floods with discharges of 1% probability and 5% probability

The scour evolution process during multiple floods of 5% probability and 7-days duration is presented on Fig. 5.10. The initial data for multiple flood model is presented in the Appendix I, Chapter 7.1. (Table A1.4 and A1.5). The gray lines display hydrographs of three floods; the continuous gray line shows the changes of flood discharge in time, the dotted gray line shows the shape of the hydrograph.

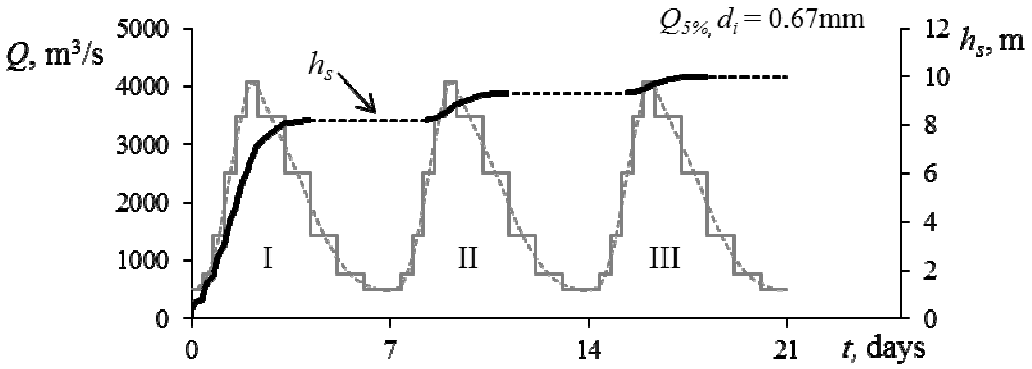

Figure 5.10 Scour development during multiple floods of 5% probability

The black lines display the process of scour development; the continuous black line- when scour develops and the dashed black line- when scour does not proceed. As can be seen from Fig. 5.10 the scour develops intensely during the first flood and stops shortly after the peak discharge of it. For the second and third flood the scour process starts only when the floods almost reach the peak discharge and stops soon after it. The intensity of sediment discharge out of the scour hole reduces with each flood and depends on the relation of the local velocity and critical velocity. Figure 5.11 presents the changes of the local velocity and critical one during multiple floods. The scour develops when the local velocity V_{lt} (continuous line) is higher than the critical velocity βV_{0t} (dashed line).

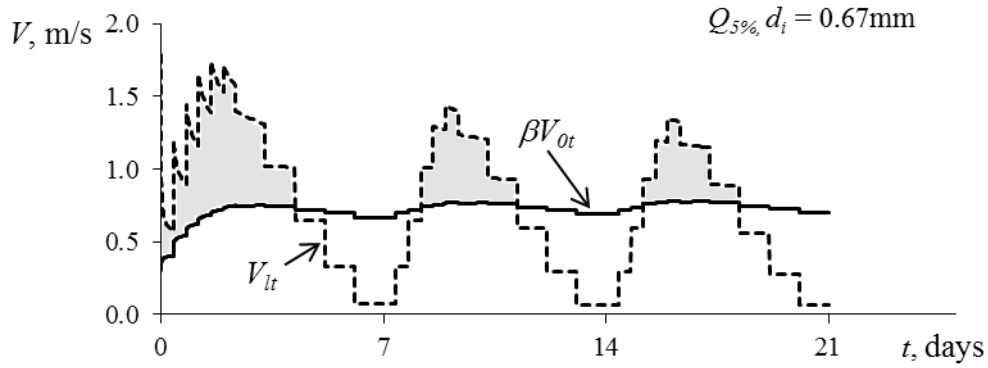

Figure 5.11 Local and critical velocity changes in time during multiple floods with equal peak discharge and duration

The intensity of scour development decreases because of the reduction in difference between the values of the local and critical velocities during the period when the local velocity is higher than the critical one (gray-marked areas in Fig. 5.11).

The joined chart of scour development and changes in local and critical velocities (Fig. 5.12) allows better understanding of the correspondence of those parameters. The gray lines display changes in the local (dashed line) and critical (continuous line) velocities. The

black line displays the scour evolution process during multiple floods. As can be seen from the figure, scour develops (black continuous line h_s) when the local velocity exceeds the critical one, and the depth of the scour hole remains the same (black dashed line h_s) when the local velocity V_{lt} is equal or less than the critical velocity βV_{0t}.

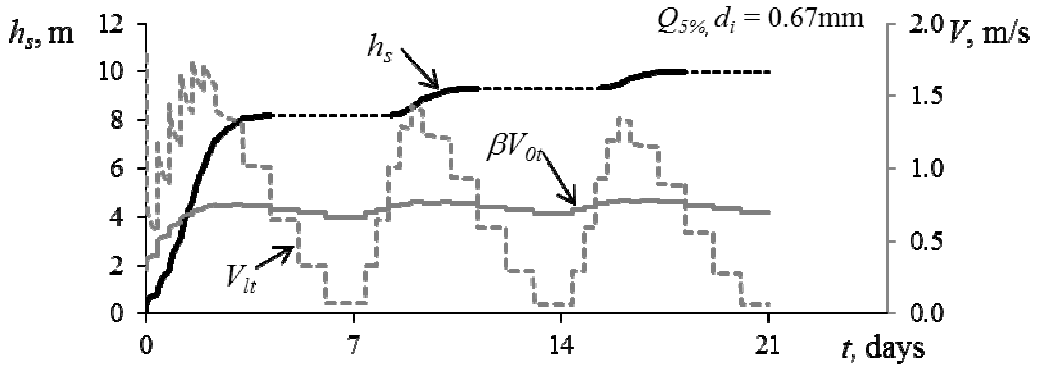

Figure 5.12 Joined chart of scour development and velocity changes during multiple floods of 5% probability

As mentioned previously, the influence of multiple floods probability on local scour development was evaluated using two series of floods with similar duration and hydrograph shape but with different discharge. The discharge of the first flood series was used according to 5% probability and the processes of scour development and velocity changes are described. The discharge of the second series of multiple floods was used according to 1% probability. The process of scour development during the series of floods of 1% probability was found similar to the described one; the high intensity of scour development during the first flood event and reduction in it with each following flood. The intensity of scour development within each flood remains higher for flood series of lower probability. The scour depth was found for each series of floods. The results were compared and it was found that the scour depth is greater for the flood series of lower probability (Fig. 5.13).

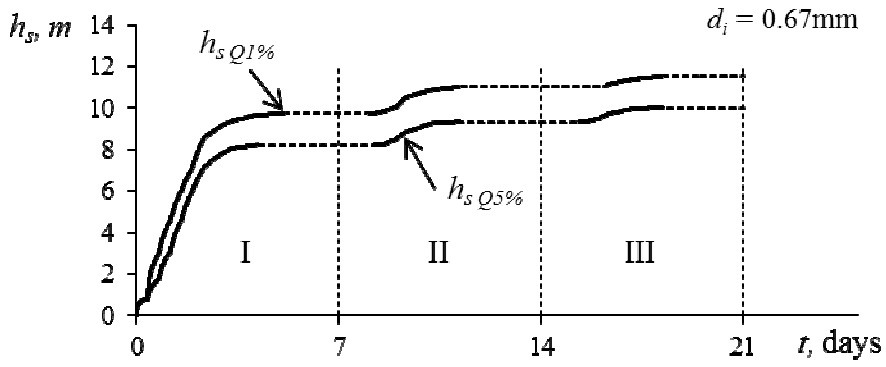

Figure 5.13 Comparison of scour development during a series of three floods with different probability

The comparison of the calculation results using different sediment sizes are presented in Appendix I, Chapter 7, Figs.A1.1 – A1.5.

5.2.2 The influence of multiple flood duration

The influence of multiple flood duration was studied for a model of multiple flood series. First the difference in scour evolution during a single flood was studied. Initial data for flood model is presented in the Appendix I, Chapter 7.3 (Table A1.6). Two single floods with similar probability and shape of hydrograph were modelled, however a duration of 7 days was chosen for first one and 14 days for the other one and the results were compared. The scour development in time for the two single floods of different duration is illustrated in Fig. 5.14. The black continuous line represents the period when scour develops, but the dotted line, the period when the depth of scour hole remains the same. In both cases scour development stops soon after peak discharge has passed and the depth of scour remains without changes throughout the flood hydrograph recession part. It is seen that the scour depth increases with the flood duration, i.e., the greater duration of the flood, the deeper the scour depth.

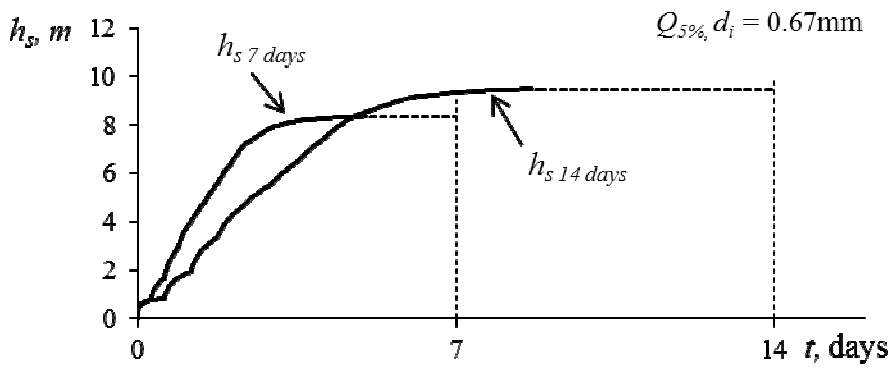

Figure 5.14 Scour development in time: 7-day duration (1) and 14-day duration (2)

Figure 5.14 shows two models of a series of three floods during certain period with equal shape of hydrograph, probability and duration *t*. While floods in the upper model have duration t_1 = 7 days, the lower flood series include floods with duration t_2 = 14 days. For both models flood hydrographs with the same discharge and steepness were used. Initial data of these models is presented in the Appendix I, Chapter 7.3 (Table A1.7).

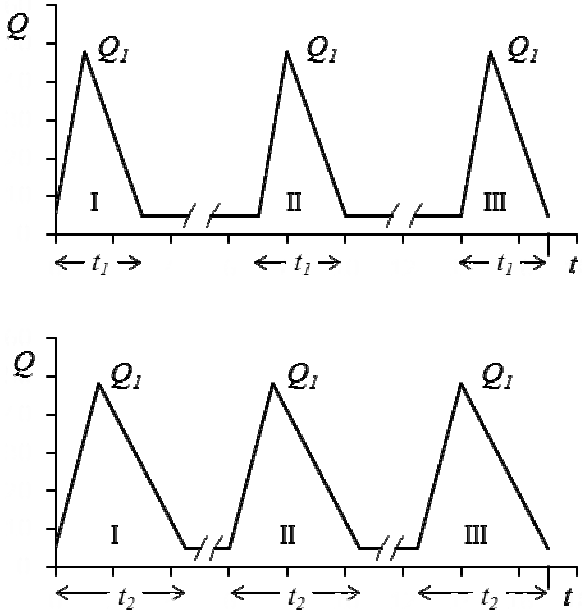

Figure 5.15 Hydrographs with the same discharge and time ratio between rising and recession parts of hydrograph

The time-dependant scour development in a series of three floods with similar discharge, hydrograph shape and duration t = 14 days (lowest model in Fig. 5.15) is illustrated in Fig. 5.16. The gray lines show the steps of hydrograph (continuous line) and average form of hydrograph shape (dashed line). The black lines (h_s) describe the process of scour development and indicate the flood hydrograph area where scour development proceeds (black continuous line). As it was confirmed previously, scour develops when the local velocity is higher than the critical velocity.

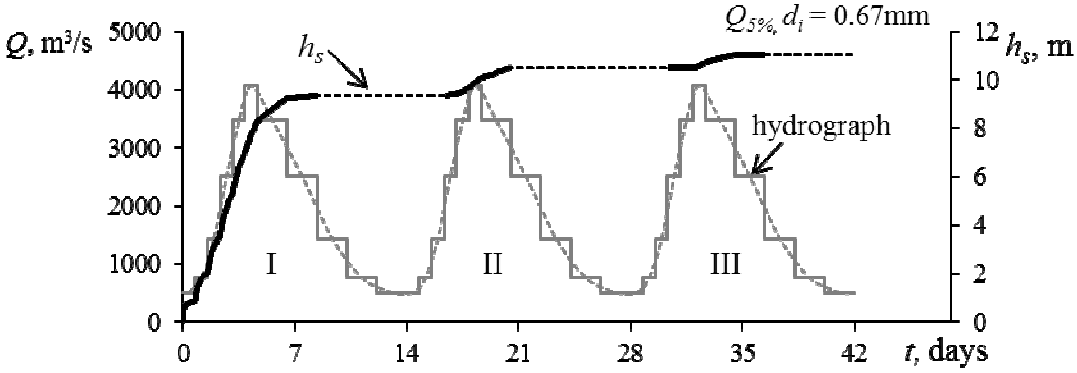

Figure 5.16 Scour development during multiple floods with a duration of 14 days each

The relation of the scour evolution process in time to the changes of the critical and local velocities of the flow is presented in Fig. 5.17 for this model. The local and critical velocities are shown by the gray lines and the black lines describe the scour process. During multiple

floods the scour develops when the value of local velocity V_{lt} exceeds the value of critical velocity βV_{0t}; scour hole develops intensely during the first flood, but a continuation of scour development proceeds only in an area around the peak discharge of the following floods (Fig. 5.17).

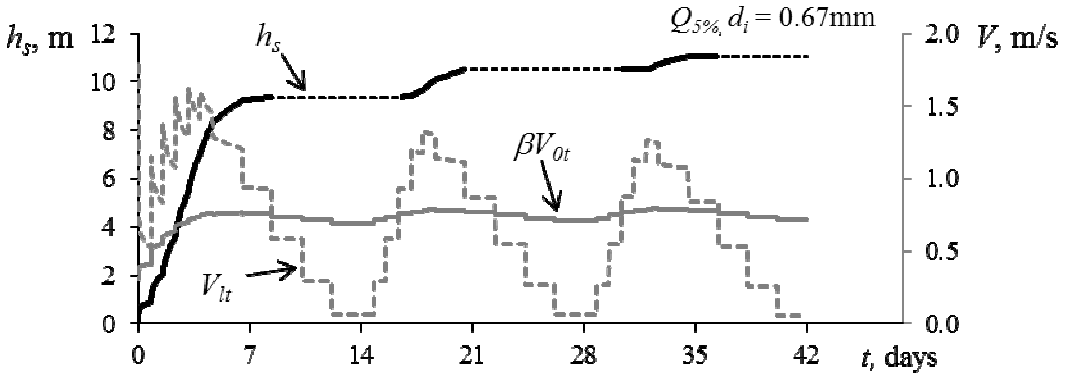

Figure 5.17 Joined chart of scour development and changes in velocities

The scour development and the depth of scour during multiple floods of 7-days and 14-days duration according to the model presented on Fig. 5.15 were compared. It is seen that the greater duration of the floods in the series, the deeper the scour depth (Fig. 5.18).

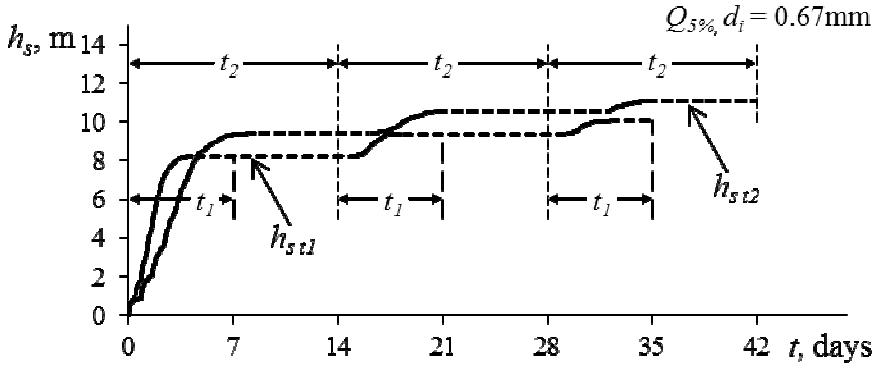

Figure 5.18 Comparison of scour depth for three following floods with 7-days or 14-days duration

Comparison of the results of scour evolution of multiple floods with different duration and using different river bed particle sizes are presented in the Appendix I, Chapter 7.4 (Figs. A1.6 – A1.9).

5.2.3 The influence of multiple flood frequency

The multiple floods with different frequency were modeled. The period of multiple floods was assumed similar however the flood number was changed during this time (Fig. 5.19). Two, three and four floods were modeled during the equal multiple floods period.

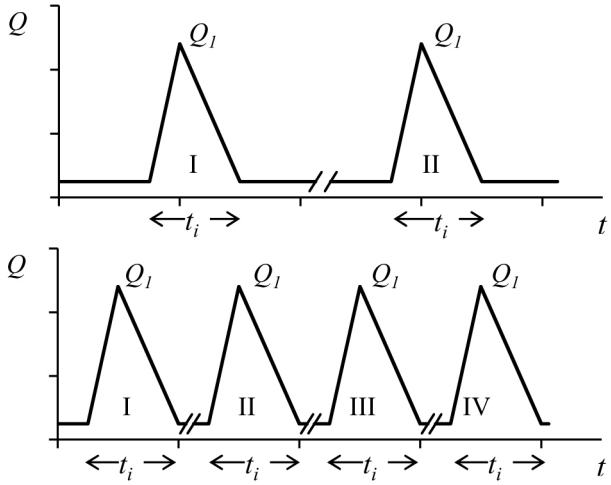

Figure 5.19 Multiple floods with different frequency; example of two and four floods are presented in top and bottom parts respectively during similar multiple floods period

To investigate the influence of the flood frequency on the scour development in time, a period of, for example, 5 years was chosen and supposed that, during this period, two or four floods of the same probability, duration and the shape of hydrograph occurred. The initial data for multiple flood model is presented in the Appendix I, Chapter 7.5. (Table A1.8). A similar discharge, duration and the form of hydrograph shape was used for all of the following floods in the series. The model of the series of two floods with 7-days duration was chosen and supplemented by two additional flood events. According to the assumption made for this research that scour depth remains the same between floods, the scour development can be described by one chart of time-dependant changes in the depth of scour for the series of four floods (Fig. 5.20).

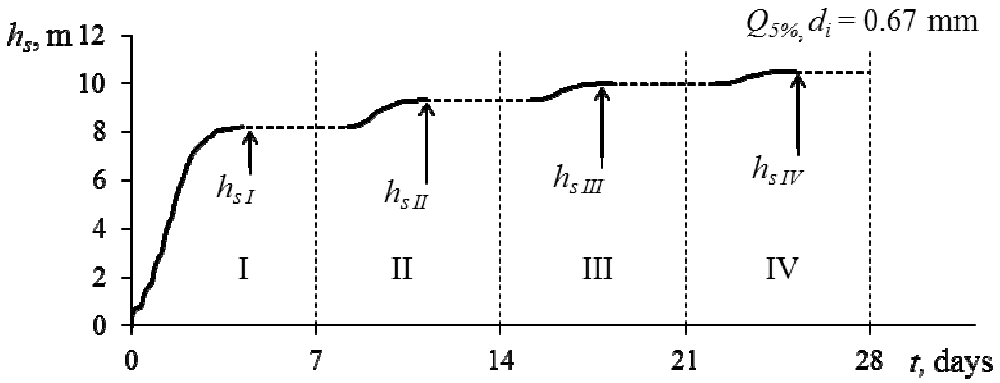

Figure 5.20 Scour development in time for floods with different frequencies; $h_{s\,I}$ to $h_{s\,IV}$ are scour depths reached after first to fourth flood respectively

The scour development intensity and additional depth of scour hole reduces with each following flood. It can be explained by the reduction of difference in the local velocity V_{lt} and the critical velocity βV_{0t} in the period when the local velocity is higher than the critical one (Fig. 5.21). In other words, the scour intensity reduces when the ratio $V_{lt}/\beta V_{0t}$ approaches 1.

The scour evolution of four frequent floods (probability 5%, duration 7 days, d_i = 0.67mm) is presented in Fig.7.20. The equilibrium depth calculated for one flood with the aformentioned parameters is 18.2m (method by Neilands [81]). As intensity of the sediment removal decreases with each forthcoming flood, the possibility to achieve the equilibrium depth by the series of floods of the accepted probability seems to be only theoretical. Because a large number of floods with same probability and duration should follow in order for the developed scour depth to reach the calculated equilibrium depth.

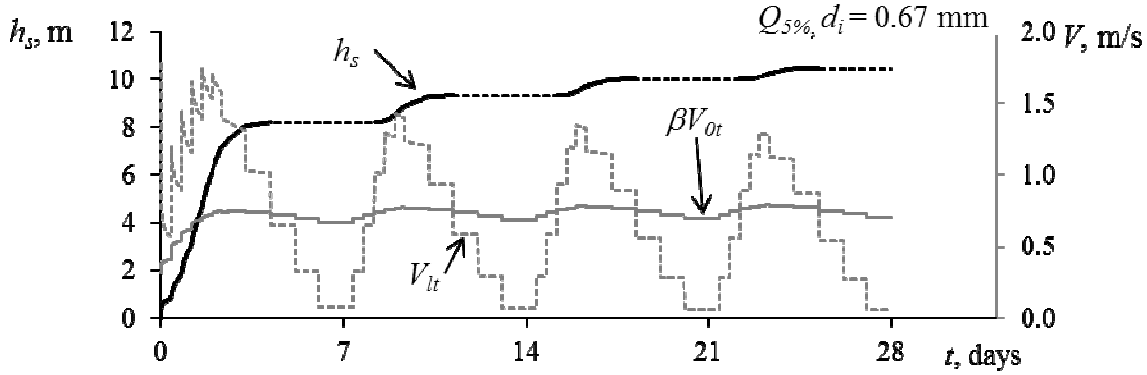

Figure 5.21 Joined chart of scour development and changes in velocities for a series of four floods

It is obvious that an increase in the frequency of the floods is accompanied by an increase in the scour depth, and it follows from Figs.5.20 and 5.21 that the scour depth after two floods h_{sII} at an accepted period of time is less than that h_{sIII} after three floods occurred

during the same period, $h_{sIV} > h_{sIII}$ etc. After every flood, the depths of scour are summed up, and tends to reach the value of the equilibrium depth.

The scour evolution was modelled by using different sediment size. The results are presented in the Appendix I, Chapter 7.6 (Fig. A1.10).

5.2.4 The influence of multiple flood sequence

The influence of the sequence of floods with a different probability on the time-dependent scour development was examined according to three scenarios (Figs. 5.22, 5.23). Figure 5.22 shows a scheme of three floods of the same probability.

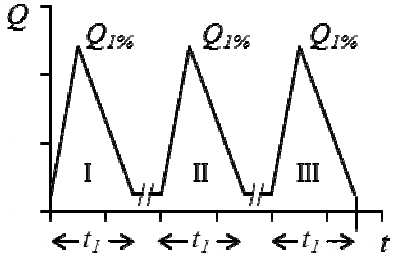

Figure 5.22 Multiple flood series with three floods of the same probability

The high flood follows by two lower floods in the left scheme and two floods with higher probability are followed by the flood with less probability in the right scheme of Fig. 5.23. The initial data of multiple flood models described are presented in Appendix I, Chapter 7.7. (Tables A1.9 – A1.11).

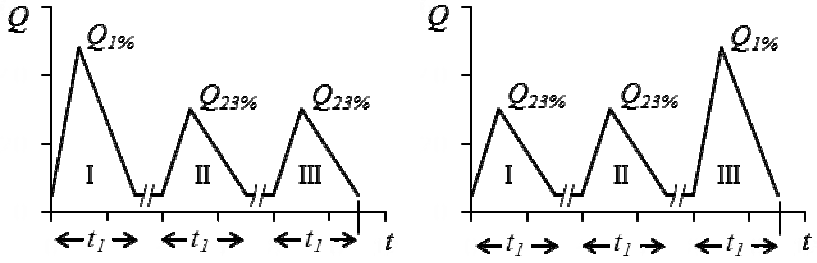

Figure 5.23 Multiple floods with different sequence

The scour development for the scenario described in Fig. 5.22 presents curve 1 in Fig. 5.24. The scour starts when the flood-plain is flooded and increases rapidly. Because of the scour hole developed during the first flood, in the second flood, the scour process starts at the step of hydrograph when $V_{lt\,II} \geq \beta V_{0t\,II}$ and has less duration, while for the third flood the velocities

change due to the scour developed after the two previous floods, and it begins at $V_{lt\,III} \geq \beta V_{0t\,III}$ (Fig. 5.24, curve 1).

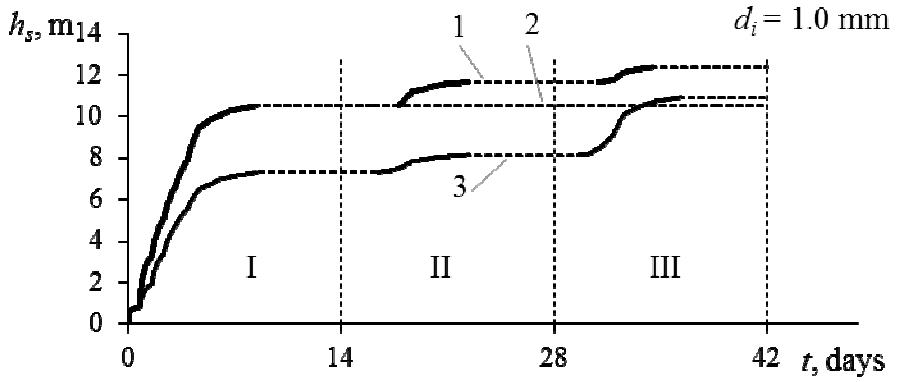

Figure 5.24 Scour development in time for floods of different sequences

The curve 2 in Fig. 5.24 shows the scour process of a multiple flood sequence scenario when the high flood is followed by two lower floods (left-side scenario in Fig. 5.23).

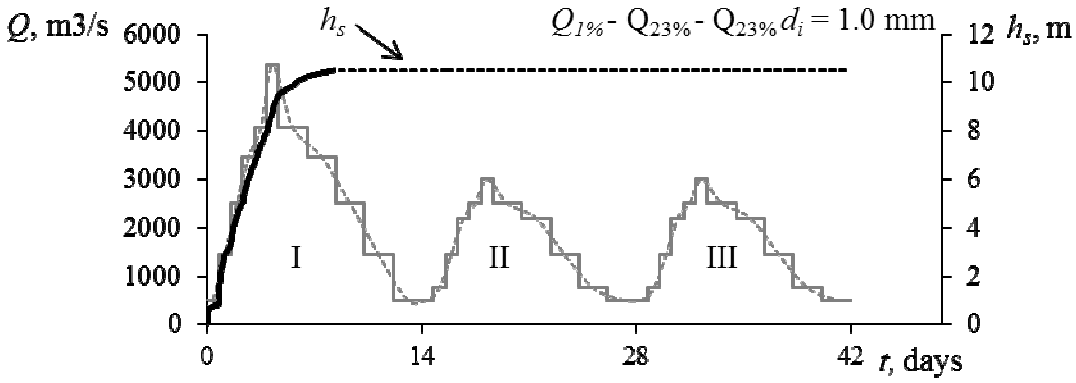

Figure 5.25 Scour development for a series of floods when the high flood is followed by two lower floods

Figures 5.25 – 5.26 present scour evolution curve joined with a flood hydrograph chart and with curves of the local and critical velocities respectively. As seen from Fig. 5.25, during the first flood, the scour depth develops and remains the same till the next flood. There is no change in the depth of the scour hole during two forthcoming floods.

An explanation of it can be described by a chart of changes in the local and critical velocities (Fig. 5.26). The local velocity V_{lt} reduces but the critical velocity V_{0t} increases because of the scour depth developed during the previous flood. In the next flood, the capacity of the flow is not sufficient to remove sediments out of the scour hole, and V_{lt} is less than βV_{0t}. In the second and third floods, the scour depth remains the same, as after the first flood (Fig. 5.26).

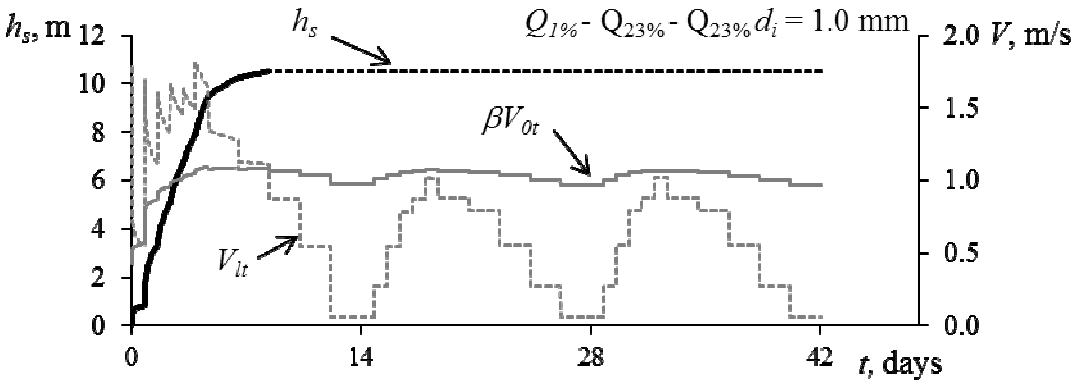

Figure 5.26 Scour development and changes in local and critical velocities for a series of floods when the high flood is followed by two lower floods

Curve 3 in Fig. 5.24 shows the scour process of a multiple flood sequence scenario when two floods with higher probability are followed by the flood with less probability (right-side scenario in Fig. 5.23). The scour starts and develops rapidly during the first flood (Fig. 5.27).

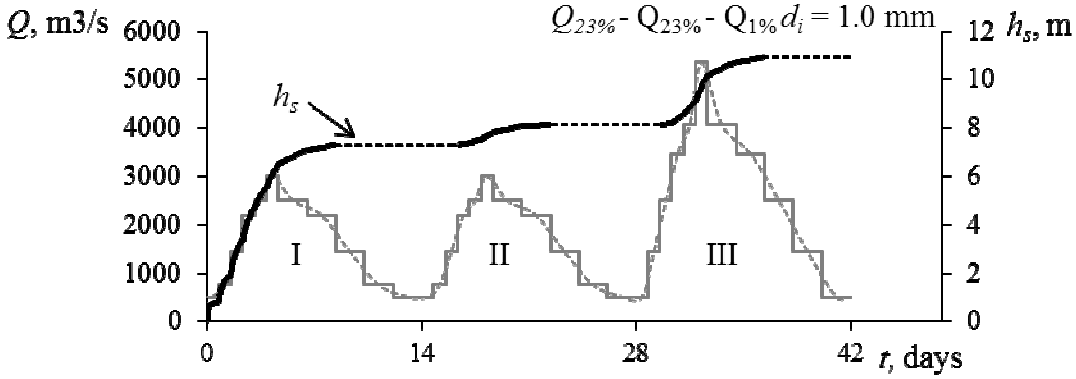

Figure 5.27 Scour development for a series of floods when the high flood is followed by two lower floods

In the second flood, the scour process starts at the step of the hydrograph when $V_{lt\ II} \geq \beta V_{0t\ II}$ and has less duration. In the third flood, the scour starts at the step of hydrograph when $V_{lt} \geq \beta V_{0t}$ and develops rapidly due to the discharge of the flow which is much higher than during the previous two floods (Fig. 5.27). Changes in the local and critical velocities are presented in Fig. 5.28 for this scenario. The intensity of scour development is well presented by the area surrounded by the curves of the local velocity and critical velocity in this figure. The higher the local velocity V_{lt} is than the critical one βV_{0t}, the more intensive scour development is.

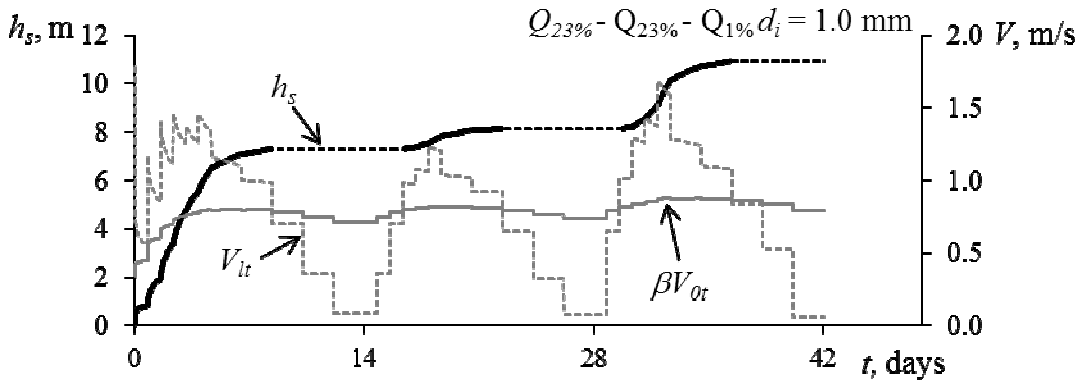

Figure 5.28 Scour development for a series of floods when the high flood is followed by two lower floods

The results of scour evolution during multiple floods of various sequence scenarios using sediment size d_i = 1.0 are presented in Figs. 7.24 – 7.28. The results of scour development with time for the sediment size 0.24mm, 0.50mm and 0.67mm are presented in Figs. (A1.11 – A1.14) of the Appendix I, Chapter 7.8.

Chapter summary

Using the differential equation of equilibrium of the bed sediment movement in clear water, a method for calculating the scour development in time at engineering structures during multiple floods was elaborated and the scour development in time during multiple floods was investigated. The following conditions are taken into account in this study: clear-water conditions and alluvial river bed with homogenous river bed material was supposed. The constant cross section of the river bed and floodplain between floods was accepted.

A computer modeling of the scour process based on the method described in Chapter 3 was performed, and the influence of floods with different probability, duration, frequency, and sequence on the scour depth at the abutments was determined. A computer modeling of the scour development in time was performed to study the influence of a triangle-shaped hydrograph shape on the time-dependent local scour under clear-water conditions.

It was established that the process of time-dependent scour formation is similar both for tests and calculations, namely the rapid development at the start of the scour process was followed by its gradual reduction in time. Since the scour process stops just after the peak of the flood, the time when the maximum depth is reached is usually smaller than the flood duration. It was also stated that the scour depth, width, and volume depended on the flow hydraulics, the river-bed parameters, the probability of multiple floods, as well as on their duration, frequency, sequence, and shape of flood hydrograph [58], [59].

It was confirmed that the scour develops if the ratio $V_{lt} / \beta V_{0t} > 1$. The scour stops if the ratio $V_{lt} / \beta V_{0t} \leq 1$. Further investigations of the flood intensity evaluation can be carried out by calculating the area incorporated by the curves of local and critical velocities (grey-marked areas in Fig. 5.11) however it was not a task for this research. Nevertheless those areas visually clearly indicate the capacity to remove sediments from the scour hole for each of the forthcoming floods in the multiple flood series.

Two types of the shape of flood hydrographs were studied. The first type of hydrograph had a fixed time of the rising part, but the time of recession was changed according to the ratios 1:2, 1:3, 1:4, 1:6 and 1:8, thus the duration of the flood was increased. The second type of hydrograph had constant flood duration and discharge, but the shape of the hydrograph was changed because of the ratio between the time of rising and recession parts. It was found that the for hydrographs with equal discharge and fixed time of the rising part, the scour depth increases if the time of recession of the flood becomes longer. The scour depth changes a little if the shape of the hydrograph with a fixed duration is varied by the ratio between the times of the rise and recession. However, the time when the maximum scour depth is reached is less for floods with a higher slope of the rising limb. Similarly, the higher value of the scour is reached during the equal period of floods with a shorter time of the hydrograph rising limb.

The results of computer modeling of the scour process during floods with different probability, duration, frequency, and sequence showed the influence on the scour depth near hydraulic structures.

The scour hole at the abutments is deeper for the flood of a lower probability- the higher discharge, the deeper the scour hole.

The scour depth increases with the flood duration, i.e., the greater duration of the tests, the deeper the scour depth.

It is obvious that an increase in the frequency of the floods is accompanied by an increase in the scour depth. The scour depth after two floods at an accepted period of time is less than that after four floods occurred during the same period. After every flood, the depths of scour are summed up. Nevertheless the equilibrium stage can be reached only theoretically, because of the decreased intensity of the removal of sediments by the each forthcoming flood of accepted probability. It can be concluded that only floods with an unexpected probability can be the reason for water engineering structure damage by the local scour at foundation.

It was found that the scour depth reaches higher value for multiple flood sequence when each forthcoming flood in sequence has less probability. The depth, width, and volume

of scour increased with each subsequent flood. Of exception was the case with varied sequence of multiple floods with different probability. The scour depth after the first flooding remained the same if the first flood probability was significantly lower than that of the forthcoming floods of a series of multiple floods. This happened due to the scour hole developed in the first flood event, which reduced the local velocity of the flow and its capacity to remove sediments.

It was determined that duration, probability, frequency and sequence as well as the hydrograph shape effect the results of a time-dependent scour depth near hydraulic structures.

CONCLUSIONS

1. An analysis of literature observed that at present there is no method for scour calculation at water engineering structures in river flow that takes into account the influence of multiple floods during the period of exploitation.
2. A differential equation of the bed sediment movement was used and a new theoretical method for computing scour depth, width and volume at engineering structures in river flow under unsteady flow conditions was developed.
3. Based on the developed method for the computer modeling of the local scour at engineering structures under unsteady flow conditions, a computer program was created allowing to evaluate the changes of the scour depth during multiple floods of different scenarios.
4. Processing of the experimental data show influence of the contraction rate of the flow and its depth, Froude number, approach flow velocity and different ratios of the local and critical velocities $\beta V_{0t}/V_{lt}$, V_0/V_{0t}, V_l/V_{lt}, on the local scour evolution and it corresponds with calculated results.
5. The comparison graphs of the local and approach velocities at different rates of the flow contraction and Froude numbers confirms that the local velocity depends on the flow contraction rate and the maximum backwater value and is several times higher than the approach velocity in the flume; with an increased Froude number and with an decreased contraction rate, the difference between local and approach velocity of the flow is decreasing. The local velocity forms a scour hole, but not the approach flow as it is accepted by different authors.
6. For the first time the relative local and critical velocity changes under unsteady flow conditions are described and calculated; in the scour process the local velocity decreases due to the formation of the scour hole and at the same time increases with the growth of the discharge; the critical velocity increases during flood intensification; erosion stops when the local velocity and the critical velocity becomes equal.
7. It was found that the time when maximum scour is reached during single wave flood differs for hydrographs of various steepness; the intensity of scour evolution increases by the increase of the slope of the hydrograph raised part

8. The effect of multiple flood probability, duration, frequency and sequence on the scour at water engineering structures in flow is established for the first time, based on the results of the computer modeling for a real recurrent flood in different scenarios.
9. It was found that the scour parameters increase with decrease in probability and with increasing duration and frequency of the floods; the sequence of floods can increase or reduce the scour evolution with time, depending on their probability; the successive floods of the same probability considerably increase the value of the scour depth.
10. It was confirmed that even with a high frequency of floods of accepted probability the equilibrium depth of scour cannot be reached and only unexpected flood event can be the source of the failure of water engineering structures caused by local scour.

REFERENCES

1. Ahmad M. Experiments on design and behavior of spur dikes // Proc. of International Hydraulics Convention 1953, pp. 145–159.

2. Armitage, N & McGahey C. Scour prediction using the Movability Number criteria for incipient motion Vol.1 // Proc. of River Flow 2004 / ed. in Greco Carravetta & Della Morte (eds) Napoli, Italy, 2004, Vol. 1, pp. 511–519.

3. Ballio F., Orsi E. Time evolution of scour around bridge abutments. Water Engineering Research 2(4) 2001, Vol. 2, № 4, pp. 243–259.

4. Baryshnikov N. Hydraulic resistance of fluvial channels. A manual St.Petersburg: RSHU Publishers, 2003, 147 p.

5. Benedict S.T. et al. Trends of abutment-scour prediction equations applied to 144 field sites in South Carolina. Open-file Report.No 2003-95 Reston VA, USA, U.S.Geological Survey, 2006, № 2003, 150 p.

6. Bertoldi, D., Jones J. Time to scour experiments as an indirect measure of stream power around bridge piers // Int. Water Resource Engineering Conference 1998, pp. 264–269.

7. Bhunya P.K., Panda S.N., Goel M.K. Synthetic Unit Hydrograph Methods : A Critical Review // The Open Hydrology Journal 2011, Vol. 5, pp. 1–8.

8. Bhunya P. et al. Parameter Estimation of Beta Distribution for Unit Hydrograph Derivation // Journal of Hydrologic Engineering 2004, Vol. 9, № 4, pp. 325–332.

9. Bombar, G. et.al. Experimental and Numerical Investigation of Bed-Load Transport under Unsteady Flows // J. Hydraul. Eng 2011, Vol. 137, № October, pp. 1276–1282.

10. Borghei S.M., Kabiri-Samani A., Banihashem S.A. Influence of unsteady flow hydrograph shape on local scouring around bridge pier // Proceedings of the ICE - Water Management 2012, Vol. 165, № 9, pp. 473–480.

11. Briaud J.L. et al. Multiflood and multilayer method for scour rate prediction at bridge piers // Journal of Geotechnical & Geoenvironmental Engineering 2001, Vol. 127, № 2, pp. 114–125.

12. Cardoso A.H., Bettess R. Effect of time and channel geometry on scour at bridge abutments. // Journal of Hydraulic Engineering 1999, Vol. 125, № 4, pp. 388–399.

13. Chang F.M., Davis S. Maryland SHA procedure for estimating scour at bridge abutments. Part 2- Clear water scour // Maryland SHA procedure for estimating scour at bridge abutments. Part 2- Clear water scour. ASCE Compendium: Stream Stability and Scour at Highway Bridges / ed. Lagasse, Richardson Reston,VA,USA: ASCE, 1999, pp. 412–416.

14. Chang H.H. Scour study for bridge design on Temecula Creek // North American Water and Environment Congress A.S.C.E. Anaheim, USA, 1996, pp. 1162–1166.

15. Chang H.H. Fluvial Processes In River Engineering Krieger Pub Co, 2001, 456 p.

16. Chang W. et al. Evolution of Scour Depth at Circular Bridge Piers // Journal of Hydraulic Engineering 2004, № 9, pp. 905–913.

17. Chin C.O., Melville B.., Raudkivi A.J. Streambed armouring // Journal of Hydraulic Enginering 1994, Vol. 120, № 8, pp. 899–918.

18. Chow V.T. Runoff. Handbook of applied hydrology New York: McGraw- Hill, 1964, pp. 14–1 – 14–54.

19. Chow V.T., Maidment D., Mays L. Applied Hydrology New York: McGraw- Hill, 1988, 572 p.

20. Christen J.H., Christen O.B. Climate modelling: Severe summertime flooding in Europe // Nature 2003, Vol. 421, pp. 805–806.

21. Ciepielowski A. Statistical methods of determining typical win- ter and summer hydrographs for ungauged watersheds // Flood Hydrology.Proc.of Int.Symposium on Flood Frequency and Risk Analyses Baton Rouge, USA: Springer Netherlands, 1987, pp. 117–124.

22. Ciscar J. Climate change impacts in Europe Luxembourg: Office for Official Publications of the European Communities, 2009, 130 p.

23. Dehghani A.A., Ghodsian M., Suzuki K. Local Scour Around Lateral Intakes in 180 Degree Curved Channel // Advances in Water Resources and Hydraulic Engineering. Proc. of 16th IAHR-APD Congress and 3rd Symposium of IAHR-ISHS. Vol.III Springer Berlin Heidelberg, 2009, pp. 821–825.

24. Dongol D. Local scour at bridge abutments. Research Report No544. Auckland, New Zealand, School of Engineering, University of Auckland, 1994, 409 p.

25. Dooge J. A general theory of the unit hydrograph // Journal of Geophysical Research 1959, Vol. 64, № 2, pp. 241–249.

26. European Commission. A new EU Floods Directive [online] / Available from: http://ec.europa.eu/environment/water/flood_risk/

27. European Commission. Directive 2007/60/EC of the European Parliament and of the Council of 23 October 2007 on the assessment and management of flood risks. [online] 2007, / Available from: http://eur-lex.europa.eu/LexUriServ/LexUriServ

28. European Environment Agency. Occurrence of major floods in Europe (1998–2009) [online] / Available from: http://www.eea.europa.eu/data-and-maps/figures/occurrence-of-flood-events-in-europe-1998

29. European Environment Agency. Impacts of Europe's changing climate - 2008 indicator-based assessment. 2008, 246 p.

30. Franzetti, S., Malavasi, S., and Piccinin C. Sull'erosione alla base delle pile di ponte in acque chiare // Proc. of XXIV Convegno di Idraulica e Costruzioni Idrauliche, Vol.II 1994, pp. 13–24.

31. Frei C. et al. Future change of precipitation extremes in Europe: Intercomparison of scenarios from regional climate models // Journal Geophysical Research-Atmospheres 2006, pp. 111–121.

32. Froehlich D.C. Local scour at bridge abutments // Proc.of National Conference on Hydraulic Engineering New Orleans,LA,USA: ASCE, 1989, pp. 922–927.

33. Garde R.J., Subramanya K., Nambudripad K.D. Study of scour around spur dikes // Journal of the Hydaraulics 1961, Vol. 87, pp. 23–37.

34. Gill M.A. Erosion of sand beds around spur dikes // Journal of Hydraulic Division 1972, Vol. 87, pp. 23–37.

35. Gjunsburgs B., Klive G., Neilands R. j. Local scour at straight guide banks in plain rivers // Proc.of 7th International Conference on Environmental Engineering Vilnius: Vilnius Gediminas Technical University Press "Technika," 2008, pp. 552–529.

36. Gjunsburgs B., Neilands R. Scour development on time at the abutment of the bridge on plain rivers // Proc.of Conference on Environmental Research, Engineering and Management, Vilnius: Kaunas Uniersity of echnology, 2001, Vol. 1, № 15, pp. 8–11.

37. Gjunsburgs B., Neilands R., Neilands R. j. Scour development at bridge abutments on plain rivers during the flood: Analysis of the method // Proc.of 2nd International Conference on Scour and Erosion Singapore: Stallion Press, 2004, pp. 199–206.

38. Gjunsburgs B., Neilands R. j., Govsha E. Scour development at elliptical guide banks during multiple floods // Proc.of 32nd Congress of IAHR Venice, Corila, 2007, pp. 589–598.

39. Gjunsburgs B., Govsha E., Jaudzems G. Riverbed layering impact on scour at the abutments // 7th International Conference on Fluvial Hydraulics, RIVER FLOW 2014 / ed. Schleiss A. et al. Switzerland, Lausanne, 3-5 September, Switzerland: CRC Press, 2014, pp. 1463–1468.

40. Gjunsburgs B., Jaudzems G., Govsha E. Scour at Elliptical Guide Banks under Stratified Bed Conditions: Equilibrium Stage // People, Buildings and Environment 2010 / ed. Hanák T., Aigel P., Dyntarová K. Krtiny, Czech Republic: Akademicke Nakladatelstvi Cerm, 2010, Vol. 1, pp. 24–30.

41. Gjunsburgs B., Jaudzems G., Govsha E. Multiple Floods Impact on Scour at Engineering Structures // 6th International Conference on Scour and Erosion Paris, 27-31 August, France: Societe Hydrotechnique de France, 2012, pp. 747–754.

42. Gjunsburgs B., Jaudzems G., Govsha E. Influence of the Flow and Bed Parameters on the Scour at Bridge Structures // First IAHR European Congress Edinburgh, United Kingdom: Heriot-Watt University - School of the Built Environment, 2010, pp. 53–58.

43. Gjunsburgs B., Jaudzems G., Govsha E. Hydrograph Shape Impact on the Scour Development with Time at Engineering Structures in River Flow // Scientific Journal of Riga Technical University. Construction Science 2010, Vol. 11, № 2, pp. 6–12.

44. Gjunsburgs B., Jaudzems G., Govsha E. Influence of the Hydrograph Shape on the Scour Development // Hydrology: from Research to Water Management: the XXVI Nordic Hydrological Conference Latvia, Riga, 9-11 August, 2010, Latvia, 2010, pp. 196–198.

45. Gjunsburgs B., Jaudzems G., Govsha E. Flood Duration and Hydrograph Shape Impact on Scour near Hydraulic Structures // WMHE 2011, Current Events in Hydraulic Engineering Gdansk, 5-8 September, Poland: Gdansk University of Technology Publishers, 2011, pp. 143–149.

46. Gjunsburgs B., Jaudzems G., Govsha J. Assessment of Flood Damage Risk for Abutments in River Floodplains // International Conference on Fluvial Hydraulics River Flow 2010 Braunshweig, Germany: Bundesanstalt fur Wasserbau, Federal Waterways Engineering and Research Institute, 2010, pp. 1185–1192.

47. Gjunsburgs B., Lauva O., Neilands R. Equilibrium time of scour near structures in plain rivers // The 9th International Conference “Environmental Engineering 2014” Vilnius, Lithuania: Vilnius Gediminas Technical University Press “Technika” 2014, 2014, № May, pp. 1–7.

48. Gjunsburgs B., Neilands R. Local Velocity at the Abutments on the Plain Rivers // River Flow 2004 : Proceedings of the Second International Conference on Fluvial Hydraulics Napoli, Italy: A.A. Balkema, 2004, Vol. 1, pp. 443–448.

49. Gjunsburgs B., Neilands R., Govsha E. Scour Development and Bridge Abutment Safety during the Floods // Flow Simulation in Hydraulic Engineering Dresden, Germany: Dresden Technical University, 2006, pp. 157–167.

50. Gray D. Synthetic unit hydrographs for small watersheds // Journal of the Hydraulics Division 1961, Vol. 87, № 4, pp. 33–53.

51. Grimaldi C. et al. Local scouring at bridge piers and abutments- time evolution and equilibrium. // Proc. of River Flow 2006, Vol.2 / ed. in Ferreira et al. (eds) Lisbon, Portugal, 2006, Vol. 2, pp. 1657–1664.

52. Grimaldi C., Gaudio R. Local scouring at bridge piers and abutments: Time evolution and equilibrium // Proc.of Conference on Fluvial Hydraulics River Flow 2006 / ed. A.A.Balkema London: Teylor&Francis, 2006, pp. 1657–1664.

53. Hager W.H., Unger J., Oliveto G. Entertainment criterion for bridge piers and abutments. // Proc.of River Flow 2002 Belgium, 2002, Vol. 2, pp. 1053–1058.

54. Hager W.H., Unger J. Bridge Pier Scour under Flood Waves // Journal of Hydraulic Engineering 2010, Vol. 136, № 10, pp. 842–847.

55. Haktanir T., Sezen N. Suitability of two-parameter gamma and three-parameter beta distributions as synthetic unit hydrographs in Anatolia // Hydrology Science 1990, Vol. 35, № 2, pp. 167–184.

56. Hamill L. Bridge Hydraulics: Theory and practice London: E&FN Spon, 1999, 384 p.

57. Inglis S. The behavior and control of rivers and canals // The behavior and control of rivers and canals. Poona, Ind 1949, pp. 327–348.

58. Jaudzems G., Gjunsburgs B. Local Scour Development at Engineering Structures during Multiple Floods // Riga Technical University 53rd International Scientific Conference: Dedicated to the 150th Anniversary and the 1st Congress of World Engineers and Riga Polytechnical Institute / RTU Alumni: Digest Latvia, Riga, 11-12 October, Latvia: RTU, 2012, pp. 417–417.

59. Jaudzems G., Gjunsburgs B., Govsha E. Multiple Flood as the Cause of Failure of Engineering Structures in River Flows // International Scientific Conference People, Buildings and Environment 2012 Czech Republic, Lednice, 7-9 November: Brno University of Technology, 2012, Vol. 2, pp. 548–557.

60. Kandasamy J.K. Abutment scour. Research Report No458 Auckland, New Zealand, School of Engineering, University of Auckland, 1989, p. 278.

61. Kothyari U.C., Garde R.J., Ranga Raju K.G. Temporal variation of scour around circular bridge piers // Journal of Hydraulic Engineering 1992, Vol. 118, № 8, pp. 1091–1106.

62. Kothyari U.C., Ranga Raju K.G. Scour around spur dikes and bridge abutments // Journal of Hydraulic Research 2001, Vol. 39, № 4, pp. 367–374.

63. Kouchakzadeh S., Townsend D.R. Maximum scour depth at bridge abutments terminating in the floodplain zone // Can. Journal of Civil Engineering 1997, Vol. 24, pp. 996–1006.

64. Kwan T.F. A study of abutment scour. Report No451 Auckland, New Zealand, 1988, 461 p.

65. Lacey G. Stable channels in alluvium // Proc.of the Institution of Civil Engineers London, UK: William Clowes and Sons Ltd., 1930, pp. 259–292.

66. Lai J. et al. Maximum Local Scour Depth at Bridge Piers Under Unsteady Flow // Journal of Hydraulic Engineering 2009, № July, pp. 609–614.

67. Lauchlan C.S., Coleman S.E., Melville B.W. Temporal scour development at bridge abutments // Proc. 29th IAHR Congress Beijing, China, 2001, pp. 738–745.

68. Laursen E.M. An analysis of relief bridge scour // Journal of the Hydraulics Division 1963, Vol. 92 (HY3), pp. 93–118.

69. Laursen E.M. Predicting Scour at Bridge Piers and Abutments: General Report. No. 3 1980, № 3, 223 p.

70. Laursen E.M., Toch A. Scour around bridge piers and abutments. Bulletin 4 Jowa, USA, Jowa Institute of Hydraulic Research, 1956, 60 p.

71. Lim S.V. Equilibrium clear-water scour around abutment // Journal of Hydraulic Engineering 1997, Vol. 123, № 3, pp. 237–243.

72. Liu H.K., Chang F.M., Skinner M.M. Effect of bridge construction on scour and backwater. Report CER 60 HKL 22 Fort Collins, CO, USA, Department of Civil Engineering, Colorado State University, 1961, 118 p.

73. May R.W., Ackers J.C., Kirby A. Manual on scour at bridges and other hydraulic structures London, Uk: CIRIA, 2002, 225 p.

74. Melihyanmaz A., Kose O. A semi-empirical model for clear-water scour evolution at bridge abutments // Journal of Hydraulic Research 2009, Vol. 47, № 1, pp. 110–118.

75. Melville B.W. Local scour at bridge abutments // Journal of Hydraulic Engineering 1992, Vol. 118, № 4, pp. 615–631.

76. Melville B.W. Pier and abutment scour: integrated approach // Journal of Hydraulic Engineering 1997, Vol. 123, № 2, pp. 125–136.

77. Melville B.W. Bridge abutments scour in compound channels // Journal of Hydraulic Engineering. 1995, Vol. 121, № 12, pp. 863–868.

78. Melville B.W., Coleman S.E. Bridge scour Water Resources Publications, CO, USA, HighLands Ranch, CO, USA, Highlands Ranch: Water Resources Publications, 2000, 550 p.

79. Melville, B. W., Chiew Y.M. Time scale for local scour at bridge piers // Hydraulic Engineering 1999, Vol. 125, № 1, pp. 59–65.

80. Mia F., Nago H. Scour at Circular Bridge Pier // Journal of Hydraulic Engineering 2003, Vol. 126, № 6, pp. 420–427.

81. Neilands R.R. Equilibrium scour depth at water intakes: promotional work Riga Technical University, 2008, 80 p.

82. Neilands R. The theoretical analysis of the method of scour development in time for engineering structures: promotional work 2010, 99 p.

83. Neilands R., Gjunsburgs B., Jaudzems G. Wastewater Treatment Plant Hydraulic Performance Improvement // The 8th International Conference Environmental

Engineering. Water Engineering,Energy for Buildings Vilnius, 19-20 May, Lithuania: Vilnius Gediminas Technical University Press “Technika,” 2011, Vol. 2, pp. 555–561.

84. Neill C. Guide to Bridge Hydraulics University of Toronto Press, 1973, 191 p.

85. Oliveto G., Hager W.H. Temporal evolution of clear water pier and abutment scour // Journal of Hydraulic Engineering, ASCE 2002, Vol. 128, № 9, pp. 811–820.

86. Oliveto G., Hager W.H. Further Results to Time-Dependent Local Scour at Bridge Elements // Journal of Hydraulic Engineering 2005, Vol. 131, № February, pp. 97–105.

87. Pilgrim D., Cordery I. Flood runoff // Handbook of hydrology / ed. Maidment D. New York: McGraw- Hill, 1993, 386 p.

88. Radice A., Franzetti S., Ballio F. Local scour at bridge abutments Vol.2 // Proc. of River Flow 2002 / ed. in Bousmar & Zech (eds) Louvain-La-Neuve, Belgium, 2002, Vol. 2, pp. 1059–1068.

89. Rahman Md.M., Haque M.A. Local scour estimation at bridge site: Modification and application of Lacey formula // International Journal of Sediment Research 2003, Vol. 18, № 4, pp. 333–339.

90. Rajaratnam N., Nwachukwu B.W. Flow near groyne-like structures // Journal of Hydraulic Engineering, 1983, Vol. 109, № 3, pp. 463–480.

91. EEA Technical Report. Mapping the impacts of natural hazards and technological accidents in Europe 2010, № 13, 144 p.

92. Richardson E.V., Davis S. Evaluating scour at bridges. 3rd Ed. Hydraulic Engineering Circular No18. Publ.No FHWA-10-90-017 Washington, DC, USA,: FHWA, USDOT, 1995, 240 p.

93. Richardson E.V., Davis S.R. Evaluating scour at bridges. 4th Ed. Hydraulic Engineering Circular 2001, Vol. No18., № Publ.No FHWA-NHI-01-001, 378 p.

94. Richardson E.V., Davis S.R. Evaluating scour at at bridges. 3rd ed. Of Hydraulic Engineering Circular, No18 Washington D.C., U.S. Department of Transportation, Federal Highway Administration, 1995, 132 p.

95. Richardson E.V., Simons D.B., Julien P. Highways in the river environment (HIRE). Report No.FHWA-HI-90-016. Washington, DC, USA: FHWA, 1990, 683 p.

96. Shen H.W., Schneider V.R., Karaki S.S. Mechanics of local scour US Department of Commerce, National Bureau of Standards, Institute of Applied Technology, 1966, 56 p.

97. Sherman L.K. Streamflow from rainfall by the unit-graph method // Engineering News Record 1932, Vol. 108, pp. 501–505.

98. Snyder F.F. Synthetic unit-graphs // Transactions, American Geophysical Union 1938, Vol. 19, № 1, pp. 447–454.

99. Sokolov A.A., Rantz S.E., Roche M. Methods of developing design flood hydrographs: Flood computation methods compiled from world experience Paris: UNESCO, 1976, 120 p.

100. Sturm T.W. Enhanced abutment scour studies for compound channels. Final Report No.FHWA-RD-99-156 McLean, VA, USA, FHWA, USDOT, 2004, 144 p.

101. Sturm T.W. Scour Around Bankline and Setback Abutments in Compound Channels // Journal of Hydraulic Engineering 2006, Vol. 132, № 1, pp. 21–32.

102. Sturm T.W., Janjua N.S. Clear-water scour around abutments in floodplains // Journal of Hydraulic Engineering 1994, Vol. 120, № 8, pp. 956–766.

103. De Sutter R., Verhoeven R. Simulation of sediment transport during flood events : laboratory work and field experiments // Hydrological Scienc 2001, Vol. 46, № 4, pp. 599–610.

104. Tey C.B. Local scour at bridge abutments. Research report No.329 Auckland, New Zealand, School of Engineering, University of Auckland, 1984, № 329, 111 p.

105. Thomas A. Discussion of local scour around bridge crossings // Transactions of the ASCE / ed. Laursen E.M. Transactions of the ASCE, 1962, Vol. 127, № 1, pp. 631–639.

106. Tregnaghi M., Marion A. Scour development at bed sills under unsteady flow conditions // Proc. of River Flow 2008, Vol.2 / ed. Altinkar et al. Izmir, Turkey, 2008, Vol. 2, pp. 1621–1628.

107. US Department of Agriculture. Hydrology // National Engineering Handbook Washington: U.S. Dept. of Agriculture, 1985, pp. 16–1 – 16–23.

108. Wong W.H. Scour at bridge abutments. Research Report No275 Auckland, New Zealand, School of Engineering, University of Auckland, 1982, 109 p.

109. Yang Z., Han D. Derivation of unit hydrograph using a transfer function approach // Water Resources Research 2006, Vol. 42, № 1, pp. 1–9.

110. Yanmaz A.M. Interpretation of hydrologic aspects of clear-water scour at bridge elements // Proc.of Conference on Fluvial Hydraulics River Flow 2008, Proc. of River Flow 2008 / ed. in Altinkar et al. (eds) Izmir, Turkey, 2008, pp. 1569–1575.

111. Yanmaz A.M., Celebi T. A reliability model for bridge abutment scour // Turkish Journal of Engineering & Environmental Sciences 2001, Vol. 28, pp. 67–83.

112. Young G.K. et al. Testing abutment scour model // Proc.of Water Resources Engineering Memphis, TN, USA: ASCE, 1998, pp. 180–185.

113. Yue S. et al. Approach for Describing Statistical Properties of Flood Hydrograph ´ // Journal of Hydrologic Engineering 2002, Vol. 7, № 2, pp. 147–153.

114. Yue S., Hashino M. Unit hydrographs to model quick and slow runoff components of streamflow // Journal of Hydrology 2000, Vol. 227, № 1-4, pp. 195–206.

115. Zagloul N.A. Analytical and experimental investigations of flow around a spur dike Ontario, Canada, University of Winsdor, 1974, 203 p.

116. Леви И.И. Динамика русловых потоков. Москва: Госэнергоиздат, 1957, 252 p.

117. Нежиховский Р.А. Русловая сеть бассейна и процесс формирования стока воды. Leningrad, Russia: Hydrometeorological, 1971, 475 p.

118. Ротенбург И., Вольнов В. Примеры проектирования мостовых переходов. Москва: Высшая школа, 1969, 284 p.

119. Ротенбург И.С., Вольнов В.С., Поляков М.П. Мостовые переходы. Москва: Высшая школа, 1977, 328 p.

120. Студеничников Б. Размывающая способность потока и методы русловых расчетов. Москва: Стройиздат, 1964, 184 p.

121. Ярославцев И.А. Расчет местного размыва у мостовых опор. Москва, 1956, Vol. 80 16 p.

LIST OF SYMBOLS

A - parameter in the Levi formula;
a - blocked flow area by the embankment and abutment;
a_1 - opening ratio;
b - parameter equal to $Am \cdot V_l^4 k$;
B - width of a scour hole;
b_d - width of cylindrical pier;
b_s - size of analogous pier;
C_0 - best-fit constant in Sturm equation;
C_r - best-fit coefficient in Sturm equation;
d - sediment size;
D - coefficient depending on flow contraction rate and kinetic parameter $P_{KB;}$
d - grain size of the bed material;
d_{16} - grain size (particle size for which 16% are finer by weight);
d_{50} - median grain size (particle size for which 50% are finer by weight);
d_{50a} - median grain size of critical armor layer;
d_{84} - medium grain size (particle size for which 84% are finer by weight);
D_i - constant parameter in steady flow time step;
d_{max} - maximum particle size;
d_s - scour depth;
f - Lacey silt factor;
F_c - Froude number when the sediment is at incipient motion condition;
F_f - Froude number of at approach section;
Fr - Froude number;
Fr_{af} - approach flow Froude number upstream of the abutment;
g - gravitational acceleration;
h - flow depth;
h_2 - total depth of flow including scour depth;
h_{af} - approach flow depth;
h_b - average depth of the flow in bridge opening;
h_c - flow depth in main channel;
h_{equil} - equilibrium scour depth;
h_f - average depth of the flow in floodplain;
$h_{f\,II}$ - depth of the floodplain of the second flood;
h_{fl} - average depth of flow in floodplain;
h_s - scour depth;
$h_{s\,I}$ - scour depth developed during first flood;
h_{s1} - depth of scour in first step of hydrograph;
i - the slope of the river bed;
k - coefficient of changes in the discharge due to the scour;
K - adjustment factor;
K_Θ - abutment alignment factor;
K_σ - sediment size factor;
K^*_Θ - adjusted alignment factor for intermediate abutments;
K_1 - abutment shape factor;
k_1 - amplification factor depending on the type of obstruction;
K_1 - coefficient for construction shape;
K_2 - coefficient for angle of embankment to flow;

k_2 - constant depending on flow intensity;
K_b - discharge module of bridge opening;
K_d - adjustment factor;
K_f - discharge module of floodplain;
k_f - spiral-flow adjustment factor;
K_G - channel geometry factor;
k_{gr} - grain roughness;
K_h - adjustment factor;
k_m - coefficient of side wall slope;
K_S - abutment shape factor;
k_s - coefficient of the angle of flow crossing;
K_s^* - adjusted shape factor for intermediate abutments;
K_{ST} - spill-through abutment shape factor;
k_v - dimensionless velocity adjustment factor;
L - channel / flume / flow width;
L' - length of active flow obstructed by embankment;
L_a - abutment length;
L_a^* - projected length of abutment panning the floodplain;
l_b - the width of bridge opening;
M - geometric constriction ratio;
m - steepness of the scour hole;
M_1 - discharge contraction ratio;
M_1 - discharge distribution factor in approach section;
M_2 - constant for a specific river;
n - Manning's roughness coefficient;
N - shape factor;
n_b - Manning's roughness coefficient for channel bed;
n_c - Manning's roughness coefficient for main channel;
n_f - Manning's roughness coefficient for floodplain;
N_i - parameter for scour calculation;
P - unsteady flow parameter;
p_f - mass density of water;
Q - flow discharge;
q - flow discharge;
q_1 - flow rate per unit width in approach section;
q_2 - flow rate per unit width in contracted section;
Q_a - flow discharge in obstructed area over a length equal to abutment length;
q_{afl} - flow rate per unit width in the approach obstructed portion of floodplain;
Q_b - discharge through the bridge opening under open-flow conditions;
Q_c - discharge in main channel for uniform flow in compound channel;
Q_{fl} - discharge in approach floodplain;
Q_s - sediment discharge out of the scour hole;
Q_w - specific discharge for a certain width w near the abutment tip;
S - shape factor / specific gravity of sediment;
t - time;
T - relative time;
t'_p - equivalent scour duration;
t_{eo} - equilibrium scour time;
t_i - time interval,
u_{*c} - approach flow critical bed shear velocity;

V - average / approach flow velocity;
V_0 - critical velocity;
$V_{0t\,II}$ - critical velocity at the depth of the scour hole $h_{s\,I}$;
V_{0t2} - critical velocity at the depth of the scour hole h_{s1};
V_{af} - average approach flow velocity;
V_{afl} - approach flow velocity in floodplain;
V_b - flow velocity in bridge opening under un-contracted conditions;
v_c - critical flow velocity;
V_c - sediment critical velocity;
V_{cc} - critical velocity for the un-constructed approach flow in the main channel evaluated for normal flow depth h_c in the main channel;
V_{flc} - critical velocity for the un-constructed approach flow in the floodplain evaluated for h_f;
V_l - the local velocity at the abutment;
$V_{l\,II}$ - local velocity of the second flood, with the flat river bed supposed;
$V_{lt\,II}$ - local velocity at the depth of the scour hole $h_{s\,I}$;
V_{lt2} - local velocity at the depth of the scour hole h_{s1};
V_{ob} - approach flow velocity in obstructed area by embankment;
V_p - approach velocity at peak discharge;
V_R - resultant flow velocity;
w - volume of scour hole;
x - parameter determined from graphical relation;
y_1 - approach flow depth;
y_2 - flow depth in contracted section after scour;
y_f - specific weight of water;
y_s - specific weight of sediment;
α - coefficient equal to 3.9;
β - the coefficient of reduction in critical velocity due to vortex;
γ - the specific weight of sediments;
Δy_s - equal to y_s - y_f;
ΔZ - difference in water levels at the corner of the abutment;
$\Delta\rho_s$ - equal to ρ_s - ρ_f;
Θ - angle of embankment to flow;
ρ_f - mass density of water;
ρ_s - mass density of sediment;
Ψ - parameter for turbulent flow;
ω_b - cross section of the flow in bridge opening;
ω_f - cross section of the flow in floodplain;
τ_0 - bed shear stress of approach flow;
τ_c - critical shear stress of sediment particles;
τ_{*c} - critical value of Shields' parameter;
σ - sediment uniformity parameter;
φ - the local velocity coefficient;

APPENDIX I

Initial data for flood models and comparison of the scour evolution results for different sediment sizes are included in this appendix. The sediment size and specific weight used for models: 0.24mm, 1.6 t/m^3; 0.50mm, 1.7 t/m^3; 0.67mm, 1.7 t/m^3; 1.00mm, 1.8 t/m^3.

5.1 Initial data for floods with different probability

Table A1.1

Initial data for single flood model of 1% probability and duration of 7 days (168 h). d_i = 0.67mm, γ_i = 1.7 t/m^3

Step N^0	N	h_f [m]	Q/Q_b	Δh [m]	Q [m^3/h]	T_{step} [h]
						1:2
1	1	0.185	1.047	0.2172	510	9.34
2	3	1.720	1.865	0.3156	1440	9.34
3	6	2.700	2.112	0.5698	3000	9.33
4	8	3.000	2.206	0.6636	3500	9.33
5	10	3.600	2.221	0.8292	4858	9.33
6	11	3.800	2.243	0.9002	5354	9.33
7	10	3.600	2.221	0.8292	4858	22.4
8	8	3.000	2.206	0.6636	3500	22.4
9	6	2.700	2.112	0.5698	3000	22.4
10	3	1.720	1.865	0.3156	1440	22.4
11	1	0.185	1.047	0.2172	510	22.4
					Total t, h	168
					Total t_{rise}, h	56
					Total t_{reces}, h	112

Table A1.2

Initial data for single flood model of 5% probability and duration of 7 days (168 h). d_i = 0.67mm, γ_i = 1.7 t/m^3

Step N^0	N	h_f [m]	Q/Q_b	Δh [m]	Q [m^3/h]	T_{step} [h]
						1:2
1	1	0.185	1.047	0.2172	510	9.34
2	3	1.720	1.865	0.3156	1440	9.34
3	5	2.500	2.052	0.4646	2500	9.33
4	6	2.700	2.112	0.5698	3000	9.33
5	7	2.900	2.124	0.6400	3470	9.33
6	9	3.250	2.177	0.7147	4065	9.33
7	7	2.900	2.124	0.6400	3470	22.4
8	6	2.700	2.112	0.5698	3000	22.4
9	5	2.500	2.052	0.4646	2500	22.4

10	3	1.720	1.865	0.3156	1440	22.4
11	1	0.185	1.047	0.2172	510	22.4
					Total t, h	168
					Total t_{rise}, h	56
					Total t_{reces}, h	112

Table A1.3

Initial data for single flood model of 23% probability and duration of 7 days (168 h). d_i = 0.67mm, γ_i = 1.7 t/m^3

Step N^0	N	h_f [m]	Q/Q_b	Δh [m]	Q [m^3/h]	T_{step} [h] 1:2
1	1	0.185	1.047	0.2172	510	9.34
2	2	0.975	1.542	0.1926	760	9.34
3	3	1.720	1.865	0.3156	1440	9.33
4	4	2.300	2.021	0.4242	2200	9.33
5	5	2.500	2.052	0.4646	2500	9.33
6	6	2.700	2.112	0.5698	3000	9.33
7	5	2.500	2.052	0.4646	2500	22.4
8	4	2.300	2.021	0.4242	2200	22.4
9	3	1.720	1.865	0.3156	1440	22.4
10	2	0.975	1.542	0.1926	760	22.4
11	1	0.185	1.047	0.2172	510	22.4
					Total t, h	168
					Total t_{rise}, h	56
					Total t_{reces}, h	112

Table A1.4

Initial data for multiple flood models of different probability. Three floods of 5% probability and duration of 7 days (168h) each. t_{rise} / t_{reces} = 1 / 2, d_i = 0.67mm, γ_i = 1.7 t/m^3

Step N^0	N	h_f [m]	Q/Q_b	Δh [m]	Q [m^3/s]	T_{step} [h]
1	1	0.185	1.047	0.2172	510	9.34
2	2	0.975	1.542	0.1926	760	9.34
3	3	1.720	1.865	0.3156	1440	9.33
4	5	2.500	2.052	0.4646	2500	9.33
5	7	2.900	2.124	0.6400	3470	9.33
6	9	3.250	2.177	0.7147	4065	9.33
7	7	2.900	2.124	0.6400	3470	22.4
8	5	2.500	2.052	0.4646	2500	22.4
9	3	1.720	1.865	0.3156	1440	22.4
10	2	0.975	1.542	0.1926	760	22.4
11	1	0.185	1.047	0.2172	510	22.4
12	1	0.185	1.047	0.2172	510	9.34
13	2	0.975	1.542	0.1926	760	9.34
14	3	1.720	1.865	0.3156	1440	9.33
15	5	2.500	2.052	0.4646	2500	9.33
16	7	2.900	2.124	0.6400	3470	9.33
17	9	3.250	2.177	0.7147	4065	9.33

18	7	2.900	2.124	0.6400	3470	22.4
19	5	2.500	2.052	0.4646	2500	22.4
20	3	1.720	1.865	0.3156	1440	22.4
21	2	0.975	1.542	0.1926	760	22.4
22	1	0.185	1.047	0.2172	510	22.4
23	1	0.185	1.047	0.2172	510	9.34
24	2	0.975	1.542	0.1926	760	9.34
25	3	1.720	1.865	0.3156	1440	9.33
26	5	2.500	2.052	0.4646	2500	9.33
27	7	2.900	2.124	0.6400	3470	9.33
28	9	3.250	2.177	0.7147	4065	9.33
29	7	2.900	2.124	0.6400	3470	22.4
30	5	2.500	2.052	0.4646	2500	22.4
31	3	1.720	1.865	0.3156	1440	22.4
32	2	0.975	1.542	0.1926	760	22.4
33	1	0.185	1.047	0.2172	510	22.4
11	1	0.185	1.047	0.2172	510	22.4
					Total *t*, h	504

Table A1.5

Initial data for multiple flood models of different probability. Three floods of 1% probability and duration of 7 days (168h) each. t_{rise} / t_{reces} = 1 / 2, d_i = 0.67mm, γ_i = 1.7 t/m^3

Step N^0	N	h_f [m]	Q/Q_b	Δh [m]	Q [m^3/s]	T_{step} [h]
1	1	0.185	1.047	0.2172	510	9.34
2	3	1.720	1.865	0.3156	1440	9.34
3	5	2.500	2.052	0.4646	2500	9.33
4	7	2.900	2.124	0.6400	3470	9.33
5	9	3.250	2.177	0.7147	4065	9.33
6	11	3.800	2.243	0.9002	5354	9.33
7	9	3.250	2.177	0.7147	4065	22.4
8	7	2.900	2.124	0.6400	3470	22.4
9	5	2.500	2.052	0.4646	2500	22.4
10	3	1.720	1.865	0.3156	1440	22.4
11	1	0.185	1.047	0.2172	510	22.4
12	1	0.185	1.047	0.2172	510	9.34
13	3	1.720	1.865	0.3156	1440	9.34
14	5	2.500	2.052	0.4646	2500	9.33
15	7	2.900	2.124	0.6400	3470	9.33
16	9	3.250	2.177	0.7147	4065	9.33
17	11	3.800	2.243	0.9002	5354	9.33
18	9	3.250	2.177	0.7147	4065	22.4
19	7	2.900	2.124	0.6400	3470	22.4
20	5	2.500	2.052	0.4646	2500	22.4
21	3	1.720	1.865	0.3156	1440	22.4
22	1	0.185	1.047	0.2172	510	22.4
23	1	0.185	1.047	0.2172	510	9.34
24	3	1.720	1.865	0.3156	1440	9.34
25	5	2.500	2.052	0.4646	2500	9.33
26	7	2.900	2.124	0.6400	3470	9.33
27	9	3.250	2.177	0.7147	4065	9.33

28	11	3.800	2.243	0.9002	5354	9.33
29	9	3.250	2.177	0.7147	4065	22.4
30	7	2.900	2.124	0.6400	3470	22.4
31	5	2.500	2.052	0.4646	2500	22.4
32	3	1.720	1.865	0.3156	1440	22.4
33	1	0.185	1.047	0.2172	510	22.4
1	1	0.185	1.047	0.2172	510	9.34
					Total *t*, h	504

5.2 Comparison of the results of multiple floods with different probability using different river bed particle sizes

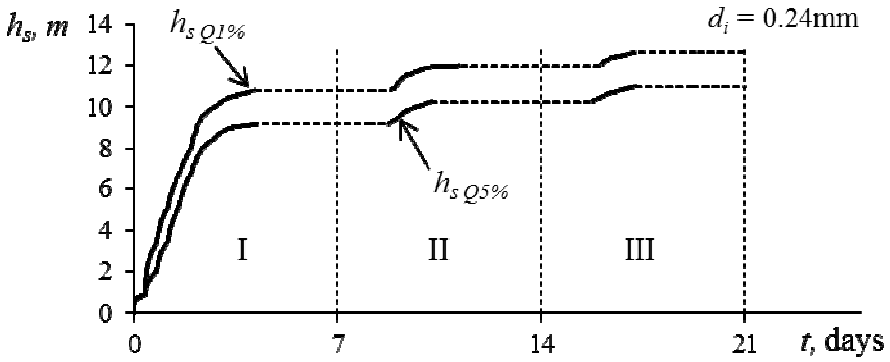

Figure A1.1. Comparison of scour development during a series of three floods with probability 1% and 5%, d_i = 0.24mm

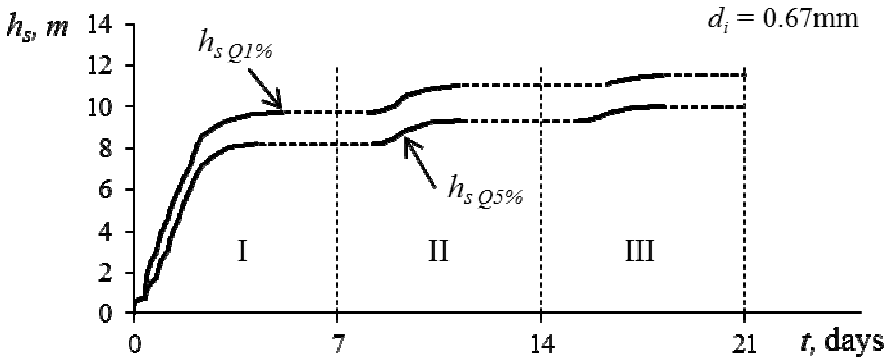

Figure A1.2. Comparison of scour development during a series of three floods with probability 1% and 5%, d_i = 0.67mm

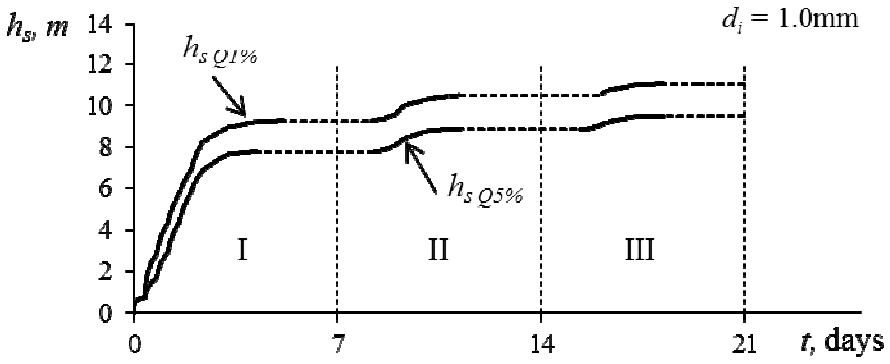

Figure A1.3. Comparison of scour development during a series of three floods with probability 1% and 5%, d_i = 1.00mm

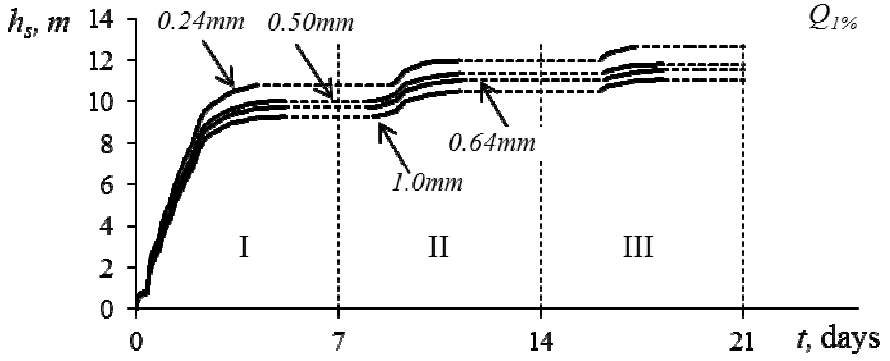

Figure A1.4. Comparison of scour development during a series of three floods with probability 1% and different sediment sizes d_i

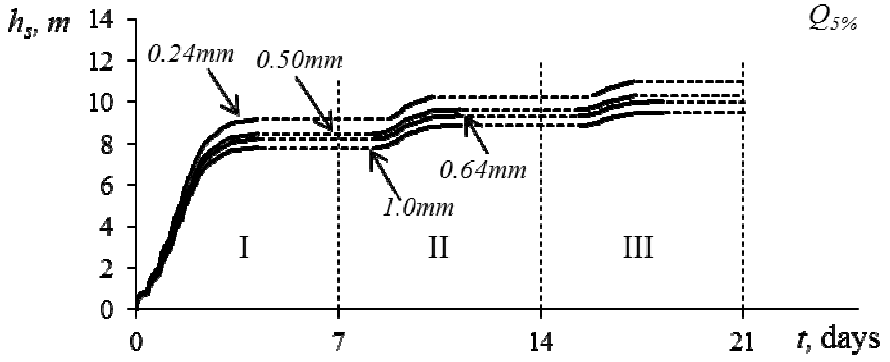

Figure A1.5. Comparison of scour development during a series of three floods with probability 5% and different sediment sizes d_i

5.3 Initial data for floods with different duration

Table A1.6

Initial data for single flood model of 5% probability. Duration 7 days (168h) and 14 days (336h). t_{rise} / t_{reces} = 1 / 2, d_i = 0.67mm, γ_i = 1.7 t/m^3

Step N^0	N	h_f [m]	Q/Q_b	Δh [m]	Q [m^3/h]	$T_{step\ 1}$ [h] 1:2	$T_{step\ 2}$ [h] 1:2
1	1	0.185	1.047	0.2172	510	7	14
2	2	0.975	1.542	0.1926	760	7	14
3	3	1.720	1.865	0.3156	1440	7	14
4	4	2.300	2.021	0.4242	2200	7	14
5	5	2.500	2.052	0.4646	2500	7	14
6	6	2.700	2.112	0.5698	3000	7	14
7	8	3.000	2.206	0.6636	3500	7	14
8	9	3.250	2.177	0.7147	4065	7	14
9	8	3.000	2.206	0.6636	3500	16	32
10	6	2.700	2.112	0.5698	3000	16	32
11	5	2.500	2.052	0.4646	2500	16	32
12	4	2.300	2.021	0.4242	2200	16	32
13	3	1.720	1.865	0.3156	1440	16	32
14	2	0.975	1.542	0.1926	760	16	32
15	1	0.185	1.047	0.2172	510	16	32
					Total t, h	168	336
					Total t_{rise}, h	56	112
					Total t_{reces}, h	112	224

Table A1.7

Initial data for a serie of three floods of 5% probability and duration for first model- 3 x 7 days (3 x 168h) and for second one – 3 x 14 days (3 x 336h). t_{rise} / t_{reces} = 1 / 2, d_i = 0.67mm, γ_i = 1.7 t/m^3

Step N^0	N	h_f [m]	Q/Q_b	Δh [m]	Q [m^3/h]	$T_{step\ 1}$ [h] 1:2	$T_{step\ 2}$ [h] 1:2
1	1	0.185	1.047	0.2172	510	9.34	18.66
2	2	0.975	1.542	0.1926	760	9.34	18.66
3	3	1.720	1.865	0.3156	1440	9.33	18.67
4	5	2.500	2.052	0.4646	2500	9.33	18.67
5	7	2.900	2.124	0.6400	3470	9.33	18.67
6	9	3.250	2.177	0.7147	4065	9.33	18.67
7	7	2.900	2.124	0.6400	3470	22.4	44.8
8	5	2.500	2.052	0.4646	2500	22.4	44.8
9	3	1.720	1.865	0.3156	1440	22.4	44.8
10	2	0.975	1.542	0.1926	760	22.4	44.8
11	1	0.185	1.047	0.2172	510	22.4	44.8
12	1	0.185	1.047	0.2172	510	9.34	18.66
13	2	0.975	1.542	0.1926	760	9.34	18.66
14	3	1.720	1.865	0.3156	1440	9.33	18.67

15	5	2.500	2.052	0.4646	2500	9.33	18.67
16	7	2.900	2.124	0.6400	3470	9.33	18.67
17	9	3.250	2.177	0.7147	4065	9.33	18.67
18	7	2.900	2.124	0.6400	3470	22.4	44.8
19	5	2.500	2.052	0.4646	2500	22.4	44.8
20	3	1.720	1.865	0.3156	1440	22.4	44.8
21	2	0.975	1.542	0.1926	760	22.4	44.8
22	1	0.185	1.047	0.2172	510	22.4	44.8
23	1	0.185	1.047	0.2172	510	9.34	18.66
24	2	0.975	1.542	0.1926	760	9.34	18.66
25	3	1.720	1.865	0.3156	1440	9.33	18.67
26	5	2.500	2.052	0.4646	2500	9.33	18.67
27	7	2.900	2.124	0.6400	3470	9.33	18.67
28	9	3.250	2.177	0.7147	4065	9.33	18.67
29	7	2.900	2.124	0.6400	3470	22.4	44.8
30	5	2.500	2.052	0.4646	2500	22.4	44.8
31	3	1.720	1.865	0.3156	1440	22.4	44.8
32	2	0.975	1.542	0.1926	760	22.4	44.8
33	1	0.185	1.047	0.2172	510	22.4	44.8
					Total *t*, h	504	1008

5.4 Comparison of the results of multiple floods with different duration using different river bed particle sizes

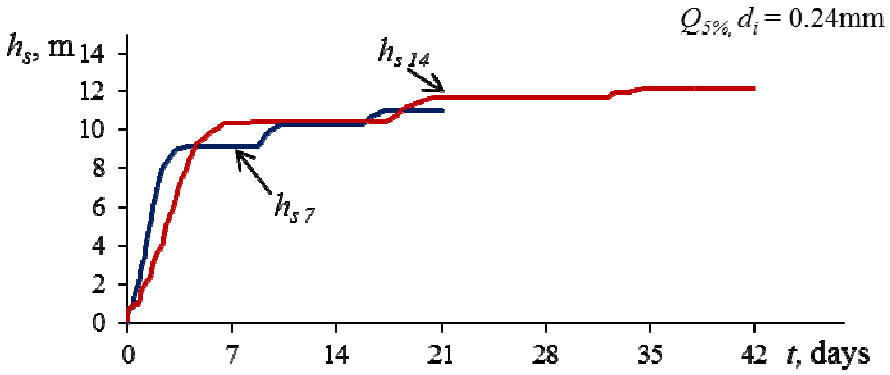

Figure A1.6. Comparison of scour depth for three following floods with 7-days or 14-days duration; sediment size d_i = 0.24mm

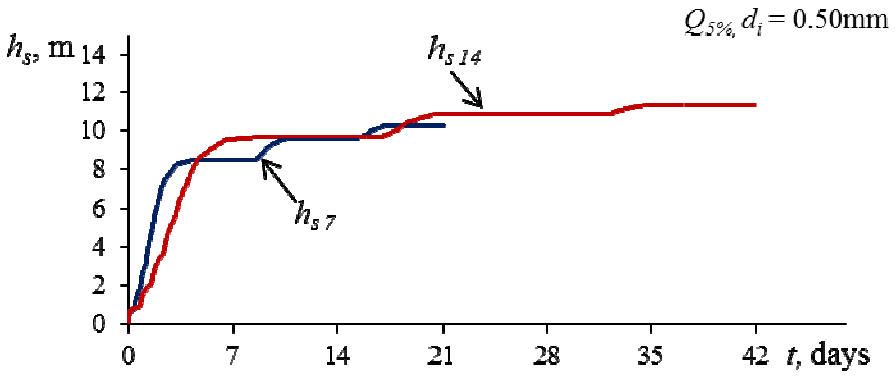

Figure A1.7. Comparison of scour depth for three following floods with 7-days or 14-days duration; sediment size d_i = 0.50mm

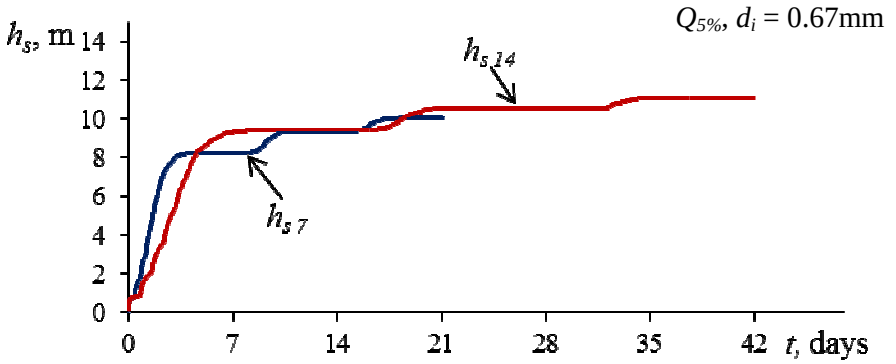

Figure A1.8. Comparison of scour depth for three following floods with 7-days or 14-days duration; sediment size d_i = 0.67mm

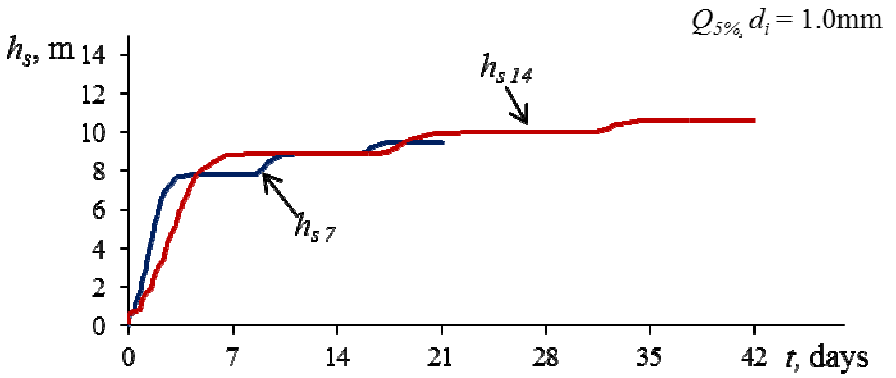

Figure A1.9. Comparison of scour depth for three following floods with 7-days or 14-days duration; sediment size d_i = 1.0mm

5.5 Initial data for multiple floods of different frequency

Table A1.8

Four floods of 5% probability and duration of 7 days (168h) each. t_{rise} / t_{reces} = 1 / 2, d_i = 0.67mm, γ_i = 1.7 t/m^3

Step N^0	N	h_f [m]	Q/Q_b	Δh [m]	Q [m^3/s]	T_{step} [h]
1	1	0.185	1.047	0.2172	510	9.34
2	2	0.975	1.542	0.1926	760	9.34
3	3	1.720	1.865	0.3156	1440	9.33
4	5	2.500	2.052	0.4646	2500	9.33
5	7	2.900	2.124	0.6400	3470	9.33
6	9	3.250	2.177	0.7147	4065	9.33
7	7	2.900	2.124	0.6400	3470	22.4
8	5	2.500	2.052	0.4646	2500	22.4
9	3	1.720	1.865	0.3156	1440	22.4
10	2	0.975	1.542	0.1926	760	22.4
11	1	0.185	1.047	0.2172	510	22.4
12	1	0.185	1.047	0.2172	510	9.34
13	2	0.975	1.542	0.1926	760	9.34
14	3	1.720	1.865	0.3156	1440	9.33
15	5	2.500	2.052	0.4646	2500	9.33
16	7	2.900	2.124	0.6400	3470	9.33
17	9	3.250	2.177	0.7147	4065	9.33
18	7	2.900	2.124	0.6400	3470	22.4
19	5	2.500	2.052	0.4646	2500	22.4
20	3	1.720	1.865	0.3156	1440	22.4
21	2	0.975	1.542	0.1926	760	22.4
22	1	0.185	1.047	0.2172	510	22.4
23	1	0.185	1.047	0.2172	510	9.34
24	2	0.975	1.542	0.1926	760	9.34
25	3	1.720	1.865	0.3156	1440	9.33
26	5	2.500	2.052	0.4646	2500	9.33
27	7	2.900	2.124	0.6400	3470	9.33
28	9	3.250	2.177	0.7147	4065	9.33
29	7	2.900	2.124	0.6400	3470	22.4
30	5	2.500	2.052	0.4646	2500	22.4
31	3	1.720	1.865	0.3156	1440	22.4
32	2	0.975	1.542	0.1926	760	22.4
33	1	0.185	1.047	0.2172	510	22.4
34	1	0.185	1.047	0.2172	510	9.34
35	2	0.975	1.542	0.1926	760	9.34
36	3	1.720	1.865	0.3156	1440	9.33
37	5	2.500	2.052	0.4646	2500	9.33
38	7	2.900	2.124	0.6400	3470	9.33
39	9	3.250	2.177	0.7147	4065	9.33
40	7	2.900	2.124	0.6400	3470	22.4
41	5	2.500	2.052	0.4646	2500	22.4
42	3	1.720	1.865	0.3156	1440	22.4
43	2	0.975	1.542	0.1926	760	22.4
44	1	0.185	1.047	0.2172	510	22.4
					Total t, h	840

5.6 Comparison of the results of multiple floods with different frequency using different river bed particle sizes

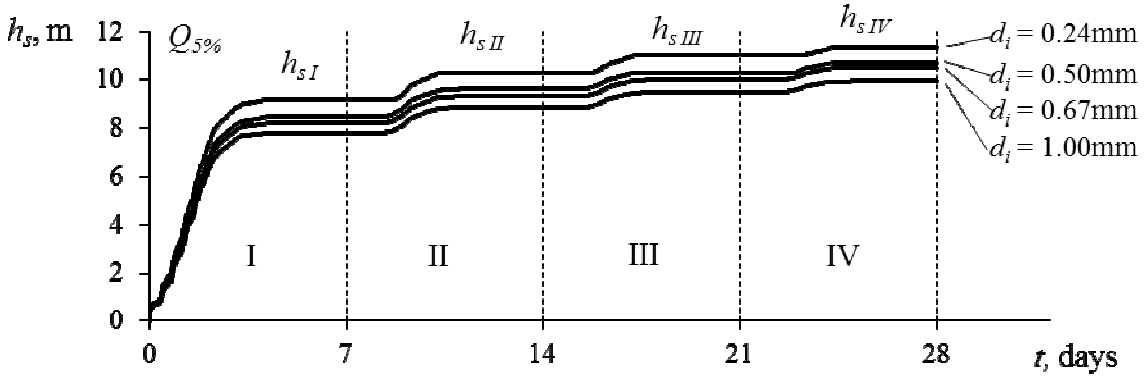

Figure A1.10. Scour development in time for floods with different frequencies and sediment sizes; $h_{s\,I}$ to $h_{s\,IV}$ are scour depths reached after first to fourth flood respectively

5.7 Initial data for multiple floods of different sequence

Three following floods of 14 days (336h) duration each were chosen. The floods of 1% probability and 23% probability were modeled in different order.

Table A1.9

Three floods of 1% probability and duration of 14 days (336h) each. t_{rise} / t_{reces} = 1 / 2, d_i = 1.00mm, γ_i = 1.8 t/m^3

Step N^0	***N***	h_f [m]	Q/Q_b	Δh [m]	***Q*** [m^3/s]	T_{step} [h]
1	1	0.185	1.047	0.2172	510	18.68
2	3	1.720	1.865	0.3156	1440	18.68
3	5	2.500	2.052	0.4646	2500	18.66
4	7	2.900	2.124	0.6400	3470	18.66
5	9	3.250	2.177	0.7147	4065	18.66
6	11	3.800	2.243	0.9002	5354	18.66
7	9	3.250	2.177	0.7147	4065	44.80
8	7	2.900	2.124	0.6400	3470	44.80
9	5	2.500	2.052	0.4646	2500	44.80
10	3	1.720	1.865	0.3156	1440	44.80
11	1	0.185	1.047	0.2172	510	44.80
12	1	0.185	1.047	0.2172	510	18.68
13	3	1.720	1.865	0.3156	1440	18.68
14	5	2.500	2.052	0.4646	2500	18.66
15	7	2.900	2.124	0.6400	3470	18.66
16	9	3.250	2.177	0.7147	4065	18.66
17	11	3.800	2.243	0.9002	5354	18.66
18	9	3.250	2.177	0.7147	4065	44.80
19	7	2.900	2.124	0.6400	3470	44.80

20	5	2.500	2.052	0.4646	2500	44.80
21	3	1.720	1.865	0.3156	1440	44.80
22	1	0.185	1.047	0.2172	510	44.80
23	1	0.185	1.047	0.2172	510	18.68
24	3	1.720	1.865	0.3156	1440	18.68
25	5	2.500	2.052	0.4646	2500	18.66
26	7	2.900	2.124	0.6400	3470	18.66
27	9	3.250	2.177	0.7147	4065	18.66
28	11	3.800	2.243	0.9002	5354	18.66
29	9	3.250	2.177	0.7147	4065	44.80
30	7	2.900	2.124	0.6400	3470	44.80
31	5	2.500	2.052	0.4646	2500	44.80
32	3	1.720	1.865	0.3156	1440	44.80
33	1	0.185	1.047	0.2172	510	44.80
					Total *t*, h	1008

Table A1.10

One flood with low probability (1%) followed by two floods of higher probability (23%), duration of each flood 14 days (336h). t_{rise} / t_{reces} = 1 / 2, d_i = 1.00mm, γ_i = 1.8 t/m^3

Step N^0	N	h_f [m]	Q/Q_b	Δh [m]	Q [m^3/s]	T_{step} [h]
1	1	0.185	1.047	0.2172	510	18.68
2	3	1.720	1.865	0.3156	1440	18.68
3	5	2.500	2.052	0.4646	2500	18.66
4	7	2.900	2.124	0.6400	3470	18.66
5	9	3.250	2.177	0.7147	4065	18.66
6	11	3.800	2.243	0.9002	5354	18.66
7	9	3.250	2.177	0.7147	4065	44.80
8	7	2.900	2.124	0.6400	3470	44.80
9	5	2.500	2.052	0.4646	2500	44.80
10	3	1.720	1.865	0.3156	1440	44.80
11	1	0.185	1.047	0.2172	510	44.80
12	1	0.185	1.047	0.2172	510	18.68
13	2	0.975	1.542	0.1926	760	18.68
14	3	1.720	1.865	0.3156	1440	18.66
15	4	2.300	2.021	0.4242	2200	18.66
16	5	2.500	2.052	0.4646	2500	18.66
17	6	2.700	2.112	0.5698	3000	18.66
18	5	2.500	2.052	0.4646	2500	44.80
19	4	2.300	2.021	0.4242	2200	44.80
20	3	1.720	1.865	0.3156	1440	44.80
21	2	0.975	1.542	0.1926	760	44.80
22	1	0.185	1.047	0.2172	510	44.80
23	1	0.185	1.047	0.2172	510	18.68
24	2	0.975	1.542	0.1926	760	18.68
25	3	1.720	1.865	0.3156	1440	18.66
26	4	2.300	2.021	0.4242	2200	18.66
27	5	2.500	2.052	0.4646	2500	18.66
28	6	2.700	2.112	0.5698	3000	18.66
29	5	2.500	2.052	0.4646	2500	44.80
30	4	2.300	2.021	0.4242	2200	44.80

31	3	1.720	1.865	0.3156	1440	44.80
32	2	0.975	1.542	0.1926	760	44.80
33	1	0.185	1.047	0.2172	510	44.80
					Total *t*, h	1008

Table A1.11

Two floods with high probability (23%) followed by one floods of low probability (1%), duration of each flood 14 days (336h), t_{rise} / t_{reces} = 1 / 2, d_i = 1.00mm, γ_i = 1.8 t/m^3

Step N^0	N	h_f [m]	Q/Q_b	Δh [m]	Q [m^3/s]	T_{step} [h]
1	1	0.185	1.047	0.2172	510	18.68
2	2	0.975	1.542	0.1926	760	18.68
3	3	1.720	1.865	0.3156	1440	18.66
4	4	2.300	2.021	0.4242	2200	18.66
5	5	2.500	2.052	0.4646	2500	18.66
6	6	2.700	2.112	0.5698	3000	18.66
7	5	2.500	2.052	0.4646	2500	44.80
8	4	2.300	2.021	0.4242	2200	44.80
9	3	1.720	1.865	0.3156	1440	44.80
10	2	0.975	1.542	0.1926	760	44.80
11	1	0.185	1.047	0.2172	510	44.80
12	1	0.185	1.047	0.2172	510	18.68
13	2	0.975	1.542	0.1926	760	18.68
14	3	1.720	1.865	0.3156	1440	18.66
15	4	2.300	2.021	0.4242	2200	18.66
16	5	2.500	2.052	0.4646	2500	18.66
17	6	2.700	2.112	0.5698	3000	18.66
18	5	2.500	2.052	0.4646	2500	44.80
19	4	2.300	2.021	0.4242	2200	44.80
20	3	1.720	1.865	0.3156	1440	44.80
21	2	0.975	1.542	0.1926	760	44.80
22	1	0.185	1.047	0.2172	510	44.80
23	1	0.185	1.047	0.2172	510	18.68
24	3	1.720	1.865	0.3156	1440	18.68
25	5	2.500	2.052	0.4646	2500	18.66
26	7	2.900	2.124	0.6400	3470	18.66
27	9	3.250	2.177	0.7147	4065	18.66
28	11	3.800	2.243	0.9002	5354	18.66
29	9	3.250	2.177	0.7147	4065	44.80
30	7	2.900	2.124	0.6400	3470	44.80
31	5	2.500	2.052	0.4646	2500	44.80
32	3	1.720	1.865	0.3156	1440	44.80
33	1	0.185	1.047	0.2172	510	44.80
					Total *t*, h	1008

5.8 Comparison of the results of multiple floods with different sequence using different river bed particle sizes

Curves in figures are marked by number 1, 2 and and 3, where 1 – scour development according to the flood sequence scenario $Q_{1\%}$ - $Q_{1\%}$ - $Q_{1\%;}$ 2 – flood sequence scenario $Q_{1\%}$ - $Q_{23\%}$ - $Q_{23\%}$ and 3 – flood sequence scenario $Q_{23\%}$ - $Q_{23\%}$ - $Q_{1\%}$.

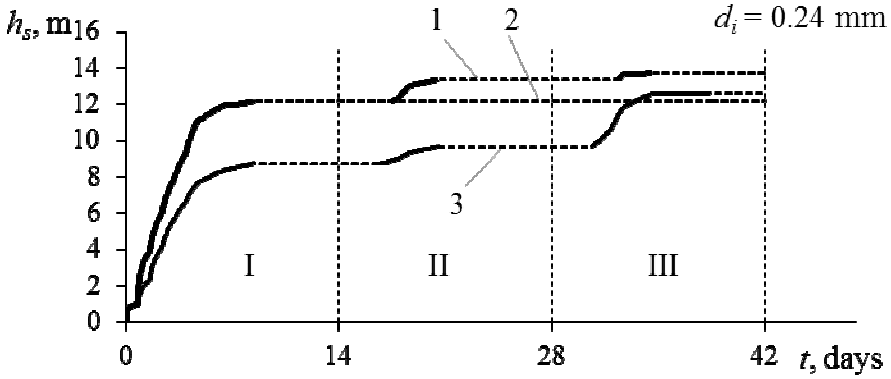

Figure A1.11. Scour development in time for floods of different sequences when the sediment size d_i = 0.24mm

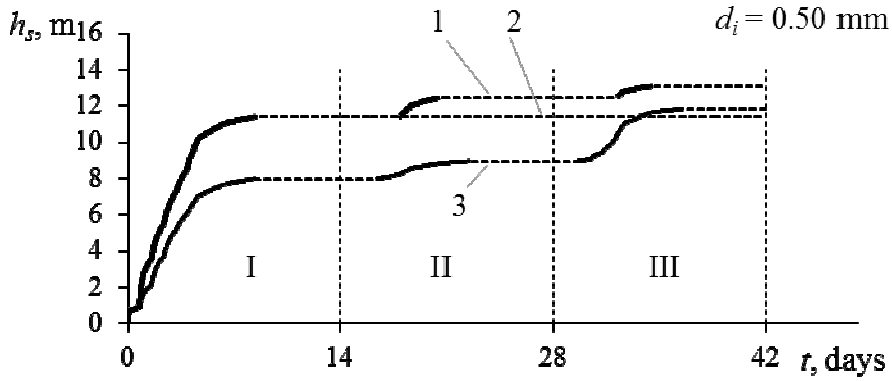

Figure A1.12. Scour development in time for floods of different sequences when the sediment size d_i = 0.50mm

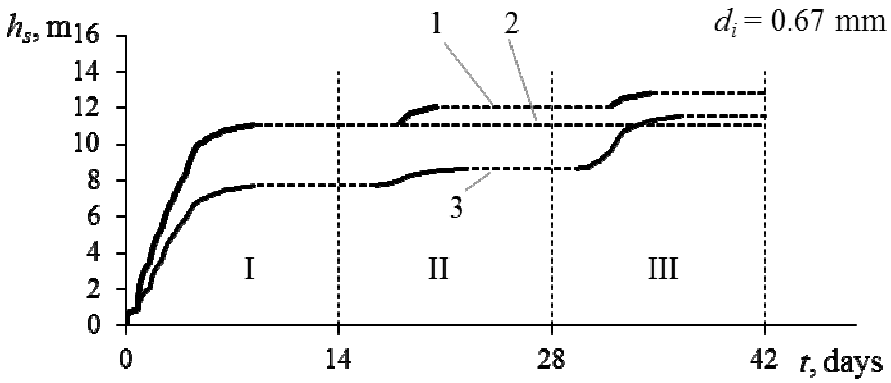

Figure A1.13. Scour development in time for floods of different sequences when the sediment size d_i = 0.67mm

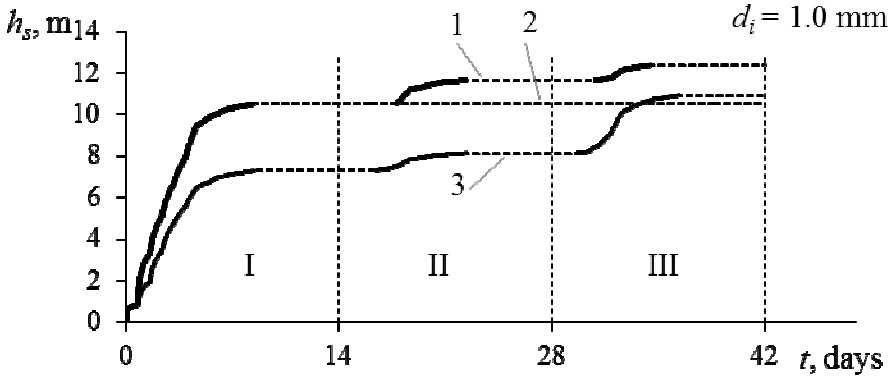

Figure A1.14. Scour development in time for floods of different sequences when the sediment size d_i = 1.0mm

5.9 Initial data for flood models in a study of hydrograph steepness influence on scour evolution

Table A1.12

Initial data for changing of hydrograph steepness if rising part has static duration and recession part changes according to ratios 1:2, 1:3, 1:4, 1:6 and 1:8, d_i = 1.00mm, γ_i = 1.8 t/m^3

Step N^0	N	h_f [m]	Q/Q_b	Δh [m]	Q [m^3/h]	T_{step} [h] 1:2	T_{step} [h] 1:3	T_{step} [h] 1:4	T_{step} [h] 1:6	T_{step} [h] 1:8
1	1	0.185	1.047	0.2172	510	4	4	4	4	4
2	2	0.975	1.542	0.1926	760	4	4	4	4	4
3	3	1.720	1.865	0.3156	1440	4	4	4	4	4
4	5	2.500	2.052	0.4646	2500	4	4	4	4	4
5	7	2.900	2.124	0.6400	3470	4	4	4	4	4
6	9	3.250	2.177	0.7147	4065	4	4	4	4	4
7	7	2.900	2.124	0.6400	3470	9.6	14.4	19.2	28.8	38.4
8	5	2.500	2.052	0.4646	2500	9.6	14.4	19.2	28.8	38.4
9	3	1.720	1.865	0.3156	1440	9.6	14.4	19.2	28.8	38.4
10	2	0.975	1.542	0.1926	760	9.6	14.4	19.2	28.8	38.4
11	1	0.185	1.047	0.2172	510	9.6	14.4	19.2	28.8	38.4
					Total t, h	72	96	120	168	216
					Total t_{rise}, h	**24**	**24**	**24**	**24**	**24**
					Total t_{reces}, h	48	72	96	144	192

Table A1.13

Initial data for changing of the ratio of hydrograph steepness 1:2, 1:3, 1:4, 1:6 and 1:8 for floods with equal duration of 9 days (216 h), , d_i = 1.00mm, γ_i = 1.8 t/m^3

Step N^0	N	h_f [m]	Q/Q_b	Δh [m]	Q [m^3/h]	T_{step} [h] 1:2	T_{step} [h] 1:3	T_{step} [h] 1:4	T_{step} [h] 1:6	T_{step} [h] 1:8
1	1	0.185	1.047	0.2172	510	12	9	7.2	5.14	4
2	2	0.975	1.542	0.1926	760	12	9	7.2	5.14	4
3	3	1.720	1.865	0.3156	1440	12	9	7.2	5.14	4
4	5	2.500	2.052	0.4646	2500	12	9	7.2	5.14	4
5	7	2.900	2.124	0.6400	3470	12	9	7.2	5.14	4
6	9	3.250	2.177	0.7147	4065	12	9	7.2	5.14	4
7	7	2.900	2.124	0.6400	3470	28.8	32.4	34.56	37.03	38.4
8	5	2.500	2.052	0.4646	2500	28.8	32.4	34.56	37.03	38.4
9	3	1.720	1.865	0.3156	1440	28.8	32.4	34.56	37.03	38.4
10	2	0.975	1.542	0.1926	760	28.8	32.4	34.56	37.03	38.4
11	1	0.185	1.047	0.2172	510	28.8	32.4	34.56	37.04	38.4
					Total t, h	**216**	**216**	**216**	**216**	**216**
					Total t_{rise}, h	72	54	43.2	30.84	24
					Total t_{reces}, h	144	162	172.8	185.16	192

APPENDIX II

Sediment discharge concept by Levi I.I. [116]

Sediment discharge is a number of particles crossing the cross section in unit time, to the weight of particles:

$$Q_S = b \cdot q_S = \gamma \frac{N \cdot V}{t} \tag{A2.1}$$

where q_S - sediment discharge in the unit width (in weight units);
N - number of particles passing the cross section on width b in time t;
V - volume of the particles;
b - width.

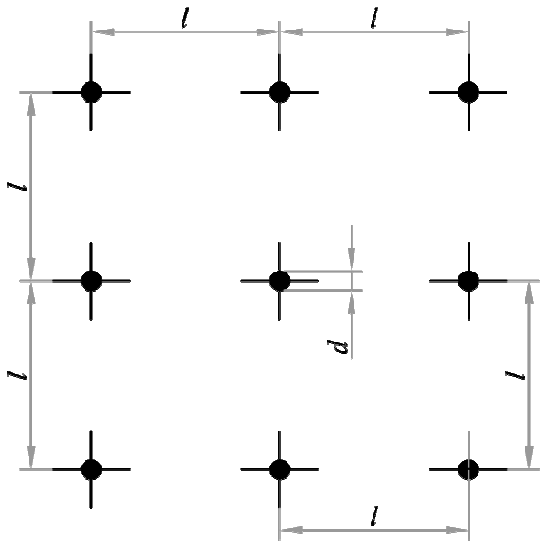

It is proposed that the particles are moving with velocity U_S, with the distance l between them. On the width b there will be $n_1 = \frac{b}{l}$ particles.

The number of particles, which cross the cross section in t [sec.], is determined as a ratio between the distance which they are passing in time t and the distance between two next following particles:

$$n_2 = \frac{U_S \cdot t}{l} \tag{A2.2}$$

where U_S - sediment particle velocity.

The common number of particles on width b is equal:

$$N = n_1 \cdot n_2 = \frac{b \cdot U_s \cdot t}{l^2} \tag{A2.3}$$

Then the sediment discharge per unit width is:

$$\frac{1}{\gamma} q_s = \frac{N \cdot V}{b \cdot t} = \frac{U_s \cdot V}{l^2} = U_s \cdot d \frac{V}{l^2 \cdot d} = U_s dm \tag{A2.4}$$

where $\frac{V}{l^2 \cdot d}$ - the ratio of of the one particle volume to the entire layer of the particles with diameter d on area l^2 - or dynamic coefficient of continuity m

$$m = \frac{V}{l^2 \cdot d} = \frac{\alpha \cdot d^2}{l^2} = f(U_s) \tag{A2.5}$$

where α - depending on the shape of particle,
d – diameter of particle

Velocity of the sediment particles:

$$U_s = f(U - U_0) \tag{A2.6}$$

where U – flow velocity,
U_0 – critical velocity.

Coefficient of the continuity:

$$m = m_1 \left(\frac{U}{\sqrt{gd}} \right)^3 \tag{A2.7}$$

where: $m_1 = f\left(\frac{d}{h}\right)$,
h – depth of the flow.

Then the sediment discharge:

$$q_s = \gamma \cdot U_s \cdot m \cdot d = f(U - U_0) \cdot \gamma \cdot m_1 \left(\frac{U}{\sqrt{gd}} \right)^3 \cdot d = f \left(\frac{U}{\sqrt{gd}} \right)^3 d(U - U_0) \cdot f\left(\frac{d}{h}\right) \cdot \gamma \tag{A2.8}$$

$$\mu_c = \frac{q_s}{q} = C_0\left(\frac{U}{\sqrt{gd}}\right)^3 \frac{d}{h}\left(1-\frac{U_0}{U}\right) f\left(\frac{d}{h}\right) \qquad \text{(A2.9)}$$

where μ_c – relative contents of sediments in flow,
q – relative flow discharge.

If we take into account that:

$$U_0 = a\sqrt{gd}\, f_1\left(\frac{h}{d}\right) \qquad \text{(A2.10)}$$

where a – coefficient 1.15,

and present $f_1\left(\frac{h}{d}\right)$ in exponential form - $\beta\left(\frac{d}{h}\right)^n$, then we have:

$$\mu_c = C\left(\frac{U}{\sqrt{gd}}\right)^3 \left(1-\frac{U_0}{U}\right)\left(\frac{d}{h}\right)^K \qquad \text{(A2.11)}$$

where $K = 1 + n_1 = 1.25$

According to the test results the figure $\mu_C\% = f\left(\frac{U}{\sqrt{gd}}\right)$ with different $\frac{d}{h}$ is presented.

The results of the data processing allow us to form an equation for Q_S.

Sediment discharge in weight units is presented:

$$Q_s = 0.002\left(\frac{U}{\sqrt{gd}}\right)^3 d\left(U-U_0\right)\cdot\left(\frac{d}{h}\right)^{0.25}, \ [T/\text{sec}] \qquad \text{(A2.12)}$$

<u>In volumetric units:</u>

$$Q_s = \frac{5.62}{\gamma}\left(1-\frac{U}{U_0}\right)\frac{1}{d^{0.25}\cdot h^{0.25}}\cdot B\cdot U^4, \ [m^3/day] \qquad \text{(A2.13)}$$

The Eq.(13) is valid for ratio:

$\frac{d}{h} > \frac{1}{500}$

or can be valid till viscosity does not affect the flow motion:

$$\frac{d}{h} > \frac{1}{5000}.$$

Critical velocity concept by Studenitcnikov B.I. [120]

The grain particles threshold stability in a river bed at clear water, steady uniform flow can be determined by using critical velocity V_0, which depends on the following parameters:

γ - specific weight of water,

γ_1 - specific weight of particle,

d - size of particle,

h - depth of flow.

A stable bed is a rectangular channel, formed in a considerable width of flow zone ($B/h \geq 2.5$-3), with normal turbulence and velocities distribution in depth.

1. Lifting force acting on the particle:

$$F_y = K_1 \gamma \frac{\alpha V_0^2}{2g} \left(\frac{h}{d}\right)^{2n} \frac{\pi d^2}{4} \qquad \text{(A2.14)}$$

where K_1 – coefficient.

2. Weight of the particle in water:

$$G = (\gamma_1 - \gamma)\frac{\pi d^3}{6} \qquad \text{(A2.15)}$$

Stability of the particle will be when:

$$K_1 \cdot \gamma \cdot \frac{\alpha V_0^2}{2g} \cdot \left(\frac{d}{h}\right)^{2n} \frac{\pi d^2}{4} = (\gamma_1 - \gamma)\frac{\pi d^3}{6} \qquad \text{(A2.16)}$$

Then the critical velocity is equal to:

$$V_0 = \frac{A_1}{\alpha}\sqrt{\frac{\gamma_1 - \gamma}{\gamma}}\sqrt{g} \cdot h^n d^{0.5-n} \qquad \text{(A2.17)}$$

where A_1 – coefficient and α – constant = 1.1

or:

$$V_0 = A\sqrt{g}\sqrt{\frac{\gamma_1 - \gamma}{\gamma}}h^n d^{0.5-n} \qquad \text{(A2.18)}$$

where $A = f(\alpha)$.

Critical velocity depends on d and h, and on the relative size of the particles $k = \frac{d}{h}$ or $d = k \cdot h$. Then:

$$V_0 = A\sqrt{g}\sqrt{\frac{\gamma_1 - \gamma}{\gamma}}k^{0.5-2n}\left(h^{0.5-n}d^n\right) \qquad \text{(A2.19)}$$

It is necessary to find n value, at which coefficient $A\sqrt{g}\sqrt{\frac{\gamma_1 - \gamma}{\gamma}}k^{0.5-2n}$ will have constant value at any relative grain size of the particles:

$$B = A\sqrt{g}\sqrt{\frac{\gamma_1 - \gamma}{\gamma}}k^{0.5-2n} = f(k) = const \qquad \text{(A2.20)}$$

Values A, γ_1, γ do not depend on the relative grain size and at any k (1/5, 1/10, 1/100 and so on) should reflect one condition $0.5 - 2n = 0$, than $k^{0.5-2n} = 0$ and $B = const$.

Solving equation $0.5-2n = 0$ we have $n = 0.25$ with: $\gamma_1 = const$

$$B = A\sqrt{g}\sqrt{\frac{\gamma_1 - \gamma}{\gamma}}k^{0.5-2n} = \frac{V_0}{h^{0.25} \cdot d^{0.25}} = const \qquad \text{(A2.21)}$$

Processing of the test results and natural experimental data in a wide range of relative depth of flow $\frac{h}{d}$ (or relative size of the particles $\frac{d}{h}$) with value of the B accepted as constant, the value B is equal to $B = 3.6$ at $\gamma_1 = 2.65$ and $\gamma = 1$, and then A is equal to 0.9

$$V_0 = 0.9\sqrt{\frac{\gamma_1 - \gamma}{\lambda}}\sqrt{g}(hd)^{0.25} \qquad \text{(A2.22)}$$

For constant specific weights of particles $\gamma_1 = 2.65$

$$V_0 = 1.15\sqrt{g}(hd)^{0.25} \qquad \text{(A2.23)}$$

or

$$V_0 = 3.6d^{0.25}h^{0.25} \qquad \text{(A2.24)}$$